Development of Electrochemical Immunosensors based on Self-Assembled Monolayers

Development of Electrochemical Immunosensors based on Self-Assembled Monolayers

Ontwikkeling van electrochemische immunosensoren
gebaseerd op zelf-assemblerende monolagen

(met een samenvatting in het Nederlands)

Proefschrift

Ter verkrijging van de graad van doctor aan de Universiteit Utrecht
op gezag van de Rector Magnificus, Prof. dr W.H. Gispen
ingevolge het besluit van het College voor Promoties
in het openbaar te verdedigen
op maandag 23 april 2001 des middags te 16.15 uur

door

Martine Dijksma
geboren op 8 februari 1973 te Delft

Promotores: Prof. dr A. Bult (Utrecht University)
Prof. dr W. R. Hagen (Delft University of Technology)

Co-promotor: Dr W. P. van Bennekom (Utrecht University)

This research was supported by the Technology Foundation (STW), applied science division of NWO and the technology programme of the Ministry of Economic Affairs.

The financial support of Eco Chemie B.V., Utrecht for the publication of this thesis is gratefully acknowledged.

ISBN 90-393-2662-2

Cover: Martijn Pieck and Martine Dijksma
Printing: Universiteitsdrukkerij Technische Universiteit Eindhoven

CONTENTS

Preface

Analysis of proteins and peptides can be performed with a wide variety of methods. Many of these techniques are based on physical separation combined with sensitive detection. High-performance liquid chromatography and capillary electrophoresis are the most frequently applied separation methods. However, prior to application of these techniques, usually, some kind of sample pretreatment, e.g., solid-phase extraction or derivatization, is required. Separation has to be followed by detection, usually with UV-VIS spectroscopy or mass spectrometry.[1]

Applications of protein analysis are, for example, the early diagnosis of certain diseases by detection of the presence of (an unusual concentration of) specific peptides and proteins in plasma or serum. Therefore, a method that is able to measure peptides and proteins *directly* in a sample, thus without any sample pretreatment or any separation, is preferred. This direct detection can be performed with methods making use of the specific interaction of proteins with antibodies (Ab).

Antibodies are proteins, which are produced in animals by an immunological response to the presence of a foreign substance (with a molecular weight larger than 1.5 kDa), a so-called antigen (Ag), and have specific affinity for this antigen. In immunoassays, the wells of a microtiter plate or tubes are coated with either antibodies or antigens, and after addition of a sample containing its complementary substance an immunocomplex is formed. For detection, a variety of labels is used.[2-6]

Immunointeraction of proteins in solution with their complementary proteins immobilized on a surface does lead to changes in, for example, refractive index, thickness and dielectric constant of the immobilized layer. With proteins immobilized on a piezoelectric material, a change in resonance frequency is detected which is proportional to the mass change on the surface. These properties are exploited in optical[7], electrochemical[8] and piezoelectric[9] immunosensors. Ideally, immunosensors are devices with a fast response, a high specificity and sensitivity. Preferably, immunosensors are also regenerable, which means that they can be reused immediately or after dissociation of the Ab-Ag complex, e.g., by using a chaotropic reagent.[10]

The aim of the work described in this Ph.D. thesis was to develop an electrochemical method for measuring unlabeled proteins, with high sensitivity and reproducibility. Initially the method described by Sadik, Wallace and co-workers[11, 12] was adopted, where proteins are detected amperometrically with antibodies immobilized in a conducting polymer (polypyrrole). However, we (and others) were and are not able to reproduce this method. Therefore, we changed the direction of our research and continued our work searching for a different type of immunosensor capable of direct electrochemical detection.

Many methods for electrochemical detection of unlabeled peptides and proteins have been described. These methods are reviewed in **Chapter 1**. One of the methods described utilizes antibodies immobilized via self-assembled monolayers (SAMs), i.e., spontaneously formed layers of sulfur-containing molecules on metal, e.g., Au, surfaces.[13] Using chronoamperometry, i.e., measurement of the current response after a potential step, proteins could be detected in concentrations in the pg mL^{-1} range. This method therefore has formed the basis of the new direction of our research.

In principle, immunosensors can be reused after disrupting the non-covalent Ab-Ag binding with a chaotropic reagent, a solution with a high ionic strength. However, because the chaotropic reagents affect SAMs, this regeneration method is less suitable for direct electrochemical detection. An attractive option for these SAM-based immunosensors is to build a complete immunosensor reproducibly, which became one of our goals.

For an immunosensor being stable and giving a reproducible response, the SAM must be stable and formed reproducibly. In the formation of stable SAMs, the characteristics and cleanliness of the gold electrode play an important role. An optimized treatment procedure for mechanically polished polycrystalline gold electrodes will be described in **Chapter 2**.

Besides the pretreatment method, also the conditions for SAM formation are important. In **Chapter 3,** the optimal conditions for repeated formation of reproducible SAMs of thioctic acid on a single gold electrode will be described. During these investigations hexacyanoferrate(II/III), a redox probe used for impedimetric characterization was found to influence the characteristics of the SAMs. In **Chapter 4** this phenomenon is further investigated. A mechanism will be proposed based on changes in the elements of the electrochemical equivalent circuit used to model the electrochemical data and optical measurement of the thickness of thin gold layers in hexacyanoferrate(II/III).

SAM-based immunosensors are described in **Chapters 5 and 6**. In **Chapter 5** an immunosensor based upon the use of thioctic acid will be described, and in **Chapter 6,** the use of SAMs of cysteine and acetylcysteine as well as the measurement methods chronoamperometry and impedimetry are compared. Further, methods for elimination of nonspecific adsorption have been investigated as described in **Chapters 5 and 6**.

Finally, in **Chapter 7**, a general conclusion and the future perspectives will be given.

REFERENCES

1 Larive, C. K.; Lunte, S. M.; Zhong, M.; Perkins, M. D.; Wilson, G. S.; Gokulrangan, G.; Williams, T.; Afroz, F.; Schöneich, C.; Derrick, T. S.; Middaugh, R.; Bogdanowich-Knipp, S. Separation and analysis of peptides and proteins, *Anal. Chem.* **1999**, *71*, 389-423.

2 Gosling, J. P. Enzyme immunoassay, *Immunoassay* **1996**, 287-308.

3 Gosling, J. P. *Enzyme immunoassay: with and without separation*, in *Principles and practice of immunoassay*, 2nd [rev.] Ed., C. P. Price and D. J. Newman, Eds. **1997**, Stockton Press: London. p. 349, 351-388.
4 Sparreboom, A.; Rongen, H. A. H.; van Bennekom, W. P. Assays for interferons and interleukins in biological matrices, *Anal. Chim. Acta* **1994**, *295*, 1-26.
5 Porstmann, T.; Kiessig, S. T. Enzyme immunoassay techniques, *J. Immunol. Methods* **1992**, *150*, 5-21.
6 Rongen, H. A. H.; Hoetelmans, R. M. W.; Bult, A.; van Bennekom, W. P. Chemiluminescence and Immunoassays, *J. Pharm. Biomed. Appl.* **1994**, *12*, 433-462.
7 Homola, J.; Yee, S. S.; Gauglitz, G. Surface plasmon resonance sensors: review, *Sens. Actuators* **1999**, *B54*, 3-15.
8 Skládal, P. Advances in electrochemical immunosensors, *Electroanalysis* **1997**, *9*, 737-745.
9 O'Sullivan, C. K.; Vaughan, R.; Guilbault, G. G. Piezoelectric immunosensors. Theory and applications, *Anal. Lett.* **1999**, *32*, 2353-2377.
10 Byfield, M. P.; Abuknesha, A. Biochemical aspects of biosensors, *Biosens. Bioelectron.* **1994**, *9*, 373-400.
11 Sadik, O. A.; Wallace, G. G. Pulsed amperometric detection of proteins using antibody containing conducting polymers, *Anal. Chim. Acta* **1993**, *279*, 209-212.
12 Riviello, J. M.; Wallace, G.; Sadik, O. A. *Method and apparatus for pulsed electrochemical detection using polymer electroactive electrodes* **1995**, US Patent **5,403,451**.
13 Berggren, C.; Johansson, G. Capacitance measurements of antibody-antigen interactions in a flow system, *Anal. Chem.* **1997**, *69*, 3651-3657.

1

Direct Electrochemical Immunosensors - Review

ABSTRACT

Many electrochemical immunosensors capable of direct and specific measurement of very low protein concentrations have been developed.

Pulsed amperometric detection of proteins with antibodies immobilized in a conducting polymer combines reusability with a detection limit of 0.01 to 0.5 mg mL^{-1}, depending on the protein. However, this method has only been described by Sadik and co-workers.

Research on impedimetric immunosensors started with those built on Si/SiO_2. An immunosensor with a detection limit of 1 ng mL^{-1} has been described, where antibodies are coupled via aminosilane, using glutardialdehyde. However, immobilization via polysiloxane membranes, with which a detection limit of 10 ng mL^{-1} can be obtained, seems to be more reliable. These sensors are regenerable with glycine hydrochloride pH 2.8.

Later, application of silanized metal as basis of these sensors is investigated. In contrast to those based on Si/SiO_2, these sensors have been applied in flow injection analysis. A regenerable sensor with a detection limit of 0.2 ng mL^{-1} has been obtained with antibodies coupled to aminosilane via glutardialdehyde. With antibodies immobilized in polypyrrole 0.5 ng mL^{-1} could be detected.

The sensors built on silanized metal have been succeeded by those built on self-assembled monolayers (SAMs) and bilayer lipid membranes (BLMs). With BLMs also detection in the ng mL^{-1} range is possible, this sensor can be reused 5 times, and regeneration is possible.

Much attention is paid to reusability. In general, nonspecifically adsorbed proteins contribute to the signal. Sometimes this contribution is disregarded, but also various methods to correct for the specificity of the signal have been applied.

Using SAMs much lower detection limits have been obtained. 20 ag mL^{-1} has been detected with antibodies immobilized on thin SAMs after activation with a mixture of carbodiimide and succinimide. Nonspecific adsorption is reduced by tuning the ionic strength. This method offers good possibilities for measurement in real samples. However, because the sensor is damaged by chaotropic reagents used for regeneration, this method can only be applied in disposable sensors.

M. Dijksma and W.P. van Bennekom, manuscript in preparation

INTRODUCTION

Among the methods described for analysis of proteins and peptides, many are based on a combination of physical separation and sensitive detection. Only immunoassay methods are capable of direct and specific detection in 'real' samples, like serum or plasma.

In these immunoassays the interaction between an antibody (Ab) and the protein that elicited its synthesis, the antigen (Ag), is exploited. The antigen is a foreign molecule with a molecular weight (MW) higher than 1.5 kDa to which the immune system of animals responds by synthesizing antibodies. Low-molecular-weight compounds cannot elicit antibodies by themselves. Antibodies to these so-called haptens can be formed when they are coupled to an immunogenic carrier protein, e.g., bovine serum albumin (BSA). Some of the antibodies formed are specific for the conjugated hapten. These antibodies can be selected and purified by means of, e.g., immunoaffinity chromatography.

Polyclonal antibodies have a specific affinity for the antigen, but they are directed to different binding sites (epitopes) on the antigen with different affinities. In immunoassays often the use of antibodies with uniform characteristics, i.e., monoclonal antibodies, is preferred. These antibodies are formed by using identical cells by the hybridoma technology, and have optimized characteristics such as high affinity or high specificity.[1]

Antibodies are structurally very similar. Of the five classes of immuno-globulins (IgA, IgD, IgE, IgG and IgM), which differ in, e.g., glycosylation and number and positions of the disulfide bridges, mainly IgG (150 kDa) is used for immunoassays. An IgG consists of two heavy and two light chains, which are interconnected by disulfide bridges (see Figure 1). All chains have a variable and a constant region. The variable regions of the heavy and light chain combine in one interaction site for the antigen, which is called the antigenic site. Thus, an IgG molecule has two identical binding locations for the antigen.[2]

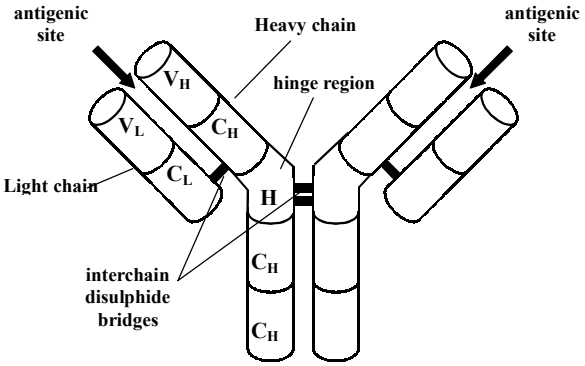

Figure 1. Basic structure of an IgG molecule.[3]

The molecular forces responsible for the Ab-Ag binding are based on non-covalent interactions including: non-polar hydrophobic interactions, Coulomb interaction, Van der Waals interaction, London dispersion attractive forces; and steric repulsion forces. The interaction is characterized with an association and a dissociation reaction rate constant, k_a and k_d respectively.

$$Ab + Ag \underset{k_d}{\overset{k_a}{\rightleftharpoons}} Ab:Ag$$

The association constant K_a, which ranges from 10^5-10^{11} M^{-1}, can be described by:

$$K_a = \frac{k_a}{k_d} = \frac{[Ab:Ag]}{[Ab][Ag]}$$

where [Ab], [Ag] and [Ab:Ag] are the concentrations of the antibody, antigen and complex in the solution, respectively.[4]

The immunoassay method is applied in interaction measurements in several approaches, a short overview of which is given in the next paragraph. After passing on to immunosensors, the focus will be on direct electrochemical detection of unlabeled proteins and peptides.

IMMUNOASSAYS

Immunoassays are in wide use as analytical tools in clinical and pharmaceutical sciences. To be able to detect the interaction, one of the immunoagents has to be labeled. Various labels have been applied, of which radioisotopes were among the first, because of their inherent sensitivity. Other frequently used labels are chemiluminescent compounds,[5, 6] and enzymes (e.g., alkaline phosphatase, horseradish peroxidase), that convert an enzyme substrate into a measurable product.[7-10]

Many different formats have been described and four generally used formats are shown in Figure 2. In a homogeneous immunoassay (Figure 2a) antibodies, antigens and labeled antigens are mixed. Free labeled antigens and those bound to an antibody, can be distinguished by an activity change of the label upon binding.

Usually, immunoassays are heterogeneous, which means that either the antibody or the antigen is immobilized on a solid carrier and an immunocomplex is formed upon contact with a solution containing the other immunoagent. The unbound proteins are removed by washing and the response obtained from the labels is proportional to the amount of protein bound.

In a sandwich immunoassay, antibodies are immobilized and after addition of the sample containing the antigen, a labeled secondary antibody is added (Figure 2b). Besides these non-competitive formats, also competitive formats can be applied. In a competitive assay, competition takes place between free and bound antigen for a limited amount of labeled antibody (Figure 2c) or between antigen (the sample) and labeled antigen for a limited amount of antibody (Figure 2d).

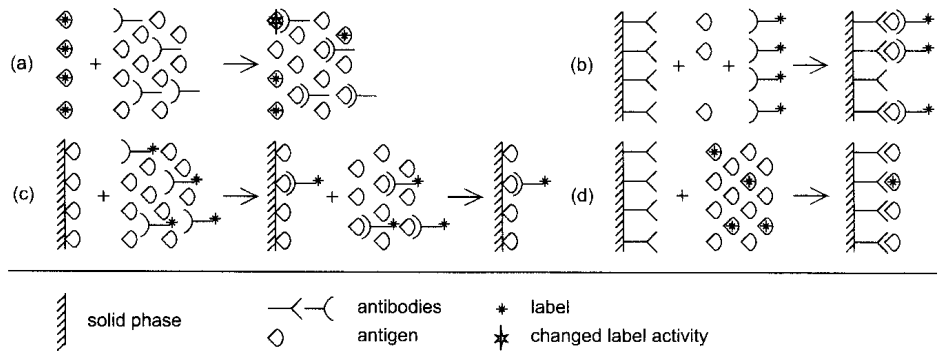

Figure 2. Generally used formats: (a) a homogeneous competitive immunoassay, (b) a heterogeneous non-competitive immunoassay, (c) a heterogeneous competitive immunoassay and (d) a heterogeneous competitive immunometric assay.[11]

Liposomes with marker molecules or enzymes encapsulated have been used to enhance the response. In these so-called liposome immunoassays, the secondary antibody is labeled with biotin and (strept)avidin is used as a bridging molecule between this antibody and biotinylated liposomes.[11]

Immunoassays are convenient for clinical practice when many, often identical, analyses have to be conducted on a routine basis. Immunoassays are often performed in (a multiple of) 96-wells microtiter plates.

Ideally, a method for detection of immunointeraction has a fast response, and a high specificity and sensitivity. In the research towards improved methods, the development of faster and more sensitive methods for direct detection are major subjects. These prerequisites may be fulfilled by immunosensors.

IMMUNOSENSORS

Generally, a sensor consists of a sensing element and a transducer (Figure 3). In case of an immunosensor, the sensing element is formed by immobilized antibodies or antigens.

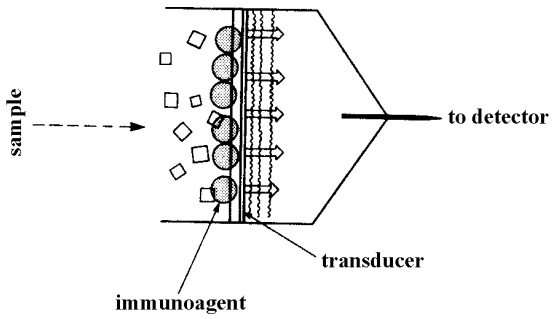

Figure 3. Principle of operation of an immunosensor.[12]

For immobilization of the immunoagents many methods have been developed, on various substrates.[13-15] The binding event is transformed into a measurable signal by the transducer.[12] Transduction has been performed using optical (e.g., surface plasmon resonance),[16] piezoelectrical (e.g., quartz crystal micro-balance),[17, 18] surface scanning (e.g., atomic force microscopy)[19-21], scanning electrochemical microscopy,[22-24] and other electrochemical techniques.[25, 26]

Electrochemical detection of immunointeraction can be performed both with and without labeling. A frequently used format in electrochemical immunosensing is an amperometric immunosensor, where proteins are labeled with enzymes producing an electroactive product from an added substrate.[26]

Direct detection without labeling can be performed by cyclic voltammetry, chronoamperometry, impedimetry, and by measuring the current during potential pulses (pulsed amperometric detection). These methods are able to detect a change in capacitance and/or resistance of the electrode induced by binding of protein. These immunosensors have been developed using various substrates. Those built on silicon, silanized metal, or polypyrrole are often regenerable, while those based on self-assembled monolayers (SAMs), that is, monolayers formed spontaneously from sulfur-containing compounds on silver or gold, are not. Chaotropic reagents, used to accomplish disruption of the Ab-Ag bond, have been reported to affect the SAM[27, 28] or to induce a decrease in the sensitivity of the sensor.[29, 30]

The various measurement methods are described in the next section, followed by an overview of publications on direct electrochemical immunosensors.

MEASUREMENT METHODS

In impedance measurements a sinusoidal potential (E_{ac}) is superimposed on a dc potential (E_{dc}). E_{ac} can be described by

$$E_{ac} = E_0 \sin \omega t \qquad \text{(Equation 1)}$$

where E_0 is the amplitude (V), t the time (s), and ω the radial frequency (rad s^{-1}). The response is a current I given by

$$I = I_0 \sin(\omega t + \phi) \qquad \text{(Equation 2)}$$

where ϕ is the phase angle between perturbation and response. The proportionality factor between E and I is the impedance Z.

The current through a resistance R is

$$I = \frac{E_0}{R} \sin \omega t \qquad \text{(Equation 3)}$$

Kinds of resistances that are found in electrochemical cells are:

- Solution resistance (R_s), which depends on the ionic strength of the solution and the distances between the working, auxiliary and reference electrode
- Polarization resistance (R_p), which arises from application of a potential other than its equilibrium potential to the electrode
- Charge transfer resistance (R_{ct}), which is due to electron transfer of a redox probe to the electrode

The current through a capacitance C is

$$I = C\frac{dE}{dt}\cos\omega t \qquad \text{(Equation 4)}$$

which implies a phase angle ($\phi = \pi/2$) between the potential and the current. The capacitance of the working electrode is built up from the capacitances of the layers on the electrode and the electrical double layer. Because the latter is relatively large, its contribution to the total capacitance is negligible. In an immunosensor, therefore, the total capacitance (C_{dl}) is determined by that of the immobilized antibodies (C_{Ab}). When antigens bind, a hydrophobic layer is formed in contact with the antibodies, with a capacitance C_{Ag}, and C_{dl} decreases according to Equation 5.

$$\frac{1}{C_{dl}} = \frac{1}{C_{Ab}} + \frac{1}{C_{Ag}} \qquad \text{(Equation 5)}$$

Data obtained by scanning ω automatically can be plotted in a Nyquist plot. Here, Z is a vector, which can be separated in an in-phase (Z') and out-of-phase (Z'') component. These systems can often be described by the Randles' equivalent circuit (Figure 4a).

From Figure 4b, R_s and R_{ct} can be calculated from the intercept with the Z'-axis, and C_{dl} from ω at Z''_{max}. Z_w is the Warburg impedance, which presence indicates mass-transfer through the boundary layer on the electrode. At low frequencies, diffusion can rule the process (mass-transfer control). In this case the impedance Z is the Warburg impedance, with $\phi = \pi/4$.[31, 32] At high frequencies, the process is kinetically controlled and the influence of Z_w is negligible, which leads to a semi-circle (see Figure 4b).

Electrodes do not behave ideally, e.g., because of the roughness of the surface and the complicated structure of an immobilized antibody layer. A constant-phase element (Q) is used to describe these systems more appropriately. Its impedance (Z_Q) is described by $Y_0 (j\omega)^{-n}$, where Y_0 is a proportionality constant, $j = \sqrt{-1}$, and n is an exponent ($-1 \leq n \leq 1$). Although the exact physical basis of Q has to be elucidated, Q can be used for fitting the data in a very flexible way. If $n = 1$ the element $Y_0 = 1/C$ and if $n = 0$ $Y_0 = R$. Usually n has values between 0.7 and 0.9 in case of solid electrodes.[32, 33]

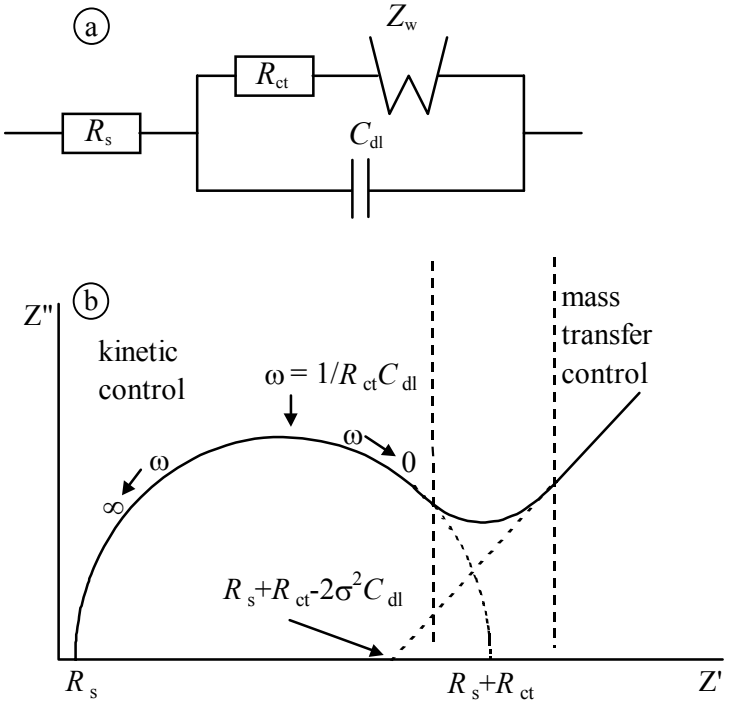

Figure 4. (a) Randles' equivalent circuit (see text), (b) Nyquist plot arising from a Randles' circuit.

The capacitance can be calculated using cyclic voltammetry (CV) or linear sweep voltammetry (LSV) by dividing the charging current in the potential scans by the scan rate.[34, 35] From the kinetics of the charge transfer of a redox probe, the amount of shielding of the electrode can be derived.

Impedimetry is most often applied for direct electrochemical immunosensing. In sensors on silanized Si/SiO_2 or silanized metal substrate this method is performed in buffer, while in sensors on SAMs also measurements have been performed in the presence of a redox probe. SAMs are often characterized in the presence of a redox probe (hexacyanoferrate(II/III) [27, 35-41] or hexaaminerutheniumchloride(II/III)) [35, 38-41] with CV or impedimetry.

In chronoamperometry, resistances and capacitances are calculated from the current response following a potential step. Swietlow et al.[42] used the Randles' equivalent circuit to calculate *C* and *R* of SAMs. Berggren et al.[27] extract *C* and *R* of an immunosensor from a fit of the first part of the current response to a *RC* circuit. In this circuit the current (*I*) as a function of time can be described by

$$I(t) = \frac{\Delta E}{R_s} \cdot \exp\left(\frac{-t}{R_s \cdot C_{dl}}\right) \qquad \text{(Equation 6)}$$

where ΔE is the potential step, and t the time after pulse application. A logarithmic plot of this function results in a straight line and R and C can be calculated from the intercept and the slope of the linear part of the curve.[27]

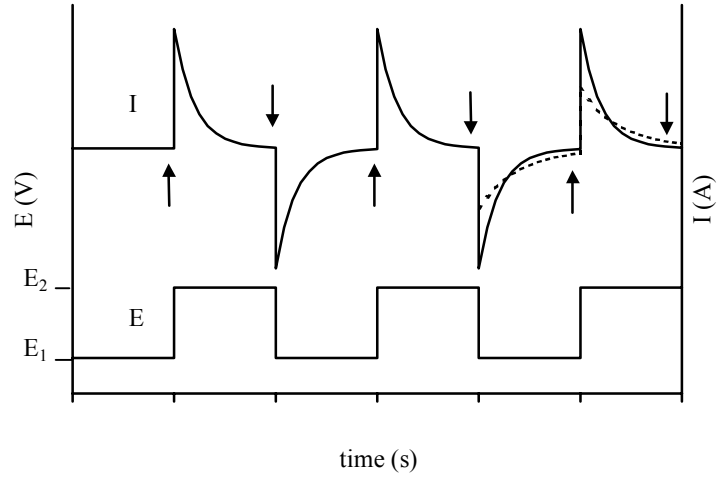

Figure 5. The principle of pulsed amperometric detection. The upper graph shows the current response to the applied potential as shown in the lower graph. The arrows indicate the moment at which the current is sampled.

In pulsed amperometric detection (PAD) the current is sampled at the end of each pulse. In Figure 5 the current-response to this pulsed potential is shown. Binding of antigen causes a change in R or C (dashed line in Figure 5), resulting in a different current at the end of the pulse. This principle has been applied by Sadik and co-workers, who used antibodies immobilized in polypyrrole as sensing layer.

APPLICATIONS

Capacitive immunosensing started in 1986.[43] The sensor developed consists of a SiO layer on copper electrodes insulated by parylene. Silanol groups of the SiO were reacted with γ-aminopropyltriethoxysilane and a hapten (tricothecene toxin T2) is bound by carbodiimide coupling. T2 specific antibodies bind to the immobilized haptens. Furthermore, they can be displaced from the immobilized haptens by free haptens. A concentration of 1 μg mL^{-1} has been detected. Later on, sensors have been developed based on antibodies (or antigens) immobilized in or on silanized Si/SiO_2, silanized metal, polypyrrole, self-assembled monolayers on gold electrodes, and bilayer lipid membranes.

POLYPYRROLE-BASED IMMUNOSENSORS

In 1991 John et al.[44] described a method for incorporation of antibodies in polypyrrole layers. Polypyrrole electrodes were prepared by galvanostatically electropolymerizing pyrrole from an aqueous solution containing anti-human serum albumin (anti-HSA) on a polished Pt electrode. Optimal conditions for preparation of these sensing layers were reported. With CV it was shown that HSA does interact with these sensing layers, while no response is obtained with polypyrrole without incorporated antibodies. This method has been extended by Sadik and Wallace,[45] who were able to detect the interaction of HSA in flow-injection analysis (FIA) using PAD.

The effect of polymer composition, the nature of the eluent, and the electrochemical waveform on the selectivity of this detection process has been investigated.[46] The principle has been patented[47] and optimized for detection of thaumatin[48] and *p*-cresol and other phenolics.[49] Detection limits achieved are in the $\mu g\ mL^{-1}$ range. A relatively small contribution (< 5%) of nonspecific proteins has been found.

However, this method has also been used to detect proteins on "non-bioactive" polymers. These polymers have been prepared from an aqueous solution containing 0.2 M pyrrole monomer and 0.1 M *p*-toluene sulfonate. The responses observed are dependent on the nature of the polymer, the nature of the electrolyte/cation as well as on the electrolyte concentration and pH, which means that these factors can be used to modify the selectivity. Detection limits in the order of nM have been reported.[50]

Polypyrrole is a conducting polymer. Its charge depends on the applied potential. By pulsing the potential between 0.4 and 0.0 V, the polymer is alternately positively charged and almost neutral. When an antibody is incorporated, the antigen is able to bind to the positively charged polymer (that is, at $E = 0.4$ V). At 0.0 V the polymer with incorporated antibodies has a net negative charge and positive ions from the solution compensate this charge and push aside the antigen. At 0.4 V these positive ions either leave the polymer, or their positive charge is neutralized by the anions in the buffer, as shown in Figure 6.[47, 51, 52]

During binding of antigen, the characteristics of the electrode are different, which results in a different current response, dependent on the concentration of antigen in the sample. The resulting positive current difference can be explained by a combination of a decrease in capacitance and an increase in resistance of the electrode (Figure 5).[53]

The characteristics of polypyrrole, with and without incorporated proteins, and the mechanism of the PAD method have been further studied using quartz crystal microbalance,[55] CV and impedance techniques.[53, 54]

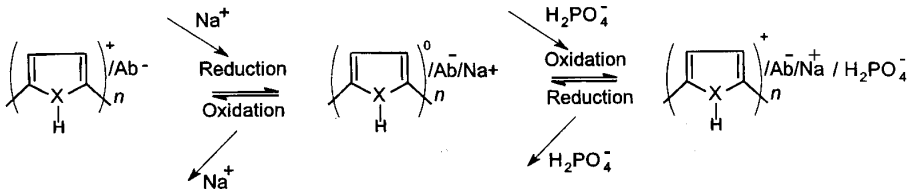

Figure 6. Mechanism of diffusion of solution-ions during pulsing.[54]

Later based on this principle, an electrochemical immunosensor for direct detection of polychlorinated biphenyls (PCBs) in water has been developed. With an analytical signal generated by applying a pulsed waveform between +0.60 V and –0.60 V with a pulse time of 120 and 480 ms, a detection limit of 0.05 μg L^{-1} could be obtained.[51, 56]

Bioaffinity sensors based on conducting polymers have been reviewed,[57] and a comparison of different sensing systems suitable for the determination of pesticides, metals and PCBs has been described.[58]

Despite the very broad applicability and reversibility, use of this method has until now not been published elsewhere. We have not been able to reproduce the results obtained. Preparation of reproducible polypyrrole layers and nonspecific adsorption of proteins to polypyrrole layers are the main problems. The applicability of this method has extensively been investigated by Higson and co-workers and the results will be published.[59]

IMMUNOSENSORS ON SILICON

Immobilization of antibodies

Immunosensors built on Si/SiO_2 structures, are prepared by covering a silicon wafer with a SiO_2 layer by thermal growth at high temperatures (~1000°C),[60-66] or by $Si_3N_4/SiO_2/Si$ structures.[67-69] In order to perform electrochemical measurements, ohmic contacts (gold[60-66] or aluminium[67-69]) have been made on the wafers. Cleaning and hydroxylation are performed by immersion of the wafer into hot organic solvents[60, 61] or into a solution of sulfuric acid and potassium dichromate,[62-66] followed by washing with water and vacuum drying at 140°C.

These hydroxylated wafers are modified with aminosilane, cyanosilane or polymeric membranes (polysiloxane or polysilsequioxane). Modification with aminosilane or cyanosilane is performed by adsorbing silanes onto the surface from a 3% (v/v) solution of the silane in isopentane, followed by removal of the solvent at −30°C under vacuum. During heating in a dry nitrogen flow for 24-48 h the surface adsorbed silane reacts with the silanol sites (a procedure often referred to as grafting) (Figure 7). The surface is cleaned with tetrahydrofuran and dried in a flow of nitrogen.[60-68]

Polysiloxane membranes are deposited from solutions of polycyanopropyl-methylsiloxane and (aminopropyl)methyldimethylsiloxane in toluene (0.1 – 1%) using a spin-coating procedure. Different concentrations of polymer were used in order to obtain a different thickness of the membrane.[65, 66] Heteropoly-silsequioxane membranes are prepared by polymerizing a mixture of 3-amino-propyltrimethylmethoxysilane (7%) and *n*-butyltrimethyl-methoxysilane at 80°C.[63, 64] The wafers are dried and washed with dichloromethane.

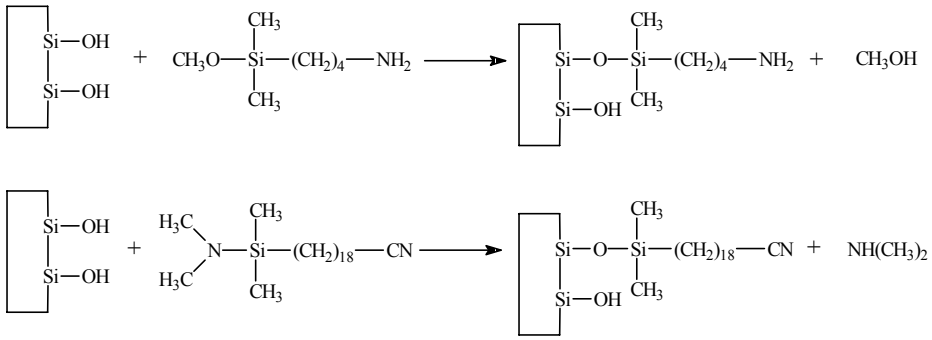

Figure 7. Modification of Si/SiO_2 surface with (a) an aminosilane and (b) a cyanosilane.[63]

Aminosilanized wafers are modified with antibodies by

– incubation in glutardialdehyde solution containing antibodies in a phosphate buffered medium at pH 7.6 at room temperature for 15 min,[62] or
– activation with glutardialdehyde followed by incubation in a solution of antibodies in phosphate buffer,[60, 61, 67, 68] or
– incubation in a solution of the coupling reagent disuccimidyl suberate (DSS) in *N,N*-dimethylformamide (DMF) for 1 h, followed by reaction of the activated surface, after chloroform washing, with a solution of antibodies in phosphate buffer for 12 h (Figure 8).[63-66]

Cyanosilanized wafers are modified with antibodies by incubation overnight in a solution of the antibody (2 mg mL^{-1} in phosphate buffer, pH 7.6). The antibodies are only bound by electrostatic interactions between a cyanogroup from the silane and a hydroxylgroup from the antibody (Figure 9). However, antibodies could not be removed by washing with a 0.1 M glycine buffer (0.4 M NaCl, pH 2.8), which is used for regeneration of the immunosensor.[62-66]

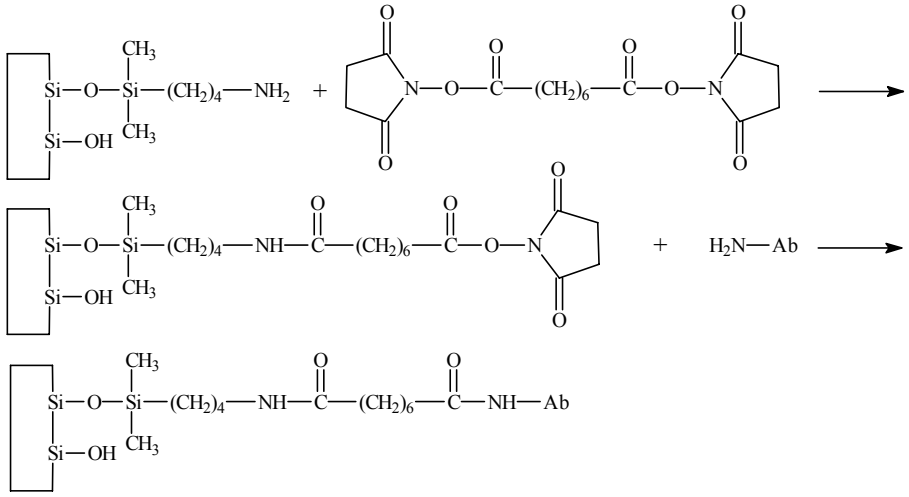

Figure 8. Antibody coupling to an aminosilanized wafer via DSS.[63]

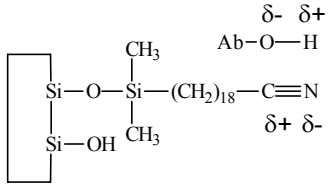

Figure 9. Antibody coupling to a cyanosilanized wafer.[63]

Results

For immunosensors on silicon, research started with the publications of Bataillard et al.[60] and Mandrand, Colin and co-workers,[61, 70] who detected α-fetoprotein (MW = 64 kDa) with monoclonal antibodies immobilized on aminosilanized wafers, with a detection limit of 1 ng mL^{-1}.

In general, measurements with these immunosensors have been performed in batch after incubation times ranging from 15 min to 1 h. Results obtained with different immobilization and coupling methods and measurement conditions are summarized in Table 1.

Detection of 1 ng mL^{-1} has only been reported by one group.[60, 61, 70] Berney et al.[68] did not observe a reproducible capacitance decrease on addition of antigen, until the layer was covered with polyethylene glycol (PEG) polymer. In a later publication examination and characterization of four device types with passively adsorbed antibodies has been described; Si/SiO_2, $Si/SiO_2/Si_3N_4$, $Si/SiO_2/Si_3N_4$ which has an area of nitride and oxide laser ablated, and $Si/SiO_2/Si_3N_4$ which has an area mechanically degraded. Only with the last device a difference signal was detected between the sensor and a reference sensor. This method has been applied to detection of various proteins.[69]

Table 1. Overview of methods and results.

Protein	Immobilization	Coupling Ab via	f (kHz)	E_{dc} (V) vs SCE	E_0 (mV)	Detection limit	Regeneration	Ref.
α-fetoprotein	aminosilane[I]	glutar-dialdehyde	10	-1 - +4	14	1 ng mL^{-1}	glycine-HCl pH 2.8	60, 61
SEB[II]	cyanosilane[III]	directly	10		14	not measurable		62
	aminosilane[IV]	glutar-dialdehyde				1 µg mL^{-1}	glycine-HCl pH 2.3	
α-fetoprotein	cyanosilane[V]	directly	10	-0.5 - +2	14	not measurable		63
	aminosilane[VI]	DSS[VII]						
	heteropolysilses-quioxanes	DSS[VII]						
α-fetoprotein	heteropolysilses-quioxanes	DSS[VII]	0.01 – 200	-1 - +1	10	10 ng mL^{-1}	glycine-HCl pH 2.8	64
α-fetoprotein	cyanosilane[VIII]	directly	1 – 100	2	10	not measurable		65
	aminosilane[IX]	DSS[VII]				not measurable		
	amino- and cyano-polysiloxane membranes	DSS[VII]/ directly				10 ng mL^{-1}	glycine-HCl pH 2.8	
α-fetoprotein	amino- and cyano-poly siloxane membranes	DSS[VII]/ directly	20-75	2	10	10 ng mL^{-1}	glycine-HCl pH 2.8	66
transferrin	aminosilane[X]	glutar-dialdehyde	1	0	100	not determined	not possible	68
transferrin and other proteins	direct adsorption		1	-1 - +1	100	25 µg mL^{-1}	not discussed	69
SEB[II]	Langmuir Blodgett	directly	10	-1 - +3	14	1 µg mL^{-1}	not discussed	71
urokinase-type plasminogen activator	aminosilane[XI]	glutar-dialdehyde	1		10	0.1 µM	glycine-HCl pH 2.4	67

[I] (4-aminobutyl)dimethylmethoxysilane
[II] enterotoxin B from *Staphylococcus Aureus*
[III] γ-cyanodecyldimethyl(dimethylamino)silane
[IV] δ-aminobutyldimethylmethoxysilane
[V] cyanooctadecyldimethyl(dimethylamino)silane
[VI] 4-aminopropyldimethylmethoxysilane
[VII] disuccimidyl suberate
[VIII] γ-cyanopropyldimethyl(dimethylamino)silane
[IX] 4-aminobutyldimethylmethoxysilane
[X] γ-aminopropyltriethoxysilane (γ-APTES) or 4-aminobutyldimethylmethoxysilane
[XI] γ-APTES

With the exception of those described by Berney et al.[68, 69] and Barraud et al.[71] immunosensors on silicon can be regenerated with glycine·hydrochloride pH 2.4 – 2.8. While all authors use a different combination of preparation and measurement method, a simple comparison between the methods can not be made. In general, antigen has not been detected on antibody coupled to aminosilanes via DSS or to cyanosilanes. With antibody coupled to aminosilane via glutardialdehyde, a detection limit of 1 ng mL^{-1} has been obtained by Bataillard et al.[60] and Gardies et al.,[61] while later Billard et al.[62] reported a detection limit of 1 µg mL^{-1}, using a slightly different immobilization procedure. Using polysiloxanes and heteropoly-silsequioxanes a detection limit of 10 ng mL^{-1} has been obtained.[64-66] However, Saby et al.[63] were not able to detect the interaction.

An explanation for the fact that detection could be performed on membranes and not on silanes has been given by Maupas et al.[65] Probably, in the case of polysiloxane membranes, the antibodies are not bound only on, but also inside the polymeric membrane, changing the electrical characteristics like the conductivity and dielectric constant.

Nonspecific adsorption

In general, only a minor contribution of nonspecific adsorption on this type of sensor has been observed. To correct for nonspecific adsorption, interaction of specific and nonspecific antigen is compared[65, 66] or a reference sensor is used in a differential setup. As reference sensor, a sensor with another protein (nonspecific antibodies or albumin) is used.[60] Klein et al.[67] first add nonspecific antigen to the solution, followed by specific antigen to compare the response. Souteyrand et al.[64] observed desorption of nonspecifically adsorbed proteins upon washing with buffer.

Interpretation of the results

In most publications, impedance results are modelled with a standard series model, which means that each molecule layer is considered as a perfect dielectric.[60-62, 69, 71] More intricate equivalent circuits have been described by Jaffrezic-Renault et al.[66] and Schyberg et al.[72] In principle, the silicon substrate acts as a conductor and the protein layers can be viewed as a series of capacitors, if they are electrically blocking (and thus behave as a dielectric). However, it seems difficult to consider the Ab-Ag interaction only as a thickening phenomenon. Another problem is the relative small capacitive effect caused by binding of the protein compared to the capacitance of the heterostructures.[66]

SILANIZED METAL BASED IMMUNOSENSORS

Immobilization of antibodies

Maupas and co-workers[73, 74] functionalized electrochemically oxidized Pt electrodes with silanes using the same procedures as described for Si/SiO_2 electrodes. Antibodies were immobilized in polypyrrole by adsorption of a mixture of pyrrole and antibody on the electrode followed by drying under reduced pressure and electropolymerisation at $E = +0.8$ V versus SCE in 0.1 M aqueous $LiClO_4$.[73, 74]

DeSilva et al.[75] immobilized anti-SEB antibodies on a Pt film deposited on a Si/SiO_2 chip. Silanization of the Pt was carried out by treating the surface with a 2% solution of 3-mercaptopropyltrimethoxysilane in dry toluene under a nitrogen atmosphere, followed by rinsing with toluene and drying in a stream of N_2. The silanized film was then reacted with *N*-γ-maleimidobutyloxysuccinimide ester (GMBS) followed by incubation in an anti-SEB solution (100 μg mL^{-1} in PBS) at 4ºC for 24 h. The influence of the substrate for immobilization of anti-SEB has been investigated using impedance and AFM measurements. Pt films showed the highest coverage of anti-SEB. On gold films, a very low coverage has been found.[76]

Varlan et al.[77] cleaned Ti with chromic acid followed by hydroxylation with 5% NaOH, silane adsorption, grafting and antibody coupling. Gebbert et al.[78] silanized Ta and immobilized antibodies after carbodiimide activation. Feng et al.[79] detected IgG potentiometrically with anti-IgG immobilized on a silanized silver electrode.

Results

In Table 2, the immobilization and measurement methods used and the results obtained are summarized.

While with sensors built on Si/SiO_2 a detection limit of 10 ng mL^{-1} seems to be feasible, with sensors built on silanized metal detection limits in the range of 0.1 ng mL^{-1} has been achieved. This detection limit has been described by Gebbert et al.[78] and DeSilva et al.[75] However, in both cases, reusability is not discussed. The method of the latter has been patented.[80]

Polypyrrole layers exhibit an even better stability to glycine washing than polysiloxane layers, and can be reused 10 times compared to 2 times for polysiloxane layers. However, due to the high polarization of the polypyrrole sensor, the antibody activity is reduced and the sensor has a lifetime of only one week.[74] Feng et al.[79] were able to regenerate their potentiometric sensor with 1.9 M HCl.

Table 2. Overview of methods and results.

Protein	Metal	Immobilization	Coupling Ab via	f (kHz)	E_{dc}	E_0 (mV)	Detection limit	Regeneration	Ref.
α-feto-protein	Pt	amino- and cyanopoly-siloxane[I]	DSS[II]/ directly	1.5			30 ng mL^{-1}	glycine-HCl pH 2.8	73
α-feto-protein	Pt	aminopoly-siloxane[III] / polypyrrole	DSS[II] / incorpo-rated	0.22	-1.5 V vs Ag/AgCl	10	30 ng mL^{-1} / 0.5 ng mL^{-1}	glycine-HCl pH 2.8	74
SEB[IV]	Pt	3-mercapto-propyltri-methoxysilane	GMBS[V]	0.1		10	0.4 ng mL^{-1}	not described	75
allostatin	Ti	aminosilane[VI] / glycidoxy-propyldimethyl ethoxysilane	glutardi-aldehyde / directly	2		20	3000x diluted serum sample	not possible	77
IgG	Ta	aminosilane[VII]	carbodi-imide[VIII]	1	100 mV		0.2 ng mL^{-1}	not described	78
IgG	Ag	aminosilane[IX]	glutardi-aldehyde	-	-	-	0.2 ng mL^{-1}	1.9 M HCl	79

[I] (aminopropyl)methylsiloxane and polycyanopropylmethylsiloxane
[II] disuccimidyl suberate
[III] polycyanopropylmethylsiloxane
[IV] enterotoxin B from *Staphylococcus Aureus*
[V] *N*-γ-maleimidobutyloxysuccinimide ester
[VI] γ-aminopropyltriethoxysilane and aminobutyldimethylmethoxysilane
[VII] (3-aminopropyl)triethoxysilane
[VIII] cyclohexyl(2-morpholinoethyl)-carbodiimide metho-*p*-toluenesulfonate
[IX] 3-aminopropyltriethoxysilane

Nonspecific adsorption

Gebbert et al.[78] compared adsorption on IgG (specific) and BSA modified and unmodified chips. On BSA a 15% change compared to IgG has been found. Denatured specific antigens cause a capacitance change of 10 – 20% compared to native antigens. Varlan et al.[77] observed only a minor effect from injection of relatively high concentrations of BSA. DeSilva et al.[75] observed desorption of nonspecifically adsorbed proteins. In the methods described by Maupas and co-workers[73, 74] the specific signal is the difference in response to injection of antigen between a working and a reference sensor.

Comparison of immunosensors built on silanized metal and built on Si/SiO_2

In contrast to immunosensors built on Si/SiO_2, immunosensors built on silanized metal have been developed for flow injection analysis. Ameur et al.[74] described that monitoring with impedimetric immunosensors based on Si/SiO_2 is

impossible, because of the small changes observed, which means that a great number of measurements has to be performed and combined to obtain reliable results.

While the impedance of a dielectric is inversely proportional to the frequency, in order for the impedance of a Si/SiO_2 structure to be negligible, measurements have to be performed at high frequencies (usually 10 kHz). Using metal electrodes it is possible to measure at more appropriate conditions. Therefore, metal electrodes functionalized with silane layers containing antibodies offer a better basis for immunosensors.[73]

SAM-BASED IMMUNOSENSORS

SAMs

The capacitance of SAM-based immunosensors can be tuned by the kind of sulfur-containing molecules used. Using long-chain alkanethiols a much more stable and shielding layer with a larger thickness, and thus a smaller capacitance, is formed than using shorter-chain or branched molecules. The stability of SAMs arises from interaction of the sulfur-atom with the metal (silver or gold) in combination with intermolecular interactions between the alkyl chains.[81, 82] Another important subject in the research on SAM application in immunosensors is the reproducibility of formation. This is largely determined by the methods used for treatment of the surface[36, 83-85]

Immunosensors

Liu et al.[28] detected the interaction of benzo[a]pyrene-bovine serum albumin (BaP-BSA) with a monoclonal antibody (Mab10c10) specific to BaP, which is immobilized on a gold electrode through a SAM of cystamine. Using linear sweep voltammetry (LSV) between +50 and –50 mV and a scan rate of 5 mV s^{-1} BaP-BSA can be detected in the range of 0.01 to 6 μM after 15 min of incubation. No cross-reactivity with BSA was observed.

Feng et al.[86] detected Human Colonic Tumor (HT29) cells with LSV on a SAM of anti-HT29 monoclonal antibody, after 1 h of incubation. In this case, the detection principle is based on the electrochemical oxidation of cells bound to antibodies. This oxidation peak is observed in a linear scan from –0.1 to +0.8 V versus SCE, only when HT29 is bound.

Direct amperometric detection was used by Snejdarkova et al.[87] The addition of human IgG to γ-chain specific anti-human IgG immobilized on mixed SAMs of 11-mercaptoundecanoic acid (MUA) and 1-dodecanethiol resulted in decrease of conductivity. The detection limit is $2 \cdot 10^{-10}$ M (= 30 μg L^{-1}). These SAMs were advantageous by their good stability and absence of nonspecific adsorption (of HSA), compared to SAMs of MUA or cysteamine or mercaptopropionic acid.

Stable monolayers were formed after gold cleaning with piranha acid (a mixture of concentrated H_2SO_4 and H_2O_2) or electrochemical cleaning with CV.[87]

In 1997 Berggren and Johansson[27] reported a method for sensitive measurement of the Ab-Ag interaction using chronoamperometry, by sampling the current after a potential step (0 – 50 mV) with 50 kHz. Antibodies were immobilized on mechanically polished and plasma-cleaned polycrystalline gold rod electrodes via a carbodiimide-activated SAM of thioctic acid, followed by post-coating with dodecanethiol. From the difference in current response before and after injection of the analyte, the proteins interleukin-2 (IL-2), human chorionic gonadotropin hormone (HCG) and human serum albumin (HSA) could be detected, with detection limits in the pg mL^{-1} range. No nonspecific adsorption (of tyrotropic hormone and serum) has been observed.[27] At least half of the electrodes did not produce any change in capacitance when antigens were injected. Different chaotropic reagents were tested for regeneration of the sensor, but they were all found to lead to a change in the response of the sensor.[27]

Detection of interleukin-6 (IL-6) has both been performed on antibodies immobilized on thioctic acid using carbodiimide activation and on cystamine using epoxy-activation, followed by postcoating with dodecanethiol. The latter has a higher sensitivity (detection limit 10 fg mL^{-1}), due to the high relative decrease in capacitance compared to that arising from antigen binding to proteins immobilized on thioctic acid SAMs. However, also total amount of binding locations on cystamine is lower, which results in a smaller detection range. The reproducibility between different electrodes was 30 – 40%. No nonspecific adsorption of IL-2 on the sensor has been observed.[88]

Hintsche et al.[89] showed that thin film gold interdigitated arrays can be used for direct electrochemical immunosensing. Binding of antibodies on antigens with thiol groups adsorbed on gold, changes the resistive and capacitive parameters.[89]

Taira et al.[90] used SAMs of long-chain dialkyl disulfide with a terminal dinitrophenyl (DNP) group to detect anti-DNP antibodies. Impedance measurements from $f = 0.1$ Hz to 65 kHz in presence of 5 mM hexacyano-ferrate(II/III), at the open circuit potential (OCP = 0.21 V versus Ag/AgCl) and $E_0 = 50$ mV could be described by a Randles' circuit (see Figure 4a). In absence of the redox probe, at $f = 100$ Hz, E_{dc} = OCP = 0.45 – 0.49 V versus Ag/AgCl a response for antibodies was found in the range $10 – 10^3$ ng mL^{-1}. However, differences are found in the impedance of the SAMs, arising from poor reproducibility of the roughness of the polished gold electrode. A way for reducing nonspecific adsorption has not been described.[90]

Göpel and co-workers[29, 30] measured the interaction between a synthetic peptide and its antibody. The peptide was modified with ω-hydroxyundecanethiol (HUT) and self-assembled on a gold electrode, prepared by sputtering gold on glass slides, using an adhesion layer of chromium. The measurements were performed in the presence of 20 mM hexacyanoferrate(II/III) at OCP, $f = 0.05$ to 1000 Hz, in

flow (60 μL min^{-1}).[29] In a further study[30] it was found that the most reproducible and insulating protein layers were formed by adsorption of the modified peptide followed by HUT. The behavior of the electrode could be described with the equivalent circuit shown in Figure 10a. Hexacyanoferrate has been found to damage SAMs or reduce the activity of the immobilized proteins.[30, 85] Therefore, further measurements were conducted in buffer, i.e., without a redox probe. The electrode was exposed to the antibody solution for 15 min and concentrations of 1.74 μg mL^{-1} could be determined. For time-dependent measurements the frequency used was 113 Hz. A relatively small change (< 5%) resulted from injection of nonspecific antibodies. Regeneration is performed with 6 M urea, because capacitances were found to return to values more similar to those before antibody binding than if acidic buffer was used.

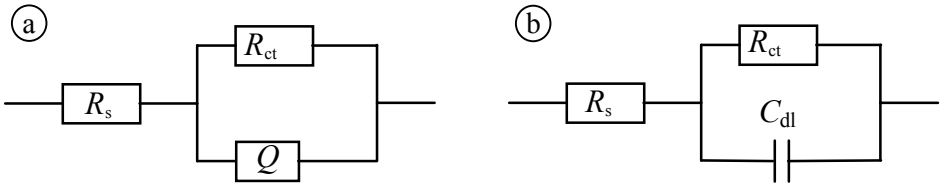

Figure 10. Equivalent circuits used by (a) Göpel and co-workers,[29, 30] and (b) Jie et al.[91] to describe their immunosensor system.

Mirsky et al.[92] used SAMs of the long-chain ω-mercaptohexadecanoic acid and ω-mercaptohexadecylamine on gold electrodes, in the development of an impedimetric immunosensor for HSA, because they are more stable than SAMs of shorter-chain molecules. Measurements have been performed at $f = 20$ Hz, $E_{dc} = 300$ mV versus Ag/AgCl, and $E_0 = 10$ mV. Different methods for immobilization of antibodies on these monolayers have been characterized using impedimetry. The *N*-hydroxysuccinimide and carbodiimide methods were identified as most suitable for protein immobilization in that they did not damage the alkanethiol layer. The detection limit of the resulting sensor is 15 nM (1 mg L^{-1}). An equivalent circuit to describe the system was derived. With polyclonal antibodies a cross-reactivity to BSA was found of 50%, with monoclonal antibodies 20%.[92]

Ameur et al.[93] immobilized α-fetoprotein specific antibodies on a gold electrode via a cystamine SAM. A sensitivity of about 700 ng mL^{-1} has been obtained. The sensor was reusable after washing with 50% ethanol in phosphate buffer.

For impedimetric detection of human mammary tumor associated glycoprotein an immunosensor has been described based on monoclonal antibodies physically adsorbed on gold.[91] Frequency scans have been measured before and after incubation for 40 min in a solution of 200 μg mL^{-1} specific antigen. Only a minor

effect has been observed with a nonspecific protein. The data have been fitted to the equivalent circuit, shown in Figure 10b.

Recently, Dijksma et al.[94] compared the use of chronoamperometry, as described by Berggren et al.,[27] and impedance measurements (at E_{dc} = +0.2 V, E_0 = 10 mV, and f = 113 Hz) for detection of interferon-γ (IFN-γ) on antibodies immobilized on a SAM of acetylcysteine. While the chronoamperometric results are rather poor, the impedance approach provides unsurpassed detection limits, as low as 0.02 fg mL^{-1} (~1 aM) IFN-γ.[94] Non-specifically adsorbed proteins are removed by injections of 100 mM KCl. SAMs can be formed reproducibly on electropolished gold electrodes, when a potential pulse method is used to remove the SAM with coupled antibodies from the electrode.[85]

From the results obtained by the different authors, it can be concluded that a low detection limit can only be obtained with sensing layers with a high capacitance (thin SAMs). The disadvantage is the relatively low stability, which means that much attention must be paid to the state of the gold and formation of the SAM. Injections of low salt concentrations, as described by Dijksma et al.,[85] can probably more generally be applied to reduce the contribution of nonspecific adsorption to the signal, which until now hindered general application of SAM-based immunosensors for measurement in real samples (e.g., plasma).

Besides SAMs also bilayer lipid membranes have been used for immunosensing.

BILAYER LIPID MEMBRANES

Bilayer lipid membranes (BLMs) have been used for immobilization of antibodies or antigens for electrochemical detection. BLMs are formed by adsorbing lipids on a hydrophobic SAM, or as a floating lipid-matrix at an air-electrolyte interface, which can be transferred to a solid support, leading to the more stable solid supported BLMs (s-BLMs).[95, 96]

In 1966, shortly after the first publications on BLMs, Del Castillo et al.[97] reported direct electrical detection of immunological reactions based on transient changes of electrical conductance in BLMs. In 1994 two further studies have been published.[98, 99]

Nikolelis et al.[100] deposited antibodies directly onto mixtures of phosphatidyl choline (PC) and dipalmitoyl phosphatidic acid (DPPA) at the air/water interface. Thyroxin was detected in the nM range by measuring differences in the transient-ion-current signal caused by dynamic changes in the electrostatic fields at the surface of the BLMs.[100]

Wang et al.[101] prepared s-BLMs with hepatitis B antigens from glycerol dioleate in squalene or from phospholipid, PC or lecithin in *n*-decane on freshly cut platinum or stainless steel or at the end of salt-bridge tubing, by immersing the material with adsorbed lipids in an aqueous solution containing antigen. Differences in R and C caused by interaction with antibodies are calculated from

CVs. A detection limit better than 1 ng mL^{-1} was found, in combination with a negligible amount of nonspecific adsorption.[101]

Filter-supported BLMs, that is, stabilized BLMs on microporous filtering (glass microfiber and polycarbonate) consisting of PC and DPPA, have been used in a flow injection immunoanalysis setup for detection in the nM range.[102] This sensor can be reused 5 times, and can easily be regenerated by recasting of the existing lipid/Ab film at the air-electrolyte interface to form fresh BLMs.

Hianik et al.[103, 104] studied the effect of addition of 2,4-dichlorophenoxyacetic acid to different antibody-modified membranes. s-BLMs have been formed on polymer coated stainless steel from 2% phospholipid solution in a mixture of *n*-decane and butanol and by immersion of a gold electrode modified with an octadecanethiol SAM into a 2% solution of phospholipids in *n*-hexane. Antibodies are modified with avidin and coupled to biotinylated phospholipids. Detection has been performed by measuring the impedance at $E_0 = 40$ mV and $f = 1$ kHz. With BLMs formed on stainless steel, a detection limit of 0.5 nM has been found, however with a poor reproducibility, while using BLMs formed on gold the detection limit was only 0.5 μM, but with a much better reproducibility. Additional information on the mechanism of interaction has been obtained from other measurement methods.[103, 104] With antibodies adsorbed directly to BLMs a detection limit of 5 μM is achieved. No contribution of nonspecific adsorption to the signal has been found.[103, 104]

CONCLUSIONS

Electrochemical immunosensors offer good possibilities for sensitive detection of unlabeled proteins. Much attention has been paid to reusability of these sensors. A problem in these sensors is the contribution of nonspecifically adsorbed proteins to the signal. Sometimes this contribution is disregarded, but also various methods to correct for the specificity of the signal have been described.

A method for detection of proteins without irreversibly binding, has been described by Sadik and co-workers. Detection limits in the μg mL^{-1} range have been accomplished, using pulsed amperometric detection of proteins with antibodies immobilized in polypyrrole. However, this method has not been used by others.

Direct immunosensors based on impedance measurements have been developed based on antibodies or antigens immobilized in or on silanized Si/SiO_2, silanized metal and polypyrrole. While with Si/SiO_2 a detectionlimit of 10 ng mL^{-1} is generally realizable, with silanized metal and polypyrrole detection limits around 0.5 ng mL^{-1} are reported. These sensors are regenerable with glycine hydrochloride pH 2.8.

With BLMs also detection in the ng mL^{-1} range is possible, this sensor can be reused 5 times, and regeneration is possible.

However, direct immunosensors based on SAMs are in fact the only ones able to detect much smaller concentrations. Using impedimetry even a detection of 20 ag mL^{-1} (~1 aM) is reported. Reduction of non-specific adsorption is accomplished by tuning the ionic strength. Therefore, this method offers good perspectives for measurement in real samples.

REFERENCES

1 Roitt, I.; Brostoff, J.; Male, D. *Immunology,* Gower Medical Publishing: London, England, **1985**.

2 Stryer, L. *Biochemistry,* 3rd Ed.; W.H. Freeman and Company: New York, **1988**.

3 Killard, A. J.; Deasy, B.; O'Kennedy, R.; Smyth, M. R. Antibodies: production, functions and applications in biosensors, *Trends Anal. Chem.* **1995**, *14*, 257-266.

4 Butler, J. E. E. *Immunochemistry of solid phase immunoassay,* CRC Press, Boca Raton, FL, USA: **1991**.

5 Sparreboom, A.; Rongen, H. A. H.; van Bennekom, W. P. Assays for interferons and interleukins in biological matrices, *Anal. Chim. Acta* **1994**, *295*, 1-26.

6 Rongen, H. A. H.; Hoetelmans, R. M. W.; Bult, A.; van Bennekom, W. P. Chemiluminescence and Immunoassays, *J. Pharm. Biomed. Appl.* **1994**, *12*, 433-462.

7 Gosling, J. P. Enzyme immunoassay, *Immunoassay* **1996**, 287-308.

8 Gosling, J. P. *Enzyme immunoassay: with and without separation*, in *Principles and practice of immunoassay*, 2nd [rev.] Ed., C. P. Price and D. J. Newman, Eds. **1997**, Stockton Press: London. p. 349, 351-388.

9 Porstmann, T.; Kiessig, S. T. Enzyme immunoassay techniques, *J. Immunol. Methods* **1992**, *150*, 5-21.

10 Tijssen, P. Principles of immunoassays. Enzymes, *Methods Immunol. Anal.* **1993**, *1*, 283-297.

11 Rongen, H. A. H.; Bult, A.; van Bennekom, W. P. Liposomes and immunoassays, *J. Immunol. Methods* **1997**, *204*, 105-133.

12 Byfield, M. P.; Abuknesha, A. Biochemical aspects of biosensors, *Biosens. Bioelectron.* **1994**, *9*, 373-400.

13 Rao, S. V.; Anderson, K. W.; Bachas, L. G. Oriented immobilization of proteins, *Mikrochim. Acta* **1998**, *128*, 127-143.

14 Scouten, W. H.; Luong, J. H. T.; Brown, R. S. Enzyme or protein immobilization techniques for applications in biosensor design, *Trends biotechnol.* **1995**, *13*, 178-185.

15 Taylor, R. F.; Marenchic, I. G.; Spencer, R. H. Antibody- and receptor-based biosensors for detection and process control, *Anal. Chim. Acta* **1991**, *249*, 67-70.

16 Homola, J.; Yee, S. S.; Gauglitz, G. Surface plasmon resonance sensors: review, *Sens. Actuators* **1999**, *B54*, 3-15.

17 Bunde, R. L.; Jarvi, E. J.; Rosentreter, J. J. Piezoelectric quartz crystal biosensors, *Talanta* **1998**, *46*, 1223-1236.

18 O'Sullivan, C. K.; Vaughan, R.; Guilbault, G. G. Piezoelectric immunosensors - Theory and applications, *Anal. Lett.* **1999**, *32*, 2353-2377.

19 Allen, S.; Chen, X.; Davies, J.; Davies, M. C.; Dawkes, A. C.; Edwards, J. C.; Roberts, C. J.; Sefton, J.; Tendler, S. J. B.; Williams, P. M. Detection of antigen-antibody binding events with the atomic force microscope, *Biochem.* **1997**, *36*, 7457-7463.

20 Perrin, A.; Lanet, V.; Theretz, A. Quantification of specific immunological reactions by atomic orce microscopy, *Langmuir* **1997**, *13*, 2557-2563.

21 Dong, Y.; Shannon, C. Heterogeneous immunosensing using antigen and antibody monolayers on gold surfaces with electrochemical and scanning probe detection, *Anal. Chem.* **2000**, *72*, 2371-2376.

22 Wittstock, G.; Yu, K.-j.; Halsall, H. B.; Ridgway, T. H.; Heineman, W. R. Imaging of immobilized antibody layers with scanning electrochemical microscopy, *Anal. Chem.* **1995**, *67*, 3578-3582.

23 Shiku, H.; Hara, Y.; Matsue, T.; Uchida, I.; Yamauchi, T. Dual immunoassay of human chorionic gonadotropin and human placental lactogen at a miocrofabricated substrate by scanning electrochemical microscopy, *J. Electroanal. Chem.* **1997**, *438*, 187-190.

24 Wijayawardhana, C. A.; Wittstock, G.; Halsall, H. B.; Heineman, W. R. Feature Articles - Electrochemical immunoassay with microscopic immunomagnetic bead domains and scanning electrochemical microscopy, *Electroanalysis* **2000**, *12*, 640-644.

25 Ghindilis, A. L.; Atanasov, P.; Wilkins, M.; Wilkins, E. Immunosensors: Electrochemical sensing and other engineering approaches, *Biosens. Bioelectron.* **1998**, *13*, 113-131.

26 Skládal, P. Advances in electrochemical immunosensors, *Electroanalysis* **1997**, *9*, 737-745.

27 Berggren, C.; Johansson, G. Capacitance measurements of antibody-antigen interactions in a flow system, *Anal. Chem.* **1997**, *69*, 3651-3657.

28 Liu, M.; Rechnitz, G. A.; Li, K.; Li, Q. X. Capacitive immunosensing of polycylic aromatic hydrocarbon and protein conjugates, *Anal. Lett.* **1998**, *31*, 2025-2038.

29 Knichel, M.; Heiduschka, P.; Beck, W.; Jung, G.; Göpel, W. Utilization of a self-assembled peptide monolayer for an impedimetric immunosensor, *Sens. Actuators* **1995**, *B28*, 85-94.

30 Rickert, J.; Göpel, W.; Beck, W.; Jung, G.; Heiduschka, P. A mixed self-assembled monolayer for an impedimetric immunosensor, *Biosens. Bioelectron.* **1996**, *11*, 757-768.

31 Bard, A. J.; Faulkner, L. R. *Electrochemical methods Fundamentals and Applications,* John Wiley & Sons Ltd: New York, USA **1980**.

32 Brett, C. M.; Oliveira Brett, A. M. *Electrochemistry, principles, methods and applications,* Oxford University Press, Inc.: New York, USA, **1993**.

33 Zoltowski, P. On the electrical capacitance of interfaces exhibiting constant phase element behaviour, *J. Electroanal. Chem.* **1998**, *443*, 149-154.

34 Chidsey, C. E. D.; Loiacono, D. N. Chemical functionality in self-assembled monolayers: structural and electrochemical properties, *Langmuir* **1990**, *6*, 682-691.

35 Cheng, Q.; Brajter-Toth, A. Permselectivity and high sensitivity at ultrathin monolayers. Effect of film hydrophobicity, *Anal. Chem.* **1995**, *67*, 2767-2775.

36 Yang, Z.; Gonzalez-Cortes, A.; Jourquin, G.; Viré, J.-C.; Kauffmann, J.-M.; Delplancke, J.-L. Analytical application of self assembled monolayers on gold electrodes: critical importance of surface pretreatment, *Biosens. Bioelectron.* **1995**, *10*, 789-795.

37 Finklea, H. O.; Avery, S.; Lynch, M. Blocking oriented monolayers of alkyl mercaptans on gold electrodes, *Langmuir* **1987**, *3*, 409-413.

38 Krysinski, P.; Brzostowska-Smolska, M. Three-probe voltammetric characterisation of octadecanethiol self-assembled monolayer integrity on gold electrodes, *J. Electroanal. Chem.* **1997**, *424*, 61-67.

39 Krysinski, P.; Brzostowska-Smolska, M. Capacitance characteristics of self-assembled monolayers on gold electrode, *Bioelectrochem. Bioenerg.* **1998**, *44*, 166-168.

40 Cheng, Q.; Brajter-Toth, A. Selectivity and sensitivity of self-assembled thioctic acid electrodes, *Anal. Chem.* **1992**, *64*, 1998-2000.

41 Cheng, Q.; Brajter-Toth, A. Permselectivity, sensitivity, and amperometric pH sensing at thioctic acid monolayer microelectrodes, *Anal. Chem.* **1996**, *68*, 4180-4185.

42 Swietlow, A.; Skoog, M.; Johansson, G. Double layer capacitance measurements of self-assembled layers on gold electrodes, *Electroanalysis* **1992**, *4*, 921-928.

43 Newman, A. L.; Hunter, K. W.; Stanbro, W. D. The capacitive affinity sensor: a new biosensor, *Proceedings of the 2nd meeting on chemical sensors, Bordeaux, France,* **1986**, 596-598.

44 John, R.; Spencer, M.; Wallace, G. G.; Smyth, M. R. Development of a polypyrrole-based human serum albumin sensor, *Anal. Chim. Acta* **1991**, *249*, 381-385.

45 Sadik, O. A.; Wallace, G. G. Pulsed amperometric detection of proteins using antibody containing conducting polymers, *Anal. Chim. Acta* **1993**, *279*, 209-212.

46 Sadik, O. A.; Wallace, G. G. Effect of polymer composition on the detection of electroinactive species using conductive polymers, *Electroanalysis* **1993**, *5*, 555-563.

47 Riviello, J. M.; Wallace, G.; Sadik, O. A. *Method and apparatus for pulsed electrochemical detection using polymer electroactive electrodes.* **1995** US Patent **5,403,451**.

48 Sadik, O. A.; John, M. J.; Wallace, G. G. Pulsed amperometric detection of thaumatin using antibody-containing poly(pyrrole) electrodes, *Analyst* **1994**, *119*, 1997-2000.

49 Barnett, D.; Laing, D. G.; Skopec, S.; Sadik, O. A.; Wallace, G. G. Determination of p-cresol (and other phenolics) using a conducting polymer based electro-immunological sensing system, *Anal. Lett.* **1994**, *27*, 2417-2429.

50 Lu, W.; Zhao, H.; Wallace, G. G. Pulsed electrochemical detection of proteins using conducting polymer based sensors, *Anal. Chim. Acta* **1995**, *315*, 27-33.

51 Sadik, O. A.; van Emon, J. M. Designing immunosensors for environmental monitoring, *Chemtech* **1997**, *june 1997*, 38-46.

52 Sadik, O. M.; van Emon, J. M. Applications of electrochemical immunosensors to environmental monitoring, *Biosens. Bioelectron.* **1996**, *11*, 1-11.

53 Sargent, A.; Loi, T.; Gal, S.; Sadik, O. A. The electrochemistry of antibody-modified conducting polymer electrodes, *J. Electroanal. Chem.* **1999**, *470*, 144-156.

54 Sargent, A.; Sadik, O. A. Monitoring antibody-antigen reactions at conducting polymer-based immunosensors using impedance spectroscopy, *Electrochim. Acta* **1999**, *44*, 4667-4675.

55 Sargent, A.; Sadik, O. A. Pulsed electrochemical technique for monitoring antibody-antigen reactions at interfaces, *Anal. Chim. Acta* **1998**, *376*, 125-131.

56 Brender, S.; Sadik, O. A.; van Emon, J. M. Direct Electrochemical Immunosensor for Polychlorinated Biphenyls, *Environ. Sci. Technol.* **1998**, *32*, 788-797.

57 Sadik, O. A. Bioaffinity sensors based on conducting polymers: A short review, *Electroanalysis* **1999**, *11*, 839-844.

58 Xu, H.; Masila, M.; Yan, F.; Sadik, O. A. Multiarray sensors for pesticides and toxic metals, *Proc. SPIE-Int. Soc. Opt. Eng.* **1999**, *3534*, 437-445.

59 Higson, S. P. J., Gibson, T. D. in preparation.

60 Bataillard, P.; Gardies, F.; Jaffrezic-Renault, N.; Martelet, C.; Colin, B.; Mandrand, B. Direct detection of immunospecies by capacitance measurements, *Anal. Chem.* **1988**, *60*, 2374-2379.

61 Gardies, F. M., C.; Colin, B.; Mandrand, B.; Feasibility of an immunosensor based upon capacitance measurements, *Sens. Actuators* **1989**, *17*, 461-464.

62 Billard, V.; Martelet, C.; Binder, P.; Therasse, J. Toxin detection using capacitance measurements on immunospecies grafted onto a semiconductor substrate, *Anal. Chim. Acta* **1991**, *249*, 367-372.

63 Saby, C.; Jaffrezic-Renault, N.; Martelet, C.; Colin, B.; Charles, M.-H.; Delair, T.; Mandrand, B. Immobilization of antibodies onto a capacitance silicon-based transducer, *Sens. Actuators* **1993**, *B15-16*, 458-462.

64 Souteyrand, E.; Martin, J. R.; Martelet, C. Direct detection of biomolecules by electrochemical impedance measurements, *Sens. Actuators* **1994**, *B20*, 63-69.

65 Maupas, H.; Saby, C.; Martelet, C.; Jaffrezic-Renault, N.; Soldatkin, A. P.; Charles, M.-H.; Delair, T.; Mandrand, B. Impedance analysis of Si/SiO_2 heterostructures grafted with antibodies: an approach for immunosensor development, *J. Electroanal. Chem.* **1996**, *406*, 53-58.

66 Jaffrezic-Renault, N.; Martelet, C. Semiconductor-based micro-biosensors, *Synmet* **1997**, *90*, 205-210.

67 Klein, M.; Kates, R.; Chucholowski, N.; Schmitt, M.; Lyden, C. Monitoring of antibody-antigen reactions with affinity sensors: Experiments and models, *Sens. Actuators* **1995**, *B27*, 474-476.

68 Berney, H.; Alderman, J.; Lane, W.; Collins, J. K. A differential capacitive biosensor using polyethylene glycol to overlay the biolayer, *Sens. Actuators* **1997**, *B44*, 578-584.

69 Berney, H.; Alderman, J.; Lane, W.; Collins, J. K. Development of a generic IC compatible silicon transducer for immunoreactions, *Sens. Actuators* **1999**, *B57*, 238-248.

70 Colin, B.; Mandrand, B.; Martelet, C.; Jaffrezic, N. *Method for detecting and/or identifying a biological substance in a liquid medium with the aid of electrical measurements, and apparatus for carrying out this method.* **1987** European Patent **EP0244326**.

71 Barraud, A.; Perrot, H.; Billard, V.; Martelet, C.; Therasse, J. Study of Immunoglobulin G thin layers obtained by the Langmuir-Blodgett method: application to immunosensors, *Biosens. Bioelectron.* **1993**, *8*, 39-48.

72 Schyberg, C.; Plossu, C.; Barbier, D.; Jaffrezic-Renault, N.; Martelet, C.; Maupas, H.; Souteyrand, E.; Charles, M.-H.; Delair, T.; Mandrand, B. Impedance analysis of Si/SiO_2 structures grafted with biomolecules for the elaboration of an immunosensor, *Sens. Actuators* **1995**, *B26-27*, 457-460.

73 Maupas, H.; Soldatikin, A. P.; Martelet, C.; Jaffrezic-Renault, N.; Mandrand, B. Direct immunosensing using differential electrochemical measurements of impedimetric variations, *J. Electroanal. Chem.* **1997**, *421*, 165-171.

74 Ameur, S.; Maupas, H.; Martelet, C.; Jaffrezic-Renault, N.; Ben Ouada, H.; Cosnier, S.; Labbe, P. Impedimetric measurements on polarized functionalized platinum electrodes: application to direct immunosensing, *Materials Science and Engineering* **1997**, *c5*, 111-119.

75 DeSilva, M. S.; Zhang, Y.; Hesketh, P. J.; Maclay, G. J.; Gendel, S. M.; Stetter, J. R. Impedance based sensing of the specific binding reaction between staphylococcus enterotoxin B and its antibody on an ultra-thin platinum film, *Biosens. Bioelectron.* **1995**, *10*, 675-682.

76 Feng, C.-D.; Ming, Y.-D.; Hesketh, P. J.; Gendel, S. M.; Stetter, J. R. Confirmation of immobilizing IgG on different surfaces with AFM and impedance investigations of a Pt electrode during the immobilization, *Sens. Actuators* **1996**, *B36*, 431-434.

77 Varlan, A. R.; Suls, J.; Sansen, W.; Veelaert, D.; De Loof, A. Capacitive sensor for the allatostatin direct immunoassay, *Sens. Actuators* **1997**, *B44*, 334-340.

78 Gebbert, A.; Alvarez-Icaza, M.; Stöcklein, W.; Schmid, R. D. Real-time monitoring of immunochemical interactions with a tantalium capacitance flow-through cell, *Anal. Chem.* **1992**, *64*, 997-1003.

79 Feng, C.; Xu, Y.; Song, L. Study on highly sensitive potentiometric IgG immunosensor, *Sens. Actuator* **2000**, *B66*, 190-192.

80 Stetter, J. R.; Hesketh, P. J.; Gendel, S. M.; MacLay, G. J. *Antibody covalently bound film immunobiosensor.* **1996** US Patent **5,567,301**.

81 Wink, T.; van Zuilen, S. J.; Bult, A.; van Bennekom, W. P. Self-assembled monolayers for biosensors (A tutorial review), *Analyst* **1997**, *122*, 43R-50R.

82 Finklea, H. O. In *Electroanalytical Chemistry*; Bard, A. J.; Rubinstein, I., Eds.; Marcel Dekker, inc.: New York, **1996**; Vol. 19, p. 110-318.

83 Hoogvliet, J. C.; Dijksma, M.; Kamp, B.; van Bennekom, W. P. Electrochemical pretreatment of gold electrode surfaces for molecular self-assembly: a study of bulk polycrystalline gold electrodes in phosphate buffer pH 7.4, *Anal. Chem.* **2000**, *72*, 2016-2021. (Chapter 2 of this Ph.D. thesis)

84 Ron, H.; Matlis, S.; Rubinstein, I. Self-assembled monolayers on oxidized metals. 2. Gold surface oxidative pretreatment, monolayer properties, and depression formation, *Langmuir* **1998**, *14*, 1116-1121.

85 Dijksma, M.; Kamp, B.; Hoogvliet, J. C.; van Bennekom, W. P. Formation and electrochemical characterization of self-assembled monolayers of thioctic acid on polycrystalline gold electrodes in phosphate buffer pH 7.4, *Langmuir* **2000**, *16*, 3852-3857. (Chapter 3 of this Ph.D. thesis)

86 Feng, J.; Zhu, L.; Ci, Y.-X.; Wang, X.-Y.; Guo, Z.-Q. A self-assembled antibody electrode for HT29 tumour cells, *Biotechnol. Appl. Biochem.* **1997**, *26*, 163-167.

87 Snejdarkova, M.; Csaderova, L.; Rehak, M.; Hianik, T. Amperometric immunosensor for direct detection of human IgG., *Electroanalysis* **2000**, *12*, 940-945.

88 Berggren, C.; Bjarnason, B.; Johansson, G. An immunological interleukin-6 capacitive biosensor using perturbation with a potentiostatic step, *Biosens. Bioelectron.* **1998**, *13*, 1061-1068.

89 Hintsche, R.; Paeschke, M.; Seitz, R. Direct electrical detection of affinity binding without labeling*, proc. Eurosensors X. 10th Eur. Conf. Solid-State Transducers, Leuven, Belgium,* **1996**, Vol 5, 1317-1319.

90 Taira, H.; Nakano, K.; Maeda, M.; Takagi, M. Electrode modification by long-chain, dialkyl disulfide reagent having terminal dinitrophenyl group and its application to impedimetric immunosensors, *Anal. Sci.* **1993**, *9*, 199-206.

91 Jie, M.; Ming, C. Y.; Jing, D.; Cheng, L. S.; Na, L. H.; Jun, F.; Xiang, C. Y. An electrochemical impedance immunoanalytical method for detecting immunological interaction of human mammary tumor associated glycoprotein and its monoclonal antibody, *Electrochem. Commun.* **1999**, *1*, 425-428.

92 Mirsky, V. M.; Riepl, M.; Wolfbeis, O. S. Capacitive monitoring of protein immobilization and antigen-antibody reactions on monomolecular alkythiol films on gold electrodes, *Biosens. Bioelectron.* **1997**, *12*, 977-990.

93 Ameur, S.; Martelet, C.; Jaffrezic-Renault, N.; Chovelon, J. M.; Plossu, C.; Barbier, D.; Ouada, H. B. Immunosensing using electrochemical impedance spectroscopy on functionalized gold electrodes, *Proc. - Electrochem. Soc.* **1997**, *97*, 1019-1023.

94 Dijksma, M.; Kamp, B.; Hoogvliet, J. C.; van Bennekom, W. P. Development of an electrochemical immunosensor for direct detection of interferon-γ at attomolar level, *Anal. Chem., accepted.* (Chapter 6 of this Ph.D. thesis)

95 Tien, H. T.; Ottova, A. L. Supported planar lipid bilayers (s-BLMs) as electrochemical biosensors, *Electrochim. Acta* **1998**, *43*, 3587-3610.

96 Nikolelis, D. P.; Hianik, T.; Krull, U. J. Biosensor based on thin lipid films and liposomes, *Electroanalysis* **1999**, *11*, 7-15.

97 Del Castillo, J.; Romero, A.; Sanchez, V. Lipid films as transducers for detection of antigen-antibody and enzyme-substrate reactions, *Science* **1966**, *153*, 185-188.

98 Mountz, J. D.; Tien, H. T. *Bioenerg. Biomembr.* **1984**, *10*, 139.

99 O'Boyle, K. P.; Siddiqi, F. A.; Tien, H. T. Antigen-antibody-complement reaction studies on micro bilayer lipid membranes, *Immunol. Commun.* **1984**, *13*, 85-103.

100 Nikolelis, D. P.; Tzanelis, M. G.; Krull, U. J. Direct electrochemical transduction of an immunological reaction by bilayer lipid membranes, *Anal. Chim. Acta* **1993**, *282*, 527-534.

101 Wang, L.-G.; Li, Y.-H.; Tien, H. T. Electrochemical transduction of an immunological reaction via s-BLMs, *Bioelectrochem. Bioenerg.* **1995**, *36*, 145-147.

102 Nikolelis, D. P.; Siontorou, C. G.; Andreou, V. G.; Viras, K. G.; Krull, U. J. Bilayer lipid membranes as electrochemical detectors for flow injection immunoanalysis, *Electroanalysis* **1995**, *7*, 1082-1089.

103 Hianik, T.; Passechnik, V. I.; Sokolikova, L.; Snejdarkova, M.; Sivak, B.; Fajkus, M.; Ivanov, S. A.; Franek, M. Affinity biosensors based on solid supported lipid membranes. Their structure, physical properties and dynamics, *Bioelectrochem. Bioenerg.* **1998**, *47*, 47-55.

104 Hianik, T.; Snejdarkova, M.; Sokolikova, L.; Meszar, E.; Krivanek, R.; Tvarozek, V.; Novotny, I.; Wang, J. Immunosensors based on supported lipid membranes, protein films and liposomes modified by antibodies., *Sens. Actuators* **1999**, *B57*, 201-212.

2

Electrochemical Pretreatment of Polycrystalline Gold Electrodes To Produce a Reproducible Surface Roughness for Self-Assembly: A Study in Phosphate Buffer pH 7.4

ABSTRACT

It has been emphasized in several studies that the state of the surface, including the surface roughness, is very important for the reproducible formation of high-quality self-assembled monolayers on gold. The pulsed-potential pretreatment procedure described in this paper can, in a reproducible way, reduce the surface roughness of mechanically polished polycrystalline gold electrodes by a factor 2. The developed procedure, in which the gold is alternately oxidized and reduced, has been optimized for use in a flow system (100 mM phosphate buffer pH 7.4). The influence of the pretreatment procedure on the surface roughness of the electrodes has been studied by in-situ oxygen adsorption measurements using cyclic voltammetry. The most effective pulse regime in producing a gold surface with a reproducible and relatively low surface roughness is a triple-potential pulse waveform, with potentials of +1.6, 0.0, and −0.8 V versus SCE and pulse widths of 100 ms for each potential. Prolonged pulsing for 2000 - 5000 s with the gold working electrode in a flow-through cell showed an electropolishing effect, i.e., a decrease of the roughness in time. Flow conditions are very important: the roughness decreased faster at higher flow rates, while an increase was observed without flow. A process of reconstruction and dissolution of gold during application of the potential pulses under flow conditions is assumed to account for the observed phenomena.

Slightly modified version of J.C. Hoogvliet, M. Dijksma, B. Kamp and W.P. van Bennekom, *Anal. Chem.* **2000**, 72(9), 2016–2021.

INTRODUCTION

Gold is a suitable substrate for the formation of self-assembled monolayers (SAMs) from thiols, sulfides, and disulfides. These SAMs can be used as intermediate layers for the coupling of a wide range of molecules, including enzymes and antibodies.[1, 2] Apart from the use of gold in electrochemistry, relatively new methodologies like surface plasmon resonance (SPR),[3] and quartz crystal microbalance (QCM)[4] mainly employ gold films as substrate. Both techniques can relatively easily be combined with electrochemical techniques (ESPR and EQCM, respectively).

As recently pointed out in the literature,[5-11] and in accordance with our own experiences with SAM formation for affinity biosensors,[12] the properties of the gold substrate - among them the surface roughness - play an important role in their overall performance. In a comparative study between vacuum-deposited thin-film and bulk polycrystalline gold electrodes as substrates for SAMs, Creager et al.[5] showed that microscopic roughness and the presence of crystal grain boundaries can have a pronounced effect on the density of defects in SAMs. Furthermore, they showed that chemical etching of bulk poly-crystalline gold with aqua regia can greatly reduce this microscopic surface roughness. Reproducible formation and stability of the monolayer systems are also dependent on the pretreatment of the gold surface, which often is applied, prior to the assembly process itself. Adsorbed impurities on the gold surface may hinder electrochemical processes and the formation of SAMs. It is mainly for these reasons that a number of mechanical,[7, 10] thermal,[13] chemical,[5, 11, 14-19] and/or electrochemical[20-22] pretreatment procedures has been described in the literature. Each of these procedures is applied shortly before (electrochemical) measurements or derivatization steps are carried out, in view of the reactive nature of the cleaned gold surface. Most (electro)chemical procedures share a common step, i.e., an oxidative treatment to decompose and remove adsorbed material, and to form a hydrophilic layer of gold oxides on the surface. Chemical oxidation with piranha acid (a mixture of concentrated H_2SO_4 and H_2O_2)[16, 17] and treatment in an oxygen plasma[18, 19] or with ozone[11, 18] are frequently applied. In some procedures a thin layer of gold is removed by the action of aqua regia.[5, 15] After oxidation, a subsequent reduction of the formed gold oxide has been reported to be necessary to obtain SAMs with a good quality. This can easily be performed by, for instance, ethanol.[8, 18]

Apart from the chemical treatments, the gold electrodes can also be pretreated electrochemically. Cycling the electrode potential between limits at which the gold surface is oxidized and reduced has been described and has proven to be effective in the removal of (adsorbed) impurities.[20-22] Bulk gold electrodes are often pretreated by polishing, which by itself has a considerable influence on the formation and characteristics of SAMs and, therefore, has to be followed by one of the above described treatments.[7, 10, 12]

For our work on affinity biosensors based on SAMs, a method to obtain SAMs with high stability and reproducible characteristics is required. Therefore, we searched for a pretreatment procedure that produces a reproducible, clean electrode surface and which is preferably suitable for on-line use in the same flow system as used for subsequent derivatizations and measurements. This cannot be achieved by mechanically polishing but was obtained after a pulsed-potential pretreatment, carried out in the flow, in a phosphate buffer of pH 7.4. A similar potential pulse regime, but at much higher pH values, has been in use for some time in the pulsed amperometric detection of carbohydrates, amines, and sulfur-containing substances at gold electrodes in liquid chromatography.[23] Using alternate detection with subsequent oxidative cleaning and reactivation of the electrode surface, electrode fouling associated with anodic oxidation of organic compounds at gold electrodes is prevented.

The potential-pulse regime was used by us as a pretreatment procedure with a double action: cleaning the electrode surface from any adsorbed impurities (including a previously formed SAM) and producing a reproducible surface roughness.

EXPERIMENTAL SECTION

Materials and reagents

All chemicals, unless mentioned otherwise, were of analytical grade and were used as received. All aqueous solutions were made with demineralized water. Phosphate buffer (100 mM, pH 7.4) was made by mixing 100 mM solutions of disodium hydrogen phosphate and sodium dihydrogen phosphate (Merck).

Hexacyanoferrate(II/III) solutions, used in the impedance measurements, consisted of phosphate buffer pH 7.4 with 2 mM of both hexacyanoferrate(II) and hexacyanoferrate(III) (Fluka, Buchs, Switzerland).

Electrochemical measurement system

Gold electrodes have been made by press-fitting a 1.00 mm diameter rod of pure gold (99.99%, Engelhard-Clal/Drijfhout, Amsterdam) into a Kel-F holder. The geometric surface area of these electrodes is 0.785 mm^2.

The gold working electrodes were used in a flow system, consisting of a LDP-5 precision piston pump (BHS-Labotron) and a confined wall-jet electrochemical flow-through cell. Details of this homemade flow cell, equipped with a saturated calomel reference electrode (SCE) and a glassy carbon auxiliary electrode, have been described previously.[24] In the current study the distance between working and auxiliary electrodes was 100 μm. Cyclic voltammetry and multiple-pulse amperometry were performed with an Autolab PGSTAT10 digital potentiostat/galvanostat, using GPES 4.5 software for electrochemical

measurements (Eco Chemie BV, Utrecht, The Netherlands). All potentials mentioned are with reference to SCE.

Pretreatment of the gold electrodes

Before each new series of measurements, the gold electrodes were polished during 30 min with Gamma micropolish B deagglomerated alumina suspension, 0.05 μm (Buehler, Lake Bluff, IL, USA) on Alphacloth (MetPrep, Coventry, U.K.), using a Metaserve grinder/polisher (Buehler, Coventry, U.K.). After being polished, the electrodes were sonicated in Milli-Q water during 15 min. Subsequently, an electrochemical pretreatment was applied.

The gold electrodes were electrochemically pretreated using a sequence of potential pulses. Several potential-pulse regimes have been investigated. A triple-potential pulse sequence with potentials and times of E_a V, 100 ms; 0.0 V, 100 ms; and E_c V, 100 ms was applied continuously during 100, 300, 1000, or 5000 s. The anodic pulse potential E_a was either +1.6 or +1.2 V. The cathodic potential E_c was 0.0, −0.3, −0.6 or −0.8 V. The last potential value in the sequence (before the cell was switched off) was always E_c.

RESULTS AND DISCUSSION

Determination of the surface roughness

For the determination of the surface roughness of electrodes, a number of methods has been reviewed by Trasatti and Petrii.[25] Because we wished to investigate the influence of the different pretreatments on the surface roughness of the gold electrodes in real-time, ex-situ methods (BET, X-ray diffraction, microscopy) could not be used. Therefore, oxygen adsorption measurement was chosen as a simple in-situ method to obtain an indication for the microscopic surface area. The method comprises oxygen chemisorption onto the gold surface in an anodic potential scan. The oxide coverage is dependent on the crystallographic orientation, anodic potential limit, and anodization time but is generally assumed to be reproducible if the same procedure is used under the same conditions. The amount of surface oxide formed can be measured by integration of the gold oxide reduction peak in a cathodic scan (Figure 1).

Usually, calculations of the real surface area, commonly expressed as a roughness factor, are based on the assumption that a monolayer of chemisorbed oxygen, with a gold:oxygen ratio of 1:1 has been formed. The current minimum that follows the gold oxidation peak in the voltammogram is usually taken as an indication that a monolayer coverage is reached.[26] The exact value of the corresponding charge required for the reduction of this monolayer depends on the composition of the exposed crystalline planes. A value of about 400 μC cm^{-2} has been mentioned in the review of Trasatti and Petrii[25] for polycrystalline gold. Oesch and Janata used a calculation of the mean surface concentration of gold

atoms based on density and atomic weight of gold, which leads to a value of 482 μ cm^{-2} for a monolayer of chemisorbed oxygen on polycrystalline gold.[26] Although oxygen adsorption measurement appears to be a somewhat arbitrary procedure to determine the real surface area, it has found widespread use.[25-31]

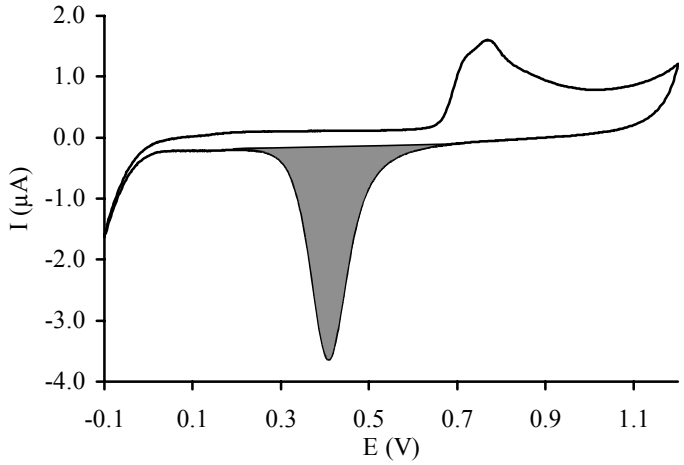

Figure 1. Determination of the surface roughness of a gold electrode by integration of the gold oxide reduction peak in the cyclic voltammogram. Phosphate buffer pH 7.4, volume flow rate 0.1 mL min^{-1}, potential scan rate 50 mV s^{-1}.

The procedure used by us was developed and optimized for 100 mM phosphate buffer pH 7.4, and consisted of two CV scans between –0.1 and +1.2 V at a scan rate of 50 mV s^{-1}. A typical example is shown in Figure 1. Oxide formation starts at +0.65 V, the current reaches a maximum at +0.75 V and a minimum at +1.0 V. Repeatedly scanning (50 CVs) in this potential range did not significantly change the area under the gold oxide reduction peak with respect to the charge measured in the second scan. The area under the gold oxide stripping peak in the second scan (oxide stripping charge Q_{AuO}, expressed in mC cm^{-2} of geometric surface area) was taken as a measure for the microscopic surface area, and thus as an indication for the surface roughness. In our study, the oxide stripping charge Q_{AuO}, as an indication for the surface roughness, is only used for comparative purposes. Additionally, a roughness factor, assuming 482 μC cm^{-2}, is given in Figures 2 - 5. This parameter is included, since it is frequently used in the literature to express surface roughness.

The measurements were automated using a facility of the GPES software package. A pulse sequence was continuously applied during a fixed period (indicated throughout this paper as the *pulse sequence duration*). Subsequently, two CVs were recorded, the area under the gold oxide stripping peak in the second scan was determined using the automatic peak search option, and the results were stored on disk. This procedure of alternated pulsing and scanning was repeated for

a predetermined number of cycles. The phrase *total pulse time* is used throughout this paper, and defined as the number of cycles multiplied by the pulse sequence duration. This automated process enabled us to measure under reproducible conditions during prolonged times.

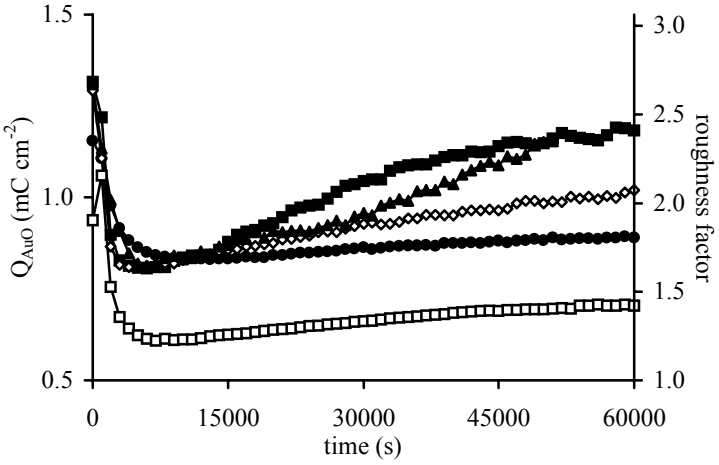

Figure 2. Influence of potential-pulse regime on the surface roughness of a gold electrode as a function of total pulse time. ●: +1.6/0.0/0.0 V; ■: +1.6/0.0/-0.3 V; ◊: +1.6/0.0/-0.6 V; □: +1.6/0.0/-0.8 V; ▲: +1.2/0.0/-0.8 V. Pulse sequence duration was 1000 s. Phosphate buffer pH 7.4, volume flow rate 0.1 mL min^{-1}. Q_{AuO}: oxide stripping charge.

The surface roughness as a function of electrode pretreatment

The gold electrodes were polished, washed and sonicated prior to (a series of) further pretreatments. Before any other further treatment, the oxide stripping charge was determined as described above.

A number of electrochemical pretreatment procedures, consisting of alternate pulsing to anodic and cathodic potentials, has been investigated. For phosphate buffer pH 7.4, the pulse regime of +1.6/0.0/–0.8 V, each potential applied during 100 ms, turned out to be the most effective one in producing a reproducible electrode surface area, with a relatively low roughness. The mean and standard deviation for a freshly polished electrode, before the application of the pulsed potential treatment, were determined as 1.17 ± 0.14 mC cm^{-2} (n = 5). After an electrochemical pretreatment of this electrode at a flow rate of 0.1 mL min^{-1}, mean and standard deviation of the oxide stripping charge at its minimum value, after ca. 6000 s of total pulse time, were 0.62 ± 0.01 mC cm^{-2} (n = 5). Both mean and standard deviation are significantly reduced compared with the corresponding data obtained in the same measurement series before the pulse treatment started. The final choice of the anodic and cathodic pulse potentials was based on the following considerations and observations. An anodic potential of +1.6 V is well beyond the onset of gold oxide formation in this medium. Decreasing the anodic pulse

potential from +1.6 to +1.2 V was still effective, but resulted in a higher minimum in the roughness, and a faster increase of roughness at prolonged pulse time (t > 10,000 s; Figure 2). The value of the cathodic potential in the triple-potential pulse regime was varied between 0.0 and –0.8 V. The lowest roughness, the least increase of the roughness at prolonged pulsing, and the best reproducibility were obtained with a cathodic pulse to –0.8 V.

Pulse sequences of only one anodic and one cathodic potential, omitting the potential of 0.0 V in between, were also investigated, but the results were inferior to those of the triple-potential pulse regimes (Figure 3). Higher values for the minimum in the roughness, and both a faster onset of the increase, and a larger absolute increase in roughness as a function of total pulse time were observed.

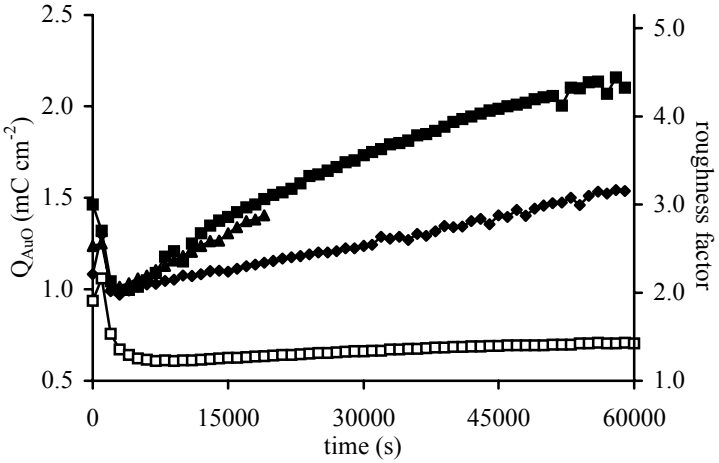

Figure 3. Comparison between the influence of a double- and triple-potential pulse regime on the surface roughness of a gold electrode as a function of total pulse time. Double-potential pulse: ■: +1.6/-0.3 V; ◆: +1.6/-0.6 V; ▲: +1.6/-0.8 V. Triple-potential pulse: □: +1.6/0.0/-0.8 V. Pulse sequence duration was 1000 s. Phosphate buffer pH 7.4, volume flow rate 0.1 mL min^{-1}. Q_{AuO}: oxide stripping charge.

Figure 4 shows the surface roughness resulting from the application of the optimum pulse regime as a function of total pulse time. Each data point in the graphs represents the recording of two CVs. The pulse sequence duration has been varied between 100 and 5000 s. After about 5000 s, the four curves of oxide stripping charge versus time, with pulse sequence durations of 100, 300, 1000, and 5000 s, tend to coincide. This is in agreement with our observation mentioned above, that during repeatedly scanning of the potential between –0.1 and +1.2 V no significant change was noticed in the charge required to reduce the formed gold oxides. Therefore, we conclude that there is no significant effect on the surface roughness by the measuring procedure itself (CV scans), compared to the effect of the potential pulse regime. It is also clear that this pretreatment yields a

reproducible roughness within about 5000 s at a volume flow rate of 0.1 mL min^{-1}, independent of the surface roughness of the freshly polished electrode at the start of the electrochemical pretreatment.

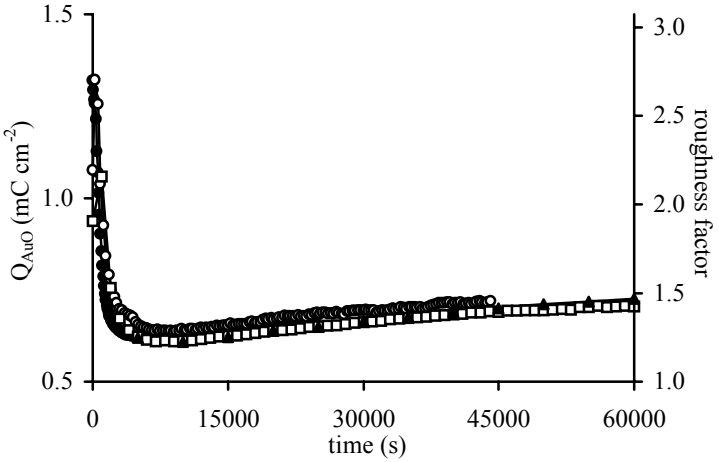

Figure 4. Change in surface roughness of a gold electrode as a function of total pulse time for a potential-pulse regime of +1.6/0.0/-0.8 V. Pulse sequence durations of ●: 100; ○: 300; □: 1000; ▲: 5000 s were used. Phosphate buffer pH 7.4, volume flow rate 0.1 mL min^{-1}. Q_{AuO}: oxide stripping charge.

Figures 2 - 5 show the electropolishing effect of this type of electrochemical pretreatment. Within the first 5000 s the oxide stripping charge decreases to a minimum value of about 0.6 mC cm^{-2}. Prolonged pulsing during another 55,000 s gradually increases the surface roughness again. To achieve this electropolishing effect, maintaining a flow of the solution along the electrode surface during the pretreatment is very important, as can be seen in Figure 5. At high flow rates, the minimum roughness is reached in a shorter time compared to low flow rates. In static solutions (no flow), there is no indication of an electropolishing effect. On the contrary, there is a relatively rapid increase in surface roughness, which is also visible as a reddish-brown colouring of the electrode surface.

The observed phenomena can be explained by reconstruction and dissolution of gold. Evidence for changes in surface topography of noble metal electrodes caused by electrochemical treatments in non-complexing electrolytes has been found already a long time ago (see Woods[20] and references therein). Both roughening and smoothing have been reported. More recently, potential-induced reconstructions have been revealed in extenso by STM (see, for instance, the review articles by Kolb,[32] Gewirth and Niece,[33] Li and Wang,[34] and by Moffat).[35]

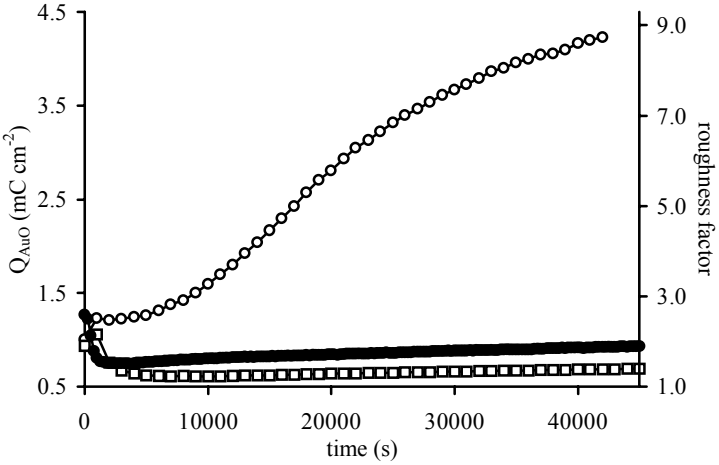

Figure 5. Influence of volume flow rate on the surface roughness of a gold electrode as a function of total pulse time for a potential-pulse regime of +1.6/0.0/-0.8 V in phosphate buffer pH 7.4. ○: 0.0 mL min^{-1} (pulse sequence duration 1000 s), □: 0.1 mL min^{-1} (pulse sequence duration 1000 s), and ●: 1.0 mL min^{-1} (pulse sequence duration 250 s). Q_{AuO}: oxide stripping charge.

Oxidative-reductive potential cycling has intentionally been used to increase the surface area of gold for surface-enhanced Raman spectroscopy (SERS).[36] A square-wave potential perturbation has been used by Chialvo et al. as a method to obtain a reproducible, controlled roughness and electrochemical response for platinum, gold, and rhodium electrodes.[37] A dissolution-redeposition mechanism for the roughening of platinum electrodes on potential cycling in 1 M H_2SO_4 has been proposed by Untereker and Bruckenstein.[38] The possibility of gold dissolution at low pH under electrochemical conditions has been proven with rotating ring-disk electrode experiments by Cadle and Bruckenstein.[28] The quantity of dissolved gold was found to increase with rotation speed. Recently, Rocklin et al. described rotating ring-disk experiments in alkalic solutions, in which they observed the same phenomena.[39] In general, optimum conditions for electropolishing are achieved under mass-transport control.[40]

It is beyond the scope of our study to determine the exact role of the phosphate anion in the gold dissolution process. Recently, Silva and Martins described the effect of the anions perchlorate, nitrate, sulphate, and phosphate on the electrochemically induced surface reconstruction of gold single crystals.[41] Phosphate showed the highest specific adsorption. It was concluded that in the presence of multi-bonded oxoanions like sulphate and phosphate, sufficient mobility of surface atoms is only achieved after desorption of those anions. An anion-enhanced mobility of gold atoms - the effect being larger, the more positive the potential and/or the stronger the anion-gold interaction - has been suggested to be the basis of electrochemical annealing.[32] It can be expected, therefore, that

specific adsorption of phosphate anions ($H_2PO_4^-$ and HPO_4^{2-}) may play an important role in the oxidation and dissolution process of gold.

CONCLUSIONS

Our results indicate, that the microscopic roughness of polycrystalline gold electrodes can be decreased compared with the roughness of mechanically polished electrodes, by a factor 2, using a triple-potential pulse regime in a flow system, in phosphate buffered media at pH 7.4. More importantly, it also appears to be possible to generate a reproducible microscopic surface area. This is of importance for the reproducible formation of stable SAMs with controlled characteristics.

The observed electropolishing effect is probably caused by reconstruction and dissolution of the gold surface under the influence of the alternating oxidizing and reducing potentials, in combination with the hydrodynamic conditions. A minimum time during which the pulse regime is applied is necessary to achieve the lowest roughness. This time is dependent on the flow conditions used. At higher flow rates, the minimum roughness is achieved faster than at lower flow rates (after 2000 s at 1.0 mL min^{-1} versus 5000 s at 0.1 mL min^{-1}, in our confined wall-jet configuration). This observation, and the fact that without flow, there is no electropolishing effect at all, can be explained by the transport of dissolved gold under the influence of the flow of buffer, away from the electrode surface, before redeposition as metallic gold at a reducing potential can occur.

ACKNOWLEDGMENT

This work has been supported by grant UFA44.3392 from the Dutch Technology Foundation STW. We thank Hans Vonk (Instrumental Service Department, Faculty of Pharmacy) for the construction of the gold electrodes.

REFERENCES

1 Finklea, H. O. In *Electroanalytical Chemistry. A Series of Advances*; Bard, A. J; .Rubinstein, I., Eds.; Marcel Dekker, Inc.: New York, Basel, 1996; Vol. 19, p. 110-318.
2 Wink, T.; van Zuilen, S. J.; Bult, A.; van Bennekom, W. P. Self-assembled monolayers for biosensors (A tutorial review), *Analyst* **1997**, *122*, 43R-50R.
3 Homola, J.; Yee, S. S.; Gauglitz, G. Surface plasmon resonance sensors: review, *Sens. Actuators* **1999**, *B54*, 3-15.
4 Bunde, R. L.; Jarvi, E. J.; Rosentreter, J. J. Piezoelectric quartz crystal biosensors, *Talanta* **1998**, *46*, 1223-1236.
5 Creager, S. E.; Hocket, L. A.; Rowe, G. K. Consequences of microscopic surface roughness for molecular self-assembly, *Langmuir* **1992**, *8*, 854-861.
6 Guo, L.-H.; Facci, J. S.; McLendon, G.; Mosher, R. Effect of gold topography and surface pretreatment on the self-assembly of alkanethiol monolayers, *Langmuir* **1994**, *10*, 4588-4593.
7 Yang, Z.; Gonzalez-Cortes, A.; Jourquin, G.; Viré, J.-C.; Kauffmann, J.-M.; Delplancke, J.-L. Analytical application of self assembled monolayers on gold electrodes: critical importance of surface pretreatment, *Biosens. Bioelectron.* **1995**, *10*, 789-795.

8 Ron, H.; Rubinstein, I. Self-assembled monolayers on oxidized metals. 3. Alkylthiol and dialkyl disulfide assembly on gold under electrochemical conditions, *J. Am. Chem. Soc.* **1998**, *120*, 13444-13452.

9 Lee, M. T.; Hsueh, C. C.; Freund, M. S.; Ferguson, G. S. Air oxidation of self-assembled monolayers on polycrystalline gold: The role of the gold substrate, *Langmuir* **1998**, *14*, 6419-6423.

10 Subramanian, R.; Lakshminarayanan, V. Effect of surface roughness on the self-assembly of octadecanethiol monolayer onto polycrystalline noble metal surfaces, *Curr. Sci.* **1999**, *76*, 665-669.

11 Tsuneda, S.; Ishida, T.; Nishida, N.; Hara, M.; Sasabe, H.; Knoll, W. Tailoring of a smooth polycrystalline gold surface as a suitable anchoring site for a self-assembled monolayer, *Thin Solid Films* **1999**, *339*, 142-147.

12 Dijksma, M.; Kamp, B.; Hoogvliet, J. C.; van Bennekom, W. P. Formation and electrochemical characterization of self-assembled monolayers of thioctic acid on polycrystalline gold electrodes: a study in phosphate buffer pH 7.4, *Langmuir* **2000**, *16*, 3852-3857. (Chapter 3 of this Ph.D. thesis)

13 Clavilier, J.; Scetlicic, V.; Zutic, V. Thionine self-assembly on polyoriented gold and sulphur-modified gold electrodes, *J. Electroanal. Chem.* **1995**, *386*, 157-163.

14 Ye, S.; Haba, T.; Sato, Y.; Shimazu, K.; Uosaki, K. Coverage dependent behavior of redox reaction induced structure change and mass transport at an 11-ferrocenyl-1-undecanethiol self-assembled monolayer on a gold electrode studied by an in situ IRRAS-EQCM combined system, *Phys. Chem. Chem. Phys.* **1999**, *1*, 3653-3659.

15 Cheng, Q.; Brajter-Toth, A. Permselectivity, sensitivity, and amperometric pH sensing at thioctic acid monolayer microelectrodes, *Anal. Chem.* **1996**, *68*, 4180-4185.

16 Creager, S. E.; Clarke, J. Contact-angle titrations of mixed w-mercaptoalkanoic acid/alkanethiol monolayers on gold. Reactive vs nonreactive spreading, and chain length effects on surface pKa values, *Langmuir* **1994**, *10*, 3675-3683.

17 Dahint, R.; Bender, F.; Morhard, F. Operation of acoustic plate mode immunosensors in complex biological media, *Anal. Chem.* **1999**, *71*, 3150-3156.

18 Ron, H.; Matlis, S.; Rubinstein, I. Self-assembled monolayers on oxidized metals. 2. gold surface oxidative pretreatment, monolayer properties, and depression formation, *Langmuir* **1998**, *14*, 1116-1121.

19 Beulen, M. W. J.; Kastenberg, M. I.; Veggel, F. C. J. M. v.; Reinhoudt, D. N. Electrochemical stability of self-assembled monolayers on gold, *Langmuir* **1998**, *14*, 7463-7467.

20 Woods, R. In *Electroanalytical Chemistry. A Series of Advances*; Bard, A. J., Eds.; Marcel Dekker, Inc.: New York, Basel, **1976**; Vol. 9, p. 24-27.

21 Fruböse, C.; Doblhofer, K. In situ quartz microbalance study of the self assembly and stability of aliphatic thiols on polarized gold electrodes, *J. Chem. Soc., Faraday Trans.* **1995**, *91*, 1949-1953.

22 Janek, R. P.; Fawcett, W. R.; Ulman, A. Impedance spectroscopy of self-assembled monolayers on Au(III): Evidence for complex double-layer structure in aqueous $NaClO_4$ at the potential of zero charge, *J. Phys. Chem.* **1997**, *B101*, 8550-8558.

23 Johnson, D. C.; Dobberpuhl, D.; Roberts, R.; Vandeberg, P. Pulsed amperometric detection of carbohydrates, amines and sulfur species in ion chromatography - the current state of research, *J. Chromatogr.* **1993**, *640*, 79-96.

24 Dalhuijsen, A. J.; van der Meer, T. H.; Hoogendoorn, C. J.; Hoogvliet, J. C.; van Bennekom, W. P. Hydrodynamic properties and mass transfer characteristics of electrochemical flow-through cells of the confined wall-jet type, *J. Electroanal. Chem.* **1985**, *182*, 295-313.

25 Trasatti, S.; Petrii, O. A. Real surface area measurements in electrochemistry, *Pure & Appl. Chem.* **1991**, *63*, 711-734.

26 Oesch, U.; Janata, J. Electrochemical study of gold electrodes with anodic oxide films. I. Formation and reduction behaviour of anodic oxides on gold., *Electrochim. Acta* **1983**, *28*, 1237-1246.

27 Brummer, S. B.; Makrides, A. C. Surface oxidation of gold electrodes, *J. Electrochem. Soc.* **1964**, *111*, 1122-1128.

28 Cadle, S. H.; Bruckenstein, S. Ring-disk electrode study of the anodic behavior of gold in 0.2 M sulfuric acid, *Anal. Chem.* **1974**, *46*, 16-20.

29 Woods, R. In *Electroanalytical Chemistry. A Series of Advances*; Bard, A. J., Eds.; Marcel Dekker, Inc.: New York, Basel, **1976**; Vol. 9, p. 119-125.

30 Gordon, J. S.; Johnson, D. C. Application of an electrochemical quartz crystal microbalance to a study of water adsorption at gold surfaces in acidic media, *J. Electroanal. Chem.* **1994**, *365*, 267-274.

31 Juodkazis, K.; Juodkazyt, J.; Juodiene, T.; Lukinskas, A. Determination of Au(III) in the surface layers formed anodically on the gold electrode, *J. Electroanal. Chem.* **1998**, *441*, 19-24.

32 Kolb, D. M. Reconstruction phenomena at metal-electrolyte interfaces, *Prog. Surf. Sci.* **1996**, *51*, 109-173.

33 Gewirth, A. A.; Niece, B. K. Electrochemical applications of in situ scanning probe microscopy, *Chem. Rev.* **1997**, *97*, 1129-1162.

34 Li, J.; Wang, E. Scanning tunneling microscopy characterization of electrode materials in electrochemistry, *Electroanalysis* **1996**, *8*, 107-112.

35 Moffat, T. P. In *Electroanalytical Chemistry. A Series of Advances*; Bard, A. J.Rubinstein, I., Eds.; Marcel Dekker, Inc.: New York, Basel, **1999**; Vol. 21, p. 211-316.

36 Pemberton, J. E. In *Electrochemical interfaces: modern techniques for in-situ interface characterization.*; Abruna, H. D., Eds.; VCH Publishers, Inc.: New York, Weinheim, Cambridge, **1991**; Vol. p. 195-256.

37 Chialvo, A. C.; Triaca, W. E.; Arvia, A. J. Changes in the electrochemical response of noble metals produces by square-wave potential perturbations. A new technique for the preparation of reproducible electrode surfaces of interest in electrocatalysis, *J. Electroanal. Chem.* **1983**, *146*, 93-108.

38 Untereker, D. F.; Bruckenstein, S. A dissolution-redeposition mechanism for the roughening of platinum electrodes by cyclic potential programs, *J. Electrochem. Soc.* **1974**, *121*, 360-362.

39 Rocklin, R. D.; Clarke, A. P.; Weitzhandler, M. Improved long-term reproducibility for pulsed amperometric detection of carbohydrated via a new quadruple-potential waveform, *Anal. Chem.* **1998**, *70*, 1496-1501.

40 Landolt, D. Review article. Fundamental aspects of electropolishing, *Electrochim. Acta* **1987**, *32*, 1-11.

41 Silva, F.; Martins, A. Surface reconstruction of gold single crystals: electrochemical evidence of the effect of adsorbed anions and the influence of steps and terraces, *Electrochim. Acta* **1998**, *44*, 919-929.

3

Formation and Electrochemical Characterization of Self-Assembled Monolayers of Thioctic Acid on Polycrystalline Gold Electrodes in Phosphate Buffer pH 7.4

ABSTRACT

Formation of self-assembled monolayers (SAMs) of thioctic acid (TA) on polycrystalline gold electrodes has been investigated. The Au electrodes are polished, first mechanically and subsequently electrochemically, until the roughness of the surface is minimal. The best TA SAMs are formed onto these electropolished electrodes from stirred solutions, while a potential $E = 0.0$ V or $E = +0.2$ V versus saturated calomel reference electrode (SCE) is applied during the adsorption process. Impedance methods are used to monitor the formation of the SAMs and to characterize these. Potentiostatically formed TA SAMs have better characteristics than those formed at open circuit. The TA SAMs are stable in 100 mM phosphate buffer pH 7.4, and when protected from light, also in buffered 2 mM hexacyanoferrate(II/III) solution. However, when the hexacyanoferrate(II/III) solutions are exposed to light, the TA SAMs are not stable. Probably, damaging of the SAM proceeds via etching of the gold surface by photochemically released cyanide ions. Using potential pulses (+1.6, 0.0, -0.8 V versus SCE, each 0.1 s) for 15 min in the flow (0.5 mL min^{-1}), the TA SAM can be removed completely, recovering the initial state of the gold electrode, as deduced from potential-step experiments. This way TA SAMs can be formed and removed repeatedly and reproducibly on a single electrode.

Slightly modified version of M. Dijksma, B. Kamp, J.C. Hoogvliet, and W.P. van Bennekom, *Langmuir* **2000**, 16(8), 3852–3857.

INTRODUCTION

In immunosensors, typically, the interaction of a protein (the antigen, Ag) and an immobilized antibody (Ab) or antibody fragment is recorded. A variety of devices has been reported, on the basis of optical, for example, surface plasmon resonance (SPR),[1] piezoelectrical, e.g., quartz crystal microbalance (QCM)[2, 3] or electrochemical methods.[4-6] For electrochemical immunosensors many approaches and strategies are exploited. Considering only those in which none of the reaction partners is labeled, the Ab-Ag interaction is directly measured, for example, using alternating current (ac) impedance methods, which can be performed in a faradaic (i.e., in the presence of a redox probe) or in a non-faradaic mode.[7-12] In the non-faradaic mode also potential-step[13, 14] and pulsed amperometric[15-17] detection methods have been reported. Both impedance and potential-step methods provide information on the resistance (*R*) and capacitance (*C*) of the sensor, from which the amount of antigen in the sample can be calculated.

In our research on electrochemical immunosensors, antibodies are attached to gold electrodes via self-assembled monolayers (SAMs) using activation of the carboxyl group of ω-mercaptoalkanoic acids with 1-ethyl-3-[3-(dimethyl-amino)propyl]carbodiimide hydrochloride and *N*-hydroxysulfo-succinimide.[7, 18, 19] With longer-chain alkanethiols (i.e., ω-mercaptohexa-decanoic acid) more stable SAMs are obtained.[7] The detection limits of these immunosensors are about 15 nM,[7] whereas with shorter-chain alkanethiols thioctic acid (TA, 1,2-dithiolane-3-pentanoic acid) and cysteamine detection limits of about 15 fM have been reported.[13, 14] It can therefore be concluded that SAMs of short-chain alkanethiols offer the best possibilities for development of sensitive immunosensors. This conclusion is supported by our own experience (see Chapters 5 and 6).

The process of SAM formation has been studied in real time with SPR,[20, 21] QCM,[22-26] atomic force microscopy (AFM),[27, 28] and scanning tunneling microscopy[29] methods. Fruböse and Doblhofer[26] studied formation of octadecane-thiol SAMs from ethanolic solutions both with QCM and impedance methods. From QCM measurements it was clear that the monolayer forms very fast. From impedance measurements a subsequent ordering was observed. Xu et al.[28] examined the mechanism and kinetics of self-assembly in solution using AFM imaging. A stepwise process for the formation of the SAM was revealed, including a structural phase transition. Thiols self-assemble onto gold surfaces initially in a lying-down phase, which subsequently rearranges to a standing-up phase. According to Fenter et al.[30] a lying-down phase is observed at low coverage and a standing-up phase at high coverage. As far as we know, only investigations of adsorption of long-chain thiols from organic solvents have been published, with the exception of Hu and Bard,[27] who studied adsorption of mercaptoundecanoic acid from aqueous solutions (pH 10.2).

Frequently, electrodes are pretreated by annealing or vapor deposition of a fresh gold layer before formation of a SAM. Ron et al.[31] describe formation of

reproducible SAMs of octadecanethiol by cleaning the electrode using a two-step procedure. First the Au surface is exposed to UV/ozone (or O_2 plasma) treatment, to oxidize organic contaminants, then the electrode is immersed in pure ethanol to reduce the gold oxide formed during the first step. Removal of gold oxides is important, because they can cause distortion of the SAM layer.[31, 32] A possibly simpler method to remove SAMs is the application of potential pulses, because SAMs are only stable in a limited potential range, depending on the kind of molecules used.[33-35]

SAMs of long-chain alkanethiols are stabilized by intermolecular Van der Waals forces. SAMs of short-chain cyclic disulfides, like TA, are therefore less stable. However, hydrogen bonding has been proposed to increase the stability of SAMs of mercaptoalkanoic acids.[36] TA SAMs have been used to assemble enzymes on electrodes.[37, 38]

For formation of stable SAMs both structure and state of the gold surface are very important. Cheng and Brajter-Toth[39] found that TA SAMs formed on aqua regia etched gold have a higher permselectivity than those formed on polished gold. Guo et al.[15] investigated the effect of gold topography and surface pretreatment on the self-assembly of alkanethiol monolayers. We recently developed a method to achieve a reproducible surface roughness of mechanically polished polycrystalline gold electrodes by prolonged treatment with potential pulses in the flow.[40]

In regenerable immunosensors the Ab-Ag complex is dissociated by the use of chaotropic reagents.[41, 42] However, this treatment is reported to damage SAMs [13, 43] or to cause a decrease in sensitivity of the sensor.[9, 44] Removal of the SAM together with antibody and antigen followed by formation of a new sensing layer is another way to achieve regenerability. An important condition for this is the reproducibility of SAM formation and coupling of the antibody.

The formation from aqueous environment (pH 7.4) and characterization of TA SAMs on electropolished Au electrodes will be described using impedance methods. The TA SAMs can be removed at pH 7.4 by application of a sequence of potential pulses to the electrode. Because of the observed limited stability of TA SAMs in solutions containing hexacyanoferrate(II/III), etching of the gold layer by this redox probe has been investigated.

EXPERIMENTAL SECTION

Chemicals

All chemicals were of analytical grade and used as received, unless mentioned otherwise. Phosphate buffer pH 7.4 was prepared by mixing 0.1 M solutions of Na_2HPO_4 and NaH_2PO_4 (both from Merck, Darmstadt, Germany).

Hexacyanoferrate(II/III) solution consisted of phosphate buffer pH 7.4 with 2 mM of both $K_3Fe(CN)_6$ and $K_4Fe(CN)_6$ (Fluka, Buchs, Switzerland).

DL-6,8-thioctic acid (> 99%) was purchased from Sigma (St. Louis, MO, USA). All water used was demineralized.

Mechanical pretreatment of electrodes

The working electrodes consist of a gold wire (99.99%, Engelhard-Clal, Amsterdam, The Netherlands) with a diameter of 1.00 mm (geometric surface area of 0.785 mm^2) and are press-fitted in Kel-F. They are polished during 30 min with Gamma micropolish B deagglomerated alumina suspension (0.05 μm, Buehler, Lake Bluff, IL, USA), using a Metaserve automatic polisher (Buehler, Coventry, U.K.), with polishing cloth Alphacloth (Metprep, Coventry, U.K.). Finally the electrodes are cleaned ultrasonically in water for 15 min.

Electrochemical equipment

For electrochemical measurements a confined wall-jet flow-through cell is used, with a saturated calomel reference electrode (SCE) and a glassy carbon disc auxiliary electrode.[45] All potentials are versus SCE. The flow system further consisted of an HPLC pump (LKB 2150, Bromma, Sweden) and PEEK capillaries.

For potential pulses, cyclic voltammetry (CV), and potential-step measurements an Autolab PGSTAT10 digital potentiostat/galvanostat with an ADC750 module was used with GPES 4.5 software (Eco Chemie, Utrecht, The Netherlands). For impedance measurements, a FRA module with software version 2.30 (Eco Chemie) was used.

Electrochemical methods

After polishing, the electrodes were pretreated by application of triple-pulse sequences (+1.6, 0.0, –0.8 V, each 0.1 s) for 30-120 min.[40] Potential pulses, CV and potential-step measurements on the electrode were performed in phosphate buffer (pH 7.4). Impedance measurements of SAM formation have been performed in batch, in phosphate buffer containing 50 mM TA, at an applied potential (E_{dc}) of 0.0 V, with a superimposed sinusoidal potential with an amplitude (E_0) of 10 mV, at a range of frequencies from 1 kHz to 0.5 Hz.

SAMs are characterized in buffered hexacyanoferrate(II/III) solution, with a flow rate of 0.1 mL min^{-1}, by measuring the impedance as a function of the frequency of the alternating potential (f = 1 kHz - 10 mHz) at a constant potential of +0.2 V.

Measurements of impedance in time have been performed in buffer at E_{dc} = 0.0 or +0.2 V, and in hexacyanoferrate(II/III) solutions at E_{dc} = +0.2 V. The real (Z') and imaginary (Z'') component of the impedance Z are plotted against time.

Measurement of the current due to application of a potential step from 0 to 50 mV (versus SCE) in buffer has been used to characterize the gold surface.

Investigation of etching of gold by hexacyanoferrate

Etching of gold by hexacyanoferrate(II/III) solutions was investigated using SPR disks, that is, thin film gold layers (about 50 nm) vapor-deposited over a titanium underlayer of 2 nm on glass (Eco Chemie, Utrecht, The Netherlands).

The thickness of the gold layer is determined by spectrophotometric transmission measurements at 550 nm using a double-beam spectrophotometer (Hitachi 100-60, Tokyo, Japan).

Formation and Removal of SAMs

SAMs were formed on potential-pulse pretreated electrodes from 50 mM solutions of DL-6,8-thioctic acid in 100 mM phosphate buffer pH 7.4 at room temperature by adsorption at open circuit or at an applied potential $E = 0.0$ V or $E = +0.2$ V.

The formation of SAMs has been monitored by impedance measurements (see Electrochemical methods).

SAMs were removed from the electrodes in 100 mM phosphate buffer pH 7.4 by application of potential pulses (+1.6, 0.0, -0.8 V versus SCE, each 0.1 s) for 15 min in the flow (flow rate 0.5 mL min^{-1}).

RESULTS AND DISCUSSION

Initially, the polished gold electrodes were further pretreated by application of potential pulses for 1000 s under flow conditions followed by the formation of TA SAMs at open circuit.[39, 46-51] These SAMs were characterized with impedance methods in buffered hexacyanoferrate(II/III) solution. In Figure 1 typical Nyquist plots are shown, indicating the large variability in characteristics.

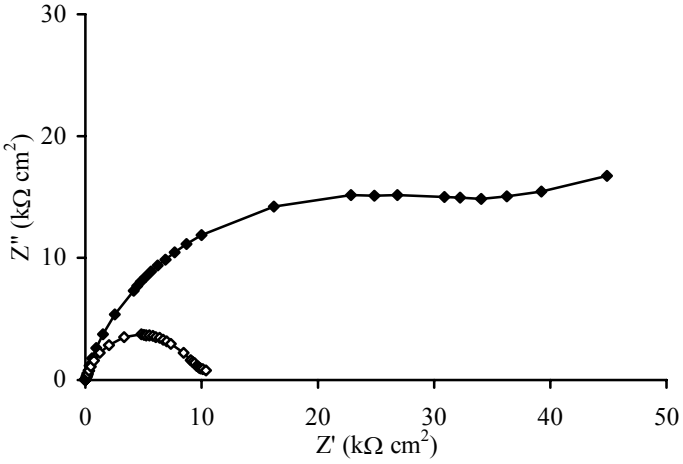

Figure 1. Typical Nyquist plots of TA SAMs in a hexacyanoferrate(II/III) solution after electrode treatment by mechanical polishing, ultrasonic cleaning and application of potential pulses during 1000 s, flow rate 0.1 mL min^{-1} (SAM 1: ♦, SAM 2: ◊). Z' is the real and Z'' the imaginary component of the impedance Z.

The characteristics of the SAMs in Figure 1 are very different, despite the fact that the procedures are identical. Generally, a larger semi-circle indicates a larger charge-transfer resistance (R_{ct}) in combination with a lower capacitance. R_{ct} can be derived roughly from the intersection of the semi-circle with the Z'-axis.[52] It is assumed that irreproducibility is mainly caused by differences in smoothness of the electrode surface.[39, 53]

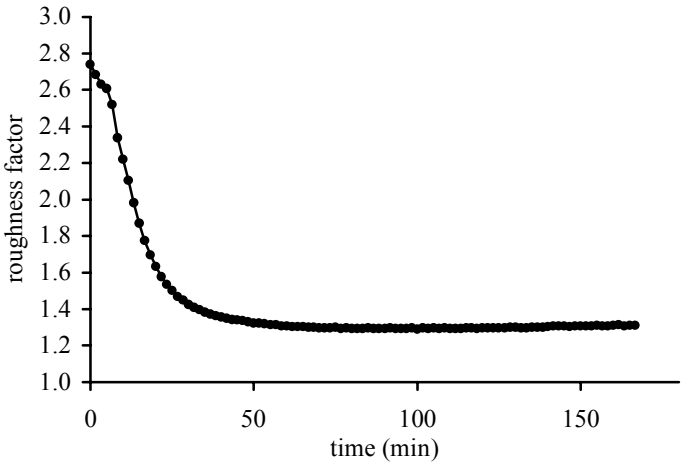

Figure 2. Typical plot of the roughness factor as a function of time during application of potential pulses (see text), measured every 100 s in phosphate buffer pH 7.4, flow rate 0.1 mL min^{-1} [40]

To find the origin of the variability, the influence of the time and potentials of the pulse treatment on the surface roughness has been investigated. The results are described in Chapter 2.[40] In Figure 2 the roughness factor (i.e., the ratio of apparent and geometric area) as a function of time is indicated during application of potential pulses. The apparent area has been determined from the gold oxide stripping peak of the second cyclic voltammetric scan from –0.1 to 1.2 V, 50 mV/s.[40, 54] An optimum pretreatment procedure was found by application of the potential pulse sequence +1.6, 0.0, –0.8 V, each 0.1 s, under flow conditions, during 30 – 120 min. With this method a smooth surface and an almost constant surface roughness is obtained.

As can be observed from Figure 2, 1000-s pulse time was not sufficient to obtain an optimal smooth surface. It can be concluded that our minor reproducibility in SAM formation can indeed arise from differences in the surface area of the electrode. Therefore, from this time on, electrodes are pretreated by potential pulses until a minimum surface roughness is reached.[40] Better characteristics for SAM formation on these electrodes are assumed.

Formation and characterization of TA SAMs

To obtain information on SAM formation, impedance measurements have been performed during this process, which imply the application of a potential to the electrode. $E = 0.0$ V has been used, because it has been observed that the open circuit potential (OCP) of an electrode with TA SAM in this solution is close to this potential. In Figure 3 the real (Z') and the imaginary (Z'') component of the impedance against time are shown, obtained at a modulation frequency of 1 kHz, in batch and without stirring.

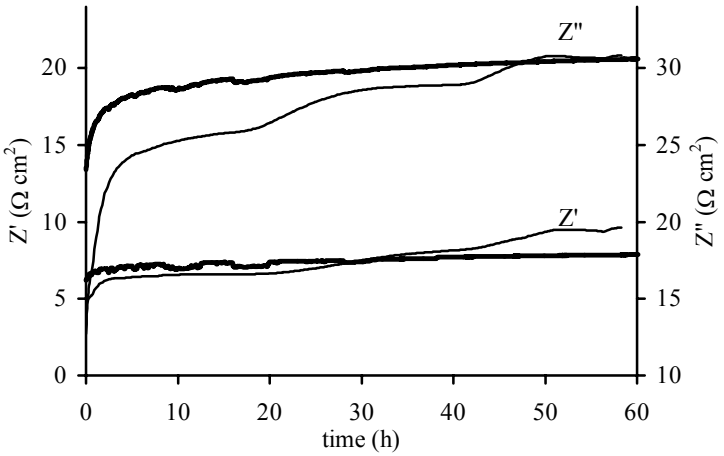

Figure 3. Real (Z') and imaginary (Z'') component of the impedance Z as a function of time during SAM formation from a 50 mM TA solution in 100 mM phosphate buffer pH 7.4 at $E = 0.0$ V and $E_0 = 10$ mV ($f = 1$ kHz) in batch, with (thick line) and without (thin line) stirring, at a constant temperature of 22.0°C.

During formation, an increase of Z' and Z'' has been observed, which can be related to both increasing amounts of TA immobilized on the surface and reorganisation. The same pattern has been observed at lower frequencies. Stirring causes the process to proceed more gently. According to Figure 3 the only difference between stirring and non-stirring is the smoothness of the process, the final results are almost identical. However, the formation time has a stronger influence on the characteristics of the SAM formed in unstirred solutions, as shown in Figure 4.

It is not possible to fit these Nyquist plots by a commonly used equivalent circuit like those shown in Chapter 1, Figures 4 and 10. However, both the real and the imaginary part of the impedance increase in time, which is assumed to arise from an increase in the mean thickness of the monolayer (i.e., decreasing amount of pin-holes), caused by rearrangement of the molecules.

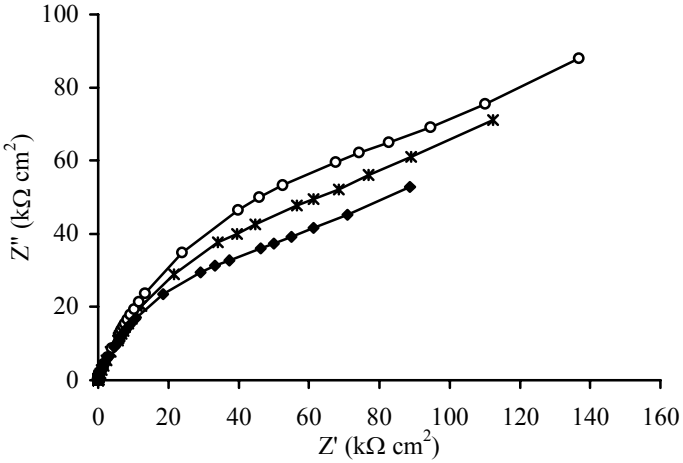

Figure 4. Typical Nyquist plots of TA SAMs formed in 17 (♦), 22 (∗), and 60 (o) h, without stirring, measured in hexacyanoferrate(II/III) solution in flow (0.01 mL min^{-1}) at E = +0.2 V and E_0 = 10 mV, f = 1 kHz – 10 mHz.

Stability

SAMs formed on electropolished Au electrodes are stable in phosphate buffer during at least 18 h, but less stable in hexacyanoferrate(II/III) solution. Krysinski and Brzostowska-Smolska[48] also reported irreversible changes in the monolayer capacitance after characterization with hexacyanoferrate(II/III) solutions. The rate of deterioration in quality depends on the initial characteristics of the SAM, that is, the amount and size of the pin-holes. We assume that damaging of the monolayer proceeds by etching of the substrate.

Therefore, the stability in buffer and hexacyanoferrate(II/III) solutions of thin (50 nm) gold layers on glass (with 2-nm titanium adhesion layer) was tested by measuring the thickness of the gold layer spectrophotometrically (λ = 550 nm). In buffer no significant etching takes place in 24 h, whereas in hexacyanoferrate(II/III) after 6 h the thickness has been diminished to 37 nm, as shown in Figure 5.

However, when the solution is protected from light, no etching effect is observed. The etching effect is probably caused by cyanide ions, which can be formed easily from displacement of one CN^- in the hexacyanoferrate(III) complex by a H_2O molecule by exposure to light.[55, 56] We found that etching of gold by hexacyanoferrate(II/III) is not limited to high pHs,[57] but also takes place in phosphate buffer pH 7.4. We assume that these results, obtained with thin gold layers, can be extrapolated to the polycrystalline gold electrodes used in immunosensors. This is emphasized because SAMs are stable in hexacyanoferrate(II/III) until the solution is exposed to light, as shown in Figures 6 and 7.

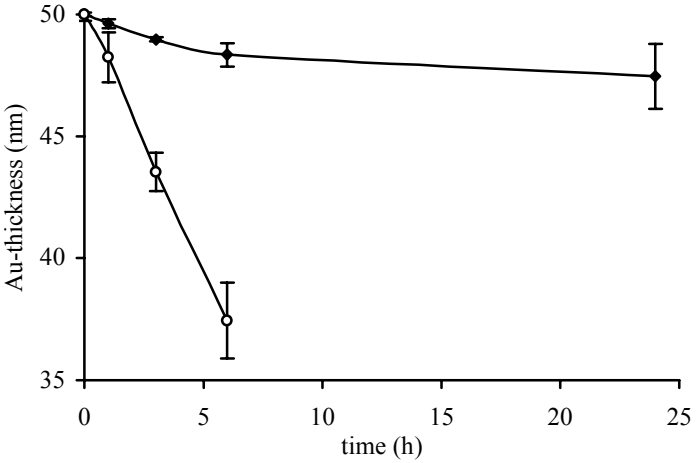

Figure 5. Thickness of a thin gold layer (50 nm) on glass as a function of time in phosphate buffer pH 7.4 (♦) and buffered hexacyanoferrate(II/III) solution (o), calculated from VIS (λ = 550 nm) measurements (n = 2).

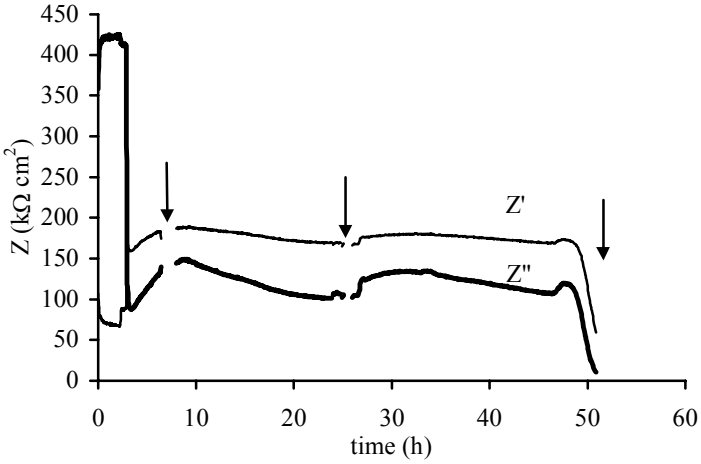

Figure 6. Real (Z') and imaginary (Z'') component of the impedance Z (f = 50 mHz; E = +0.2 V) of a TA SAM measured in phosphate buffer pH 7.4 for 2 h, in hexacyanoferrate(II/III) in the dark for 46 h, followed by exposure of the solution to light, flow rate 0.1 mL min^{-1}. At the times indicated by arrows, frequency scans have been recorded which are shown in Figure 7.

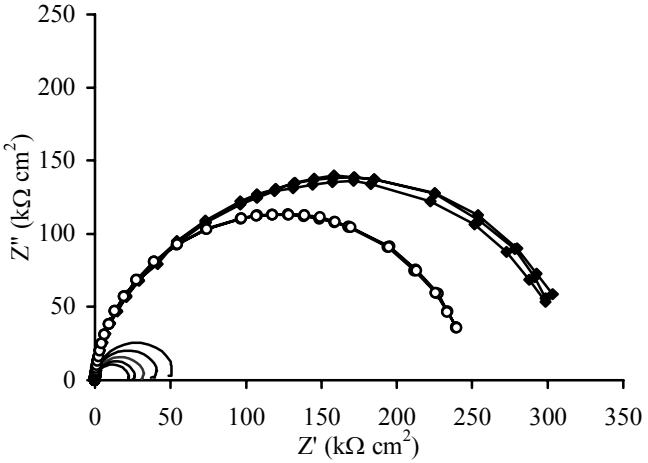

Figure 7. Influence of light on the long-term stability of a TA SAM in buffered hexacyanoferrate(II/III) solution. 3 successive scans have been measured after 6 h (♦) and after 25 h (o) in the dark (see Figure 6). After exposure of the solution to light, i.e., after 46 h, 5 successive scans have been measured (unmarked). Flow rate 0.1 mL min^{-1}, E = +0.2 V, E_0 = 10 mV, f = 1 kHz – 10 mHz.

Repeated removal and formation

The Ab-Ag complex can be dissociated by using chaotropic reagents: solutions with a low pH or a high ionic strength (or both). For electrochemical immuno-sensors based on SAMs, no suitable regeneration procedure has been published as far as we know. Damaging of the SAM by chaotropic reagents[13, 43] and irreversible adsorption of denatured proteins to the SAM[41, 42] have been reported.

When sensors can be formed reproducibly, regeneration can also be done by removal of the SAM with antibody and antigen still attached. TA SAMs can be removed by applying a series of potential pulses. For complete regeneration about 15 min of potential pulses (+1.6, 0.0, -0.8 V, each 0.1 s) are applied in a flow of 0.5 mL min^{-1}.

An indication of the cleanliness of the gold after removal of a SAM from an electrode can be obtained from impedance measurements. However, the results are influenced by rapid contamination of the gold. Fast characterization can be performed by measuring the impedance at a single frequency. However, more information can be obtained in a short time from potential-step experiments, where the current due to application of a potential step from 0 to 50 mV (versus SCE) in buffer is measured during the first few milliseconds. From Figure 8 it can be observed that the curves of the cleaned gold electrode before SAM formation and after SAM removal by potential pulses are almost exactly identical. Therefore, we conclude that the SAM is completely removed by this potential-pulse procedure in the flow.

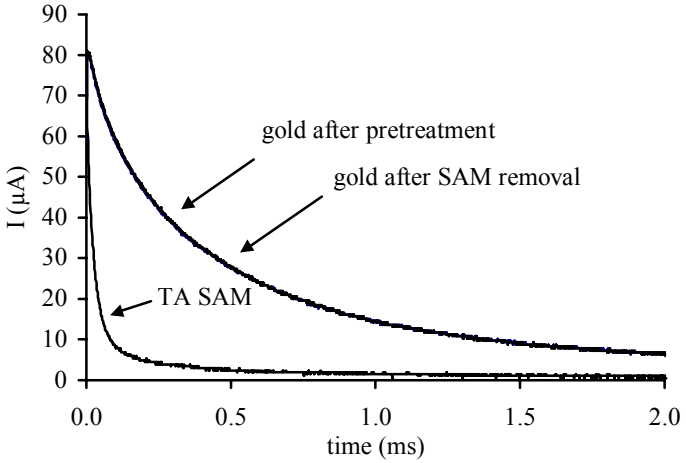

Figure 8. Characterization of gold electrodes with a potential step from 0 to 50 mV (versus SCE) in phosphate buffer pH 7.4. Clean gold response before the SAM formation, response when a TA SAM is deposited, and the response after removal of this SAM returning to the clean gold state.

In Figure 9 the Nyquist plots of TA SAMs formed successively on the same electrode at 0.0 V without stirring are shown. From this figure, it can be concluded that TA SAMs can be formed reproducibly.

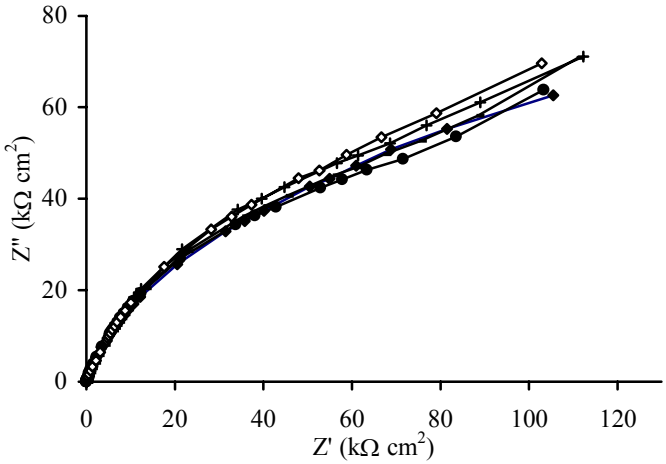

Figure 9. Nyquist plots of TA SAMs formed from 50 mM TA in batch during 22 h (at $E = 0.0$ V without stirring) on a gold electrode after removal of the previous SAM by potential pulses (see text), measured in hexacyanoferrate(II/III) solution in the flow (0.01 mL min^{-1}) at $E = +0.2$ V and $E_0 = 10$ mV, $f = 1$ kHz – 10 mHz.

However, as can be concluded from some additional measurements, the cleaning method used in this study is not generally applicable. It is found that gold that is contaminated during storage overnight can not fully be cleaned this way, and SAMs of long-chain alkanethiols (e.g., dodecanethiol) can only be partly removed from the electrode. Although some of the dodecanethiol is removed during potential-pulse treatment, the response expected from a completely clean surface is not reached within 1 h.

Influence of applied potential during SAM formation

Apart from the pulsed-potential treatment of the electrode and stirring, also the applied potential during formation influences the characteristics of the SAM. The SAMs shown in Figure 9 are formed at $E = 0.0$ V. SAMs formed overnight at 0.0 V have a higher R and lower C than SAMs formed at open circuit, and have also a better stability. In Figure 10 a typical course of the impedance in time ($f = 50$ mHz) is shown of a SAM formed at open circuit.

A possible explanation for this difference is the presence of gold oxides after potential-pulse treatment. By application of a potential of 0.0 V to the electrode these oxides are electrochemically reduced. Gold oxides can be encapsulated under the SAM, which may result in distortion of the monolayers.[58] However, although no gold oxides could be detected with stripping voltammetry[32] on pulsed-potential pretreated electrodes, the possibility of another mechanism must be considered.

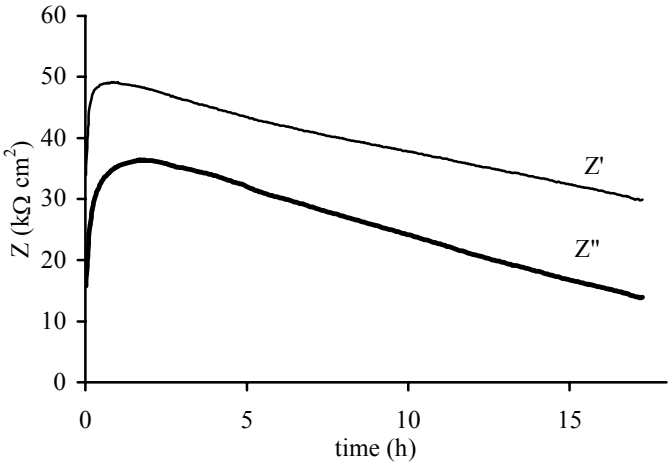

Figure 10. Real (Z') and imaginary (Z'') component of the impedance Z ($f = 50$ mHz) of a TA SAM formed at open circuit, measured in a hexacyanoferrate(II/III) solution in the dark at $E = +0.2$ V and $E_0 = 10$ mV ($f = 50$ mHz) in the flow (0.1 mL min^{-1}).

Because the OCP of an electrode with a SAM is about 0.0 V, the difference in characteristics of the SAMs is expected to arise from the initial adsorption of the molecules to the gold surface.

An even higher R and lower C have been observed at +0.2 V compared with 0.0 V. Apparently the mechanism of TA SAM formation is influenced by the potential of the substrate. We assume that SAM formation occurs more ordered when the disulfide groups of TA are attracted directly to the gold, by means of a combination of dipolar attraction and attraction between sulfur and gold. At open circuit first a disordered monolayer is formed that slowly rearranges to an ordered monolayer. Formation of SAMs at OCP has been found to proceed in different steps and it has been observed that the sulfur usually is not directed to the gold during the first adsorption step.[28, 30] Another possible explanation can be found in reconstruction of the gold surface.[59]

CONCLUSIONS

The best TA SAMs are formed when the Au electrode is first mechanically and subsequently electrochemically polished, until the roughness of the surface is minimal, and when a potential $E = 0.0$ V or $E = +0.2$ V is applied during the adsorption process. Impedance methods are used to monitor the formation and to characterize the SAMs. In stirred solutions the formation develops more gradually than in static solutions. Potentiostatically formed SAMs have better characteristics than these formed at open circuit.

The SAMs are stable in 100 mM phosphate buffer pH 7.4 and when protected from light in buffered 2 mM hexacyanoferrate(II/III) solution. However, when exposed to light, the TA SAMs are not stable in the hexacyanoferrate(II/III) solutions. Probably, damaging of the SAM proceeds via etching of the gold surface by photochemically released cyanide ions.

Using potential pulses (+1.6, 0.0, -0.8 V, each 0.1 s) for 15 min in the flow, the SAM can be removed completely, recovering the initial state of the gold electrode, as deduced from potential-step experiments. This way SAMs can be formed and removed repeatedly and reproducibly on a single electrode.

ACKNOWLEDGMENT

This work has been supported by grant UFA44.3392 from the Dutch Technology Foundation STW. We acknowledge the Instrumental Service Department, Faculty of Pharmacy, for the skillfull construction of the gold electrodes.

REFERENCES

1 Homola, J.; Yee, S. S.; Gauglitz, G. Surface plasmon resonance sensors: review, *Sens. Actuators* **1999**, *B54*, 3-15.

2 Bunde, R. L.; Jarvi, E. J.; Rosentreter, J. J. Piezoelectric quartz crystal biosensors, *Talanta* **1998**, *46*, 1223-1236.

3 Ben-Dov, I.; Willner, I. Piezoelectric immunosensors for urine specimens of *Chlamidia trachomatis* employing quartz crystal microbalance microgravimetric analysis, *Anal. Chem.* **1997**, *69*, 3506-3512.

4 Gizeli, E.; Lowe, C. R. Immunosensors, *Curr. Opin. Biotechnol.* **1996**, *7*, 66-71.

5 Ghindilis, A. L.; Atanasov, P.; Wilkins, M.; Wilkins, E. Immunosensors: Electrochemical sensing and other engineering approaches, *Biosens. Bioelectron.* **1998**, *13*, 113-131.

6 Blonder, R.; Levi, S.; Tao, G. L.; Bendov, I.; Willner, I. Development of amperometric and microgravimetric immunosensors and reversible immunosensors using antigen and photoisomerizable antigen monolayer electrodes, *J. Am. Chem. Soc.* **1997**, *119*, 10467-10478.

7 Mirsky, V. M.; Riepl, M.; Wolfbeis, O. S. Capacitive monitoring of protein immobilization and antigen-antibody reactions on monomolecular alkythiol films on gold electrodes, *Biosens. Bioelectron.* **1997**, *12*, 977-990.

8 Taira, H.; Nakano, K.; Maeda, M.; Takagi, M. Electrode modification by long-chain, dialkyl disulfide reagent having terminal dinitrophenyl group and its application to impedimetric immunosensors, *Anal. Sci.* **1993**, *9*, 199-206.

9 Rickert, J.; Göpel, W.; Beck, W.; Jung, G.; Heiduschka, P. A mixed self-assembled monolayer for an impedimetric immunosensor, *Biosens. Bioelectron.* **1996**, *11*, 757-768.

10 Souteyrand, E.; Martin, J. R.; Martelet, C. Direct detection of biomolecules by electrochemical impedance measurements, *Sens. Actuators* **1994**, *B20*, 63-69.

11 Saby, C.; Jaffrezic-Renault, N.; Martelet, C.; Colin, B.; Charles, M.-H.; Delair, T.; Mandrand, B. Immobilization of antibodies onto a capacitance silicon-based transducer, *Sens. Actuators* **1993**, *B15-16*, 458-462.

12 Patolsky, F.; Filanovsky, B.; Katz, E.; Willner, I. Photoswitchable antigen-antibody interactions studied by impedance spectroscopy, *J. Phys. Chem.* **1998**, *B102*, 10359-10367.

13 Berggren, C.; Johansson, G. Capacitance measurements of antibody-antigen interactions in a flow system, *Anal. Chem.* **1997**, *69*, 3651-3657.

14 Berggren, C.; Bjarnason, B.; Johansson, G. An immunological interleukin-6 capacitive biosensor using perturbation with a potentiostatic step, *Biosens. Bioelectron.* **1998**, *13*, 1061-1068.

15 Guo, L.-H.; Facci, J. S.; McLendon, G.; Mosher, R. Effect of gold topography and surface pretreatment on the self-assembly of alkanethiol monolayers, *Langmuir* **1994**, *10*, 4588-4593.

16 Sadik, O. A.; Wallace, G. G. Pulsed amperometric detection of proteins using antibody containing conducting polymers, *Anal. Chim. Acta* **1993**, *279*, 209-212.

17 Sadik, O. M.; van Emon, J. M. Applications of electrochemical immunosensors to environmental monitoring, *Biosens. Bioelectron.* **1994**, *11*, 1-11.

18 O'Shannessy, D. J.; Brigham-Burke, M.; Peck, K. Immobilization chemistries suitable for use in the BIAcore surface plasmon resonance detector, *Anal. Biochem.* **1992**, *205*, 132-136.

19 Disley, D. M.; Cullen, D. C.; You, H.-X.; Lowe, C. R. Covalent coupling of Immunoglobulin G to self-assembled monolayers as a method for immobilizing the interfactial recognition layer of a surface plasmon resonance immunosensor, *Biosens. Bioelectron.* **1998**, *13*, 1213-1225.

20 Peterlinz, K. A.; Georgiadis, R. In situ kinetics of self-assembly by surface plasmon resonance spectroscopy, *Langmuir* **1996**, *12*, 4731-4740.

21 Debono, R. F.; Loucks, G. D.; Dellamanna, D.; Krull, U. J. Self assembly of short and long chain n-alkyl thiols onto gold surfaces . A real time study using surface plasmon resonance techniques, *Can. J. Chem.* **1996**, *74*, 677-688.

22 Karpovich, D. S.; Blanchard, G. J. Direct measurement of the adsorption kinetics of alkanethiolate self assembled monolayers on a microcrystalline gold surface, *Langmuir* **1994**, *10*, 3315-3322.

23 Pan, W.; Durning, C. J.; Turro, N. J. Kinetics of alkanethiol adsorption on gold, *Langmuir* **1996**, *12*, 4469-4473.

24 Schneider, T. W.; Buttry, D. A. Electrochemical quartz crystal microbalance studies of adsorption and desorption of self-assembled monolayers of alkyl thiols on gold, *J. Am. Chem. Soc.* **1993**, *115*, 12391-12397.

25 Kim, Y. T.; Mccarley, R. L.; Bard, A. J. Observation of n-octadecanethiol multilayer formation from solution onto gold, *Langmuir* **1993**, *9*, 1941-1944.

26 Fruböse, C.; Doblhofer, K. In situ quartz microbalance study of the self assembly and stability of aliphatic thiols on polarized gold electrodes, *J. Chem. Soc. Faraday Trans.* **1995**, *91*, 1949-1953.

27 Hu, K.; Bard, A. J. In situ monitoring of kinetics of charged thiol adsorption on gold using an atomic force microscope, *Langmuir* **1998**, *14*, 4790-4794.

28 Xu, S.; Cruchon-Dupeyrat, S. J. N.; Garno, J. C.; Liu, G. Y.; Jennings, G. K.; Yong, T. H.; Laibinis, P. E. In situ studies of thiol self assembly on gold from solution using atomic force microscopy, *J. Chem. Phys.* **1998**, *108*, 5002-5012.

29 Edinger, K.; Gölzhäuser, A.; Demota, K.; Wöll, C.; Grunze, M. Formation of self-assembled monolayers of n-alkanthiols on gold: a scanning tunneling microscopy study on the modification of substrate morphology, *Langmuir* **1993**, *9*, 4-8.

30 Fenter, P.; Schreiber, F.; Berman, L.; Scoles, G.; Eisenberger, P.; Bedzyk, M. J. On the structure and evolution of the buried S/Au interface in self-assembled monolayers: X-ray standing wave results, *Surf. Sci.* **1998**, *412/413*, 213-235.

31 Ron, H.; Matlis, S.; Rubinstein, I. Self-assembled monolayers on oxidized metals. 2. gold surface oxidative pretreatment, monolayer properties, and depression formation, *Langmuir* **1998**, *14*, 1116-1121.

32 Ron, H.; Rubinstein, I. Alkanethiol monolayers on preoxidized gold. Encapsulaton of gold oxide under an organic monolayer, *Langmuir* **1994**, *10*, 4566-4573.

33 Beulen, M. W. J.; Kastenberg, M. I.; van Veggel, F. C. J. M.; Reinhoudt, D. N. Electrochemical stability of self-assembled monolayers on gold, *Langmuir* **1998**, *14*, 7463-7467.

34 Pan, J.; Tao, N.; Lindsay, S. M. An atomic force microscopy study of a self-assembled octadecyl mercaptan monolayer adsorbed on gold (111) under potential control, *Langmuir* **1993**, *9*, 1556-1560.

35 Sondag-Huethorst, J. A. M.; Fokkink , L. G. J. Electrochemical characterization of functionalized alkanethiol monolayers on gold, *Langmuir* **1995**, *11*, 2237-2241.

36 Cooper, E.; Leggett, G. J. Influence of tail-group hydrogen bonding on the stabilities of self-assembled monolayers of alkylthiols on gold, *Langmuir* **1999**, *15*, 1024-1032.

37 Blonder, R.; Katz, E.; Willner, I.; Wray, V.; Buckmann, A. F. Application of a nitrospiropyran fad reconstituted glucose oxidase and charged electron mediators as optobioelectronic assemblies for the amperometric transduction of recorded optical signals. Control of the on off direction of the photoswitch, *J. Am. Chem. Soc.* **1997**, *119*, 11747-11757.

38 Liu, H. Y.; Liu, S. G.; Echegoyen, L. Remarkably stable self assembled monolayers of new crown ether annelated tetrathiafulvalene derivatives and their cation recognition properties, *Chem. Commun.* **1999**, 1493-1494.

39 Cheng, Q.; Brajter-Toth, A. Permselectivity, sensitivity, and amperometric pH sensing at thioctic acid monolayer microelectrodes, *Anal. Chem.* **1996**, *68*, 4180-4185.

40 Hoogvliet, J. C.; Dijksma, M.; Kamp, B.; van Bennekom, W. P. Electrochemical pretreatment of gold electrode surfaces for molecular self-assembly: a study of bulk polycrystalline gold electrodes in phosphate buffer pH 7.4, *Anal. Chem.* **2000**, *72*, 2016-2021. (Chapter 2 of this Ph.D. thesis)

41 Lu, B.; Smyth, M. R.; Quinn, J.; Bogan, D.; O'Kennedy, R. Development of a regenerable amperometric immunosensor for 7-hydroxycoumarin, *Electroanalysis* **1996**, *8*, 619-622.

42 Gebbert, A.; Alvarez-Icaza, M.; Peters, H.; Jäger, V.; Bilitewski, U.; Schmid, R. D. On-line monitoring of monoclonal antibody production with regenerable flow-injection immuno systems, *J. Biotechnol.* **1994**, *32*, 213-220.

43 Liu, M.; Rechnitz, G. A.; Li, K.; Li, Q. X. Capacitive immunosensing of polycylic aromatic hydrocarbon and protein conjugates, *Anal. Lett.* **1998**, *31*, 2025-2038.

44 Knichel, M.; Heiduschka, P.; Beck, W.; Jung, G.; Göpel, W. Utilization of a self-assembled peptide monolayer for an impedimetric immunosensor, *Sens. Actuators* **1995**, *B28*, 85-94.

45 Dalhuijsen, A. J.; van der Meer, T. H.; Hoogendoorn, C. J.; Hoogvliet, J. C.; van Bennekom, W. P. Hydrodynamic properties and mass transfer characteristics of electrochemical flow-through cells of the confined wall-jet type, *J. Electroanal. Chem.* **1985**, *182*, 295-313.

46 Shen, H.; Mark, J. E.; Seliskar, C. J.; Mark, H. B.; Heineman, W. R. Blocking behavior of self-assembled monolayers on gold electrodes, *J. Solid State Electrochem.* **1997**, *1*, 148-154.

47 Krysinski, P.; Brzostowska-Smolska, M. Three-probe voltammetric characterisation of octadecanethiol self-assembled monolayer integrity on gold electrodes, *J. Electroanal. Chem.* **1997**, *424*, 61-67.

48 Krysinski, P.; Brzostowska-Smolska, M. Capacitance characteristics of self-assembled monolayers on gold electrode, *Bioelectrochem. Bioenerg.* **1998**, *44*, 166-168.

49 Finklea, H. O.; Snider, D. A.; Fedyk, J.; Sabatani, E.; Gafni, Y.; Rubinstein, I. Characterization of octadecanethiol-coated gold electrodes as microarray electrodes by cyclic voltammetry and ac impedance spectroscopy, *Langmuir* **1993**, *9*, 3660-3667.

50 Cheng, Q.; Brajter-Toth, A. Selectivity and sensitivity of self-assembled thioctic acid electrodes, *Anal. Chem.* **1992**, *64*, 1998-2000.

51 Cheng, Q.; Brajter-Toth, A. Permselectivity and high sensitivity at ultrathin monolayers. Effect of film hydrophobicity, *Anal. Chem.* **1995**, *67*, 2767-2775.

52 Bard, A. J.; Faulkner, L. R. *Electrochemical methods. Fundamentals and Applications,* John Wiley & Sons Ltd: New York, **1980**.

53 Creager, S. E.; Hocket, L. A.; Rowe, G. K. Consequences of microscopic surface roughness for molecular self-assembly, *Langmuir* **1992**, *8*, 854-861.

54 Oesch, U.; Janata, J. Electrochemical study of gold electrodes with anodic oxide films. I. Formation and reduction behaviour of anodic oxides on gold., *Electrochim. Acta* **1983**, *28*, 1237-1246.

55 Trotman-Dickinson, A. F. In *Comprehensive Inorganic Chemistry*; Bailar, J. C., Emeléus, H. J.Nyholm, R., Eds.; Pergamon Press Ltd.: Oxford, **1973**; Vol. 3, p. 1031 and 1047.

56 Zamborini, F. P.; Crooks, R. M. *Langmuir* **1997**, *13*, 122-126.

57 Xia, Y.; Zhao, X.-M.; Kim, E.; Whitesides, G. M. A selective etching solution for use with patterned self-assembled monolayers of alkanethiolates on gold, *Chem. Mater.* **1995**, *7*, 2332-2337.

58 Ron, H.; Rubinstein, I. Self-assembled monolayers on oxidized metals. 3. Alkylthiol and dialkyl disulfide assembly on gold under electrochemical conditions, *J. Am. Chem. Soc.* **1998**, *120*, 13444-13452.

59 Silva, F.; Martins, A. Surface reconstruction of gold single crystals: electrochemical evidence of the effect of adsorbed anions and influence of steps and terraces, *Electrochim. Acta* **1998**, *44*, 919-929.

4

Effect of Hexacyanoferrate(II/III) on Self-Assembled Monolayers of Thioctic Acid and 11-Mercaptoundecanethiol on Gold

ABSTRACT

Hexacyanoferrate (II/III) is a redox probe commonly applied in the characterization of SAMs. However, it has been reported that the redox probe influences the characteristics of the SAM. Since the stability of the SAM is of paramount importance in sensitive detection of unlabeled peptides and proteins with impedimetric immunosensors, the effect of this redox probe has been further investigated.

The change in characteristics of SAMs of thioctic acid (TA) and 11-mercapto-undecanoic acid (MUA) in time in buffered hexacyanoferrate(II/III) (HCF(II/III)) solutions pH 7.4 has been studied with impedimetry. Frequency scans are recorded at regular time intervals at 0.2 V versus SCE and a superimposed sinusoidal potential with an amplitude of 10 mV, in the frequency range of 10 kHz to 50 mHz. The stability is studied in the dark and during subsequent exposure of the solution to light.

A TA SAM, a MUA SAM and clean gold can be modelled with the same equivalent circuit. From this model it was found that, as expected, charge transfer and diffusion of the redox probe through the MUA SAM is more inhibited than through the TA SAM. Further, the MUA SAM has a larger mean monolayer-thickness, as is revealed from the lower value of the capacitive component.

After exposure of the solution to light, a relatively rapid decrease in the resistances and increase in the double layer capacitance is observed. The characteristics of the MUA SAM change faster than that of the TA SAM, and after 6 h of exposure, the equivalent circuit has to be modified to be able give an appropriate fit.

The manner in which the values of the elements describing the TA SAM change suggests that TA molecules are gradually removed. A possible mechanism is etching of the gold substrate by CN^- ions through pin-holes in the SAM. Support of this mechanism is obtained from the large difference in characteristics of the gold electrode before SAM formation and after long-term incubation in illuminated buffered hexacyanoferrate(II/III) solution, pointing to a change in the structure of the gold, and by the observation that thin gold layers are etched in this solution.

M. Dijksma, B.A. Boukamp, B. Kamp, W.P. van Bennekom, manuscript in preparation

INTRODUCTION

Immunosensors are devices for measuring the interaction between antibodies and antigens with usually one of the binding partners immobilized. Self-assembled monolayers (SAMs), i.e., monolayers that are spontaneously formed from sulfur-containing compounds in contact with gold or silver surfaces,[1-4] provide a convenient basis for protein immobilization. Attachment of proteins to the carboxylic endgroups of the SAM-forming compounds using carbodiimide activation, usually in combination with succinimide, is the most generally applied method.[5-9]

Because stability is an important requirement of an impedimetric immunosensor, a stable SAM is required. Stability depends on the structure and the pretreatment of the gold substrate,[10, 11] on the solubility of the SAM-molecules in the measurement solution and on the Van der Waals interactions between these molecules. The Van der Waals interactions are related to the length of the alkyl chain and the degree of branching.[3, 12, 13]

Many different methods can be used for the characterization of the SAMs. These methods can give information on the structure at a defined location, e.g., scanning tunneling microscopy (STM),[14, 15] atomic force microscopy,[16, 17] and Fourier transform infrared (FTIR) spectroscopy,[14] or average characteristics, e.g., contact angle measurements,[14] surface plasmon resonance,[18, 19] quartz crystal microbalance,[20, 21] and electrochemical methods.[3, 22] Electrochemical methods used in the SAM characterization are mainly cyclic voltammetry (CV) and impedimetry.

Although CV has been used, in absence of a redox probe,[23, 24] to calculate the capacitance, more often the kinetics of a redox probe, usually hexacyanoferrate(II/III) (HCF(II/III)),[9, 23, 25-31] or hexaaminеruthenium(II/III) (HRC(II/III)) is investigated.[23, 28-33] More information can be obtained from impedimetry, because this method is more sensitive and gives information on both capacitance and resistance and pin-holes when performed in presence of HCF(II/III)[34-36] or HRC(II/III).[32, 37, 38]

A reason why HCF(II/III) and HRC(II/III) are preferred to other redox probes has been given by Cheng and Brajter-Toth.[23] They found that these probes showed fast kinetics on hydrophilic thioctic acid (TA) monolayers, which became slower as the hydrophobicity of the film increased with the coadsorption of hexanethiol. For the uncharged catecholamine and quinone probes, slower kinetics were observed, independent of the monolayer composition. Which of the charged probes is preferred, depends on the electrostatic interactions between this probe and the SAM, and thus on the charge of the SAM. In some cases, additional information can be obtained when the response of both probes is compared.[23, 28-31]

In electrochemical immunosensing without labeling, impedimetry is frequently applied. Although the differences measured in absence of a redox probe are

smaller,[39] immunosensors used both in absence[6, 39] and in presence of a redox probe (HCF(II/III))[34, 40-42] have been described.

Besides, HCF(III) has also been applied for selective etching of gold in a solution containing thiosulfate.[43] A mechanism is proposed in which HCF(III) acts as the oxidant, while thiosulfate co-ordinates the gold ion. It was reported that patches of gold, which are not protected by a SAM, are etched.[43]

As has been known for a long time, both in HCF(II) and HCF(III), a cyanide ion can be exchanged with a water molecule by the action of light.[44] Due to a downward shift in the oxidation potential of gold caused by the presence of the CN^- from +1.50 to –0.60 versus NHE, gold atoms may be oxidized by HCF(III) ($E_{½}$ = +0.36 V versus NHE), usually to Au^+. This leads to formation of $Au(CN)_n^{-(n-1)}$ (where n = 2 – 4) complexes.[45]

The etching of gold by CN^- in alkaline solution is a generally known chemical process, of which the mechanism is shown in Equation 1 (see, e.g., Li et al.,[46] and references therein).

$$Au + CN^- \rightarrow AuCN^-_{ads}$$
$$AuCN^-_{ads} \rightarrow AuCN_{ads} + e^- \qquad \text{(Equation 1)}$$
$$AuCN_{ads} + CN^- \rightarrow Au(CN)^-_2$$

Li et al.[46] used electrochemical STM to study the behaviour of unmodified and hexadecanethiol-modified Au(111) surfaces in CN^--containing solutions. It was found that gold is stable in solutions containing 1 mM CN^- at potentials cathodic of -770 mV versus Ag/AgCl. However, at open circuit or at potentials anodic of -520 mV, Au dissolves in these cyanide solutions. When the surface is modified with a well-ordered, compact SAM of hexadecanethiol, no etching is observed in the potential-range from -770 to -520 mV. However, gold modified with a less ordered SAM is etched.[46]

From the above information it is clear that characterization of SAMs with HCF(II/III) may influence the results. Indeed, Krysinsky and Brzostowska-Smolska[29] observed changes in SAMs after measurements in HCF containing solutions. Rickert et al.[39] found a reduction in the activity of the sensor when stored for a long time in buffered HCF(II/III) solution.

Although long-chain SAMs are much less easily damaged, in an immunosensor for direct detection of small amounts of protein, thin sensing layers are preferred. Then the relative change in capacitance caused by binding of antigens to antibodies immobilized on the thin layer is larger. Therefore, we developed a method for preparing a stable SAM of TA on polycrystalline gold electrodes. Stable SAMs are reproducibly formed by incubation of electropolished gold electrodes in a solution of TA in phosphate buffer pH 7.4 at +0.2 V versus SCE.[47, 48] It was found that our characterization method, impedimetry in buffered HCF(II/III) solution, influences the characteristics of the SAM.[48]

TA:

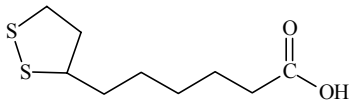

MUA:

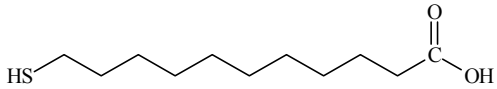

Figure 1. Structure of thioctic acid (TA) and 11-mercaptoundecanethiol (MUA).

SAMs of TA and 11-mercaptoundecanoic acid (MUA) (Figure 1), which have both been used in our work on the development of an impedimetric immunosensor, were subjected to stability studies in buffered HCF(II/III) solution, both in the dark and exposed to light. A mechanism is proposed based on the interpretation of the obtained data with an equivalent circuit, and with the results obtained from measurement of the thickness of thin gold layers with VIS spectrophotometry.

EXPERIMENTAL METHODS

Chemicals

All chemicals were of analytical grade and used as received, unless mentioned otherwise. All water used was demineralized. HCF(II/III) was prepared freshly before each experiment by adding 2 mM of each $K_3Fe(CN)_6$ and $K_4Fe(CN)_6$ (Fluka, Buchs, Switzerland) to 0.1 M phosphate buffer pH 7.4, which is a mixture of 0.1 M solutions of Na_2HPO_4 and NaH_2PO_4 (Merck, Darmstadt, Germany). Phosphate solution pH 10.4 has been prepared by adding NaOH (Merck) to 0.1 M Na_2HPO_4. 11-mercaptoundecanethiol has been obtained from Aldrich (Milwaukee, WI, USA), and DL-6,8-thioctic acid from Sigma (St. Louis, MO, USA).

Mechanical polishing of the electrode

The working electrodes (WE) consist of a gold wire (99.99%, Engelhard-Clal, Amsterdam, The Netherlands) with a diameter of 1.00 mM (geometric surface area of 0.785 mm^2) and are press-fitted in Kel-F. They are polished during 30 min with gamma-micropolish B deagglomerated alumina suspension (0.05 µm, Buehler, Lake Bluff, IL, USA) using a Metaserve automatic polisher (Buehler, Coventry, U.K.), and the electrodes are cleaned ultrasonically in water for 15 min.

Electrochemical equipment

For electrochemical measurements, a confined wall-jet flow-through cell is used,[49] with a saturated calomel reference electrode (RE, SCE) and a glassy-carbon disk auxiliary electrode (AE, Ø 1 cm). The distance between the working and auxiliary electrode is 100 µm. Details of this homemade flow-through cell have been described previously.[49] All potentials mentioned are versus SCE. The

flow system further consisted of an HPLC pump (LC-10AD, Shimadzu, Kyoto, Japan), a packed HPLC column for additional reduction of flow variations, PEEK capillaries and injector, and a thermostat (Julabo F12, Julabo Labortechnik, Seelbach, Germany).

For potential pulses, an Autolab PGSTAT10 digital potentiostat/ galvanostat with GPES 4.7 software (Eco Chemie, Utrecht, The Netherlands), and for impedance measurements a FRA2 module with FRA 4.7 software (Eco Chemie) was used.

Electrochemical methods

After mechanical polishing, the Au electrodes are electropolished by application of potential pulses (+1.6, 0.0, -0.8 V, each 0.1 s) in 0.1 M phosphate buffer, flow 0.5 mL min^{-1} for 30 – 120 min, until a minimum surface roughness has been obtained.[47]

SAMs of TA and MUA were formed from stirred solutions of 50 mM TA in 0.1 M phosphate buffer pH 7.4, and saturated solutions of MUA in 0.1 M phosphate buffer pH 10.4, respectively, at $E = +0.2$ V during 60 h. After thoroughly rinsing with water, the electrode with the SAM is transferred to a thermostatted (23.0°C) flow-through cell.

Monitoring of SAM characteristics has been performed with impedimetry, at an applied potential (E_{dc}) of +0.2 V, with a superimposed sinusoidal potential with an amplitude (E_0) of 10 mV, at a range of frequencies 10 kHz $\geq f \geq$ 50 mHz.

The resulting impedance, which is a complex quantity: $Z(\omega) = Z'(\omega) + jZ''(\omega)$, is presented in the complex plane. Z' represents the in-phase component, while Z'' is the out-of-phase component. The data sets are modelled with an 'equivalent circuit', using a Complex Non-linear Least Squares (CNLS) procedure.[50] The validity of the data sets is checked with a 'Kramers-Kronig transformation test'.[51] This test specifically discriminates for time-variant behavior of the electrochemical cell. For high-quality data the pseudo-χ^2_{KK} value is related to the noise level and values between 10^{-5} and 10^{-6} can be achieved.

Investigation of etching of gold by hexacyanoferrate

Etching of gold by buffered HCF(II/III) solution was also investigated using surface plasmon resonance (SPR) disks, i.e., thin-film gold layers (about 50 nm) vapor deposited over a titanium underlayer of 2 nm on glass (Eco Chemie, Utrecht, The Netherlands). The thickness of the gold layer is determined from transmission measurements at $\lambda = 550$ nm using a double-beam spectrophotometer (100-60, Hitachi, Tokyo, Japan).

RESULTS AND DISCUSSION

Characterization of SAMs of TA and MUA

After formation, the SAMs are first stabilized in 100 mM phosphate buffer pH 7.4 for 10 h. Then the solution is replaced by a buffered HCF(II/III) solution. In Figure 2a, a frequency scan of a bare gold electrode, and in Figure 2b of a TA and a MUA SAM are shown.

The system can be described with the equivalent circuit as shown in Figure 3, using the CNLS-method described by Boukamp.[50] The corresponding values for the different elements in the fits are shown in Table 1. The viability of the model circuit is (in part) indicated by the weighted error sum or 'pseudo'-χ^2.[50] In general, a value below $1 \cdot 10^{-5}$ can be taken as an excellent fit, provided that the pseudo-χ^2 is mostly due to statistical noise. For both SAMs this criterion is fulfilled. However, for the bare gold electrode, using the same equivalent circuit, the pseudo-χ^2 is much larger. This is most likely caused by the known instability of the impedance, due to rapid fouling of a "clean" gold electrode.

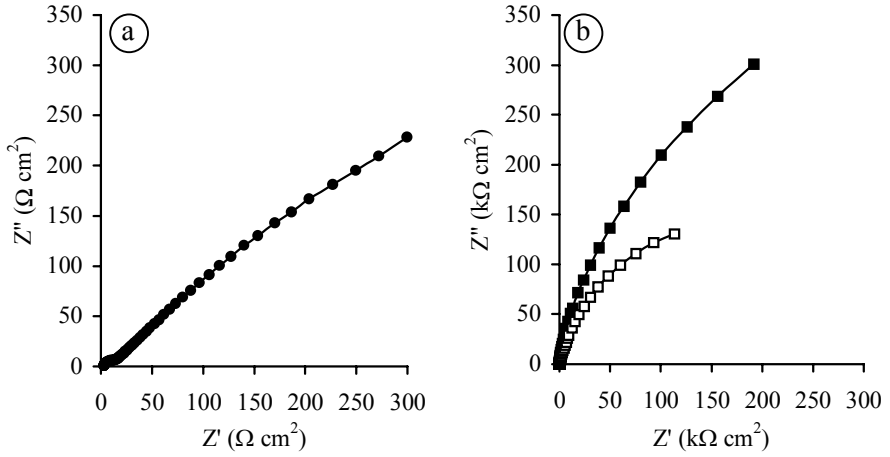

Figure 2. Nyquist plots of a (a) clean gold electrode and (b) (□) TA and (■) MUA SAM deposited on gold, measured in buffered HCF(II/III) solution pH 7.4 (flow rate = 10 μL min^{-1}, f = 10 kHz – 50 mHz, E_{dc} = +0.2 V, E_o = 10 mV).

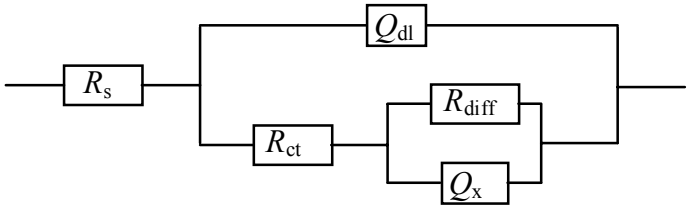

Figure 3. Equivalent circuit used to fit the frequency scans shown in Figure 2. The elements are explained in the text, the corresponding values are shown in Table 1.

The model circuit consists of resistances (R) and constant-phase elements (Q), and is described by the shorthand notation $R_s(Q_{dl}[R_{ct}(R_{diff}Q_x)])$. R_s is the solution resistance, R_{ct} the resistance against charge transfer, Q_{dl} the double layer capacitance, and R_{diff} and Q_x give information on the amount of diffusion through the SAM. A constant-phase element is frequency dependent. Its impedance is described by $Z_Q = (j\omega)^{-n}/Y_0$,[50] where Y_0 is a proportionality constant, containing the diffusion coefficient and other parameters which depend on the characteristics of the electrochemical system, $j = \sqrt{-1}$, $\omega = 2\pi f$ is the angular frequency, and n is an exponent ($-1 \leq n \leq 1$). The interfacial capacitance often shows frequency dispersion, which can be modelled by a constant phase element (Q) with n close to one. In fact the Q represents a very general dispersion relation. For $n = 1$ it models a capacitance with $C = Y_0$; for $n = 0$ a resistance with $R = Y_0^{-1}$; and for $n = -1$ an inductance with $L = Y_0^{-1}$. A special case is obtained for $n = ½$, i.e., the so-called Warburg element, which models semi-infinite diffusion. For the SAMs in this study the Warburg represents the diffusion of Red and Ox from and to the electrode. Assuming charge transfer can only take place at the 'bare' gold surface, the occurrence of a Warburg dispersion indicates the presence of pin-holes in the SAMs. On the interpretation of a constant-phase element in electrochemical systems several articles have been published.[52-55]

The Kramers-Kronig data validation test showed that most data was of high quality. Yet, it was not possible to find a simple model circuit that would result in satisfactory fit to the entire frequency dispersion (50 mHz – 10 kHz). The low frequency part ($f < 100$ Hz) could be modelled well with the equivalent circuit presented in Figure 3. The high-frequency (hf) region ($f > 1$ kHz) could also be fitted perfectly with a much simpler $R_s(RQ)_{hf}Q_{dl}$ circuit, where R_s is the electrolyte resistance and Q_{dl} the double layer capacitance.

Table 1. Values of R_s R_{ct}, R_{diff} and Q_{dl} (Y_0 and n), and Q_x (Y_0 and n) found for TA and MUA SAMs obtained from fitting the frequency scans from 1 kHz – 50 mHz to the equivalent circuit shown in Figure 2, using the CNLS-method.[50]

	Bare gold	TA	MUA
R_s (Ω cm^2)	2.93 ± 0.03	16.4 ± 0.5	12.2 ± 0.2
R_{ct} (Ω cm^2)	10.0 ± 0.3	(41 ± 2)·10^3	(106 ± 10)·10^3
R_{diff} (Ω cm^2)	1.7 ± 0.2	(0.37 ± 0.06)·10^3	(1.5 ± 0.1)·10^3
Q_{dl}: Y_0 (Ω^{-1} cm^{-2} s^n)	(1.4 ± 0.2)·10^{-4}	(8.81 ± 0.05)·10^{-6}	(4.99 ± 0.02)·10^{-6}
n	0.88 ± 0.01	0.932 ± 0.001	0.970 ± 0.007
Q_x: Y_0 (Ω^{-1} cm^{-2} s^{-n})	(9.65 ± 0.07)·10^{-5}	(4.47 ± 0.04)·10^{-6}	(2.57 ± 0.05)·10^{-6}
n	0.521 ± 0.004	0.746 ± 0.007	0.55 ± 0.02

This high-frequency dispersion can possibly be explained by the special geometry of the electrochemical cell.[49] As the RE is placed well outside the region between the WE and AE, it will be very sensitive for small changes in the current

distribution between these two electrodes. Considering the large differences in size between the WE and AE (∅ 1 and 10 mm, respectively) in combination with the small distance between these electrodes (100 μm), a significant change in the current distribution as function of frequency may be expected.

In order to circumvent this problem only the low-frequency part (f < 1 kHz) was modelled with the circuit of Figure 3. The influence of the high-frequency end (10 Hz – 1 kHz) was reduced by modifying the weighting factors with a $\omega^{-½}$ term. This procedure allowed us to obtain a much better description of the process occurring at the WE, as the effects studied are far more distinct at lower frequencies. Although the configuration of the cell limits the frequency range for a simple CNLS-modelling procedure, it has proven to be very well suited for applications in immunosensing.[56]

The value of R_s is only dependent on the solution and therefore on the distance between the electrodes. In principle, the differences found arise from variations in the cell geometry, since the distance between the RE and the other electrodes is not fully fixed. However, the difference in R_s of bare gold and the SAMs is too large to have arisen from this effect only. It is assumed to arise from a deviation of the experimental results from the model at frequencies higher than 1 kHz.

For the MUA SAM, Y_0 is lower, and R_{ct} and R_{diff} are 1.5 and 4 times larger than for the TA SAM. This is in agreement with the expected higher ordering and thickness of a MUA SAM, which means that both the charge transfer and diffusion of HCF(II/III) through the MUA SAM is more inhibited than through the TA SAM. The deviation of Q_{dl} from full capacitive behavior (n = 1) is in both cases relatively small (n = 0.932 and 0.970, respectively), and less than that found for the bare gold (n = 0.88). Because deviation from ideal capacitive behavior may originate from a non-ideal smoothness of the surface,[57] this difference may be explained by a further etching of the gold. However, also the SAM itself influences n.

The behavior of the element Q_x seems to be less obvious. In the TA SAM the value of this element is smaller than in the MUA SAM. However, the value of n is close to ½ in case of a MUA SAM and bare gold, and 0.746 in case of a TA SAM. Therefore, it can be derived that the behavior of the clean gold and the MUA SAM is diffusive, while that of the TA SAM is much more capacitive. However, this is in contrast with the 4 times larger value of R_{diff} of the MUA SAM, which means that less diffusion takes place through a MUA SAM compared to a TA SAM.

Stability of SAMs of TA and MUA in buffered HCF(II/III) solution in the dark

A good indication of the stability of SAMs in buffered HCF(II/III) solution can be obtained from recording frequency scans at regular time intervals and plotting the Nyquist plots, as shown in Figures 4a and b. It can be observed that the

difference between successive scans is larger in Figure 4a than in 4b. This means that a MUA SAM is more stable in buffered HCF(II/III) solution than a TA SAM.

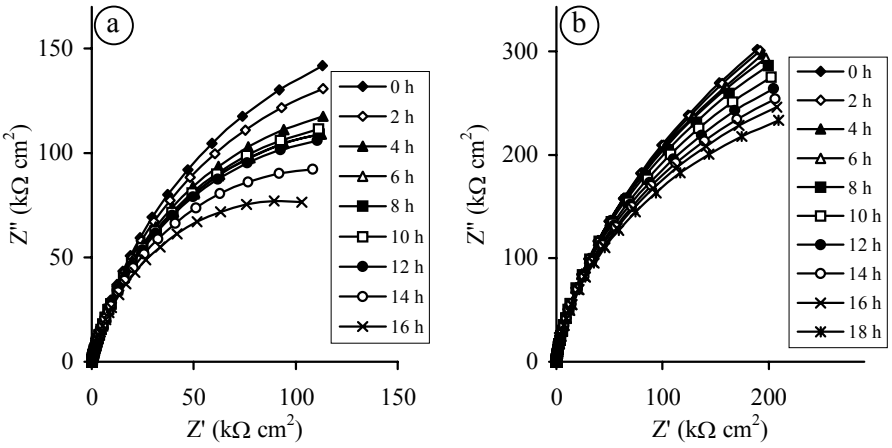

Figure 4. Nyquist plots of frequency scans measured every 2 h of the (a) TA, and (b) MUA SAM in buffered HCF(II/III) solution pH 7.4 in the dark (flow rate = 10 μL min^{-1}, f = 10 kHz – 50 mHz, E_{dc} = +0.2 V, E_0 = 10 mV).

Effect of exposure of the solution to light

After about 16 h (TA) and 18 h (MUA) this solution is exposed to light. Frequency scans measured at regular intervals are shown in Figure 5. Compared to Figure 4 the impedance decreases much faster, indicating a rapid change in SAM characteristics.

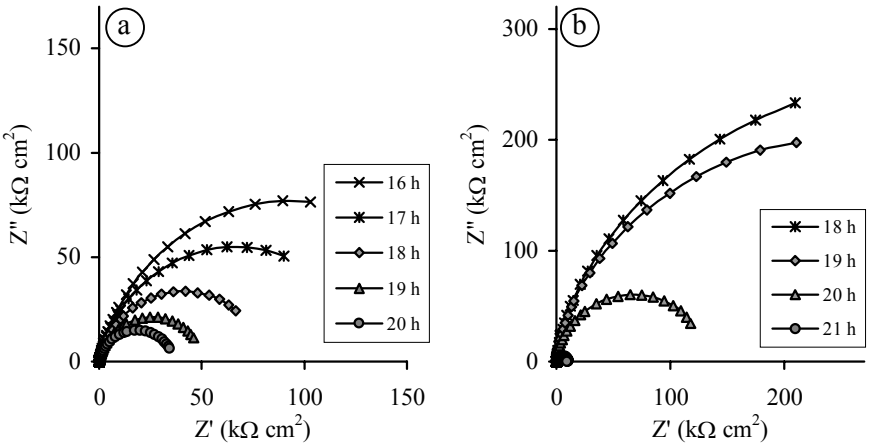

Figure 5. Nyquist plots of frequency scans measured each hour of the (a) TA, and (b) MUA SAM in buffered HCF(II/III) solution pH 7.4, when exposed to light (flow rate = 10 μL min^{-1}, f = 10 kHz – 50 mHz, E_{dc} = +0.2 V, E_0 = 10 mV).

Interpretation of the changes in terms of the equivalent circuit

Frequency scans measured at regular time-intervals have been fitted to the equivalent circuit shown in Figure 3. From these results, the influence of HCF(II/III) on the electrochemical characteristics of the SAMs can be derived. In Figures 6 and 7 the results of the fit are plotted as a function of time. Most of the frequency scans could properly be fitted to the equivalent circuit. However, CNLS-modelling is only possible when the properties of the WE are constant or change slowly, an indication of which can be obtained with a Kramers-Kronig test (from the value of χ^2_{KK}).[51] It appeared that from 34 to 40 h under the influence of light the properties of the TA SAM change so rapidly with time that the Kramers-Kronig stability condition is violated. In Figure 6a and 6b the corresponding points are indicated by a dashed line.

In general, as can be observed from Figures 6 to 8, during incubation in the dark, R_{diff} decreases slowly. Because the other elements of the MUA SAM remain constant, it can be concluded that a reorganization process of the SAM takes place. This process leaves the total amount of exposed gold (indicated by R_{ct}) more or less constant, but leads to a redistribution where larger holes in the SAM are present and diffusion through the SAM is increased.

In the TA SAM, the decrease in R_{ct} is accompanied by a slight decrease in R_{diff} and increase in Q_{dl}. It can be concluded that the total area of exposed gold increases. This is caused by removal of TA molecules from the SAM, which also leads to a decrease in the mean monolayer thickness, explaining the increase of Q_{dl}.

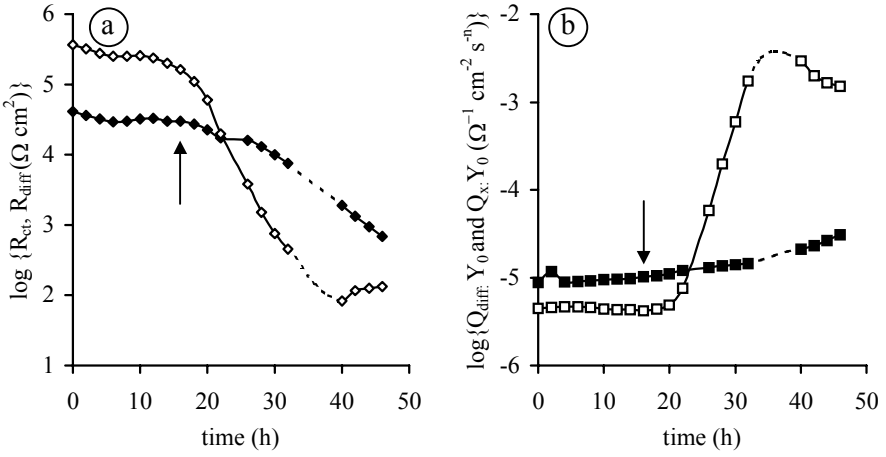

Figure 6. Change of the logarithm of (a) R_{ct}(◆), R_{diff} (◊), and (b) Q_{dl}:Y_0(■)and Q_x: Y_0 (□) in time in buffered HCF(II/III) solution of the **TA** SAM in the dark, followed by exposure to light from 16 h on (indicated by arrows). The values of these elements have been derived from fitting the frequency scans (flow rate = 10 μL min^{-1}, f = 1 kHz – 50 mHz, E_{dc} = +0.2 V, E_0 = 10 mV) to the equivalent circuit shown in Figure 3.

This difference in behaviour of the TA and the MUA SAM is explained by structural differences of these molecules. While MUA is only slightly soluble at pH 7.4, TA is soluble up to 50 mM. Further, because of the relatively long alkyl chain MUA is more suitable for formation of stable monolayers.

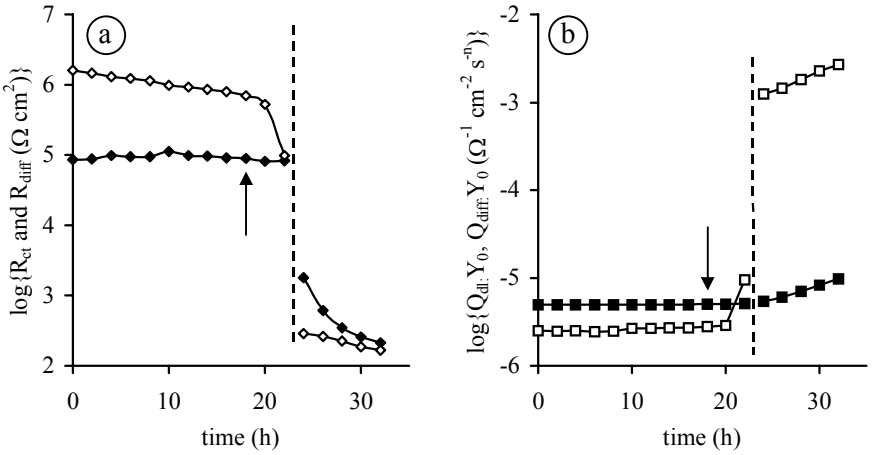

Figure 7. Change of the logarithm of (a) R_{ct}(◆), R_{diff} (◊), and (b) Q_{dl}:Y_0(■)and Q_x: Y_0 (□) in time in buffered HCF(II/III) solution of the **MUA** SAM in the dark, followed by exposure to light from 18 h on (indicated by arrow). The values of these elements have been derived from fitting the frequency scans (flow rate = 10 μL min^{-1}, f = 1 kHz – 50 mHz, E_{dc} = +0.2 V, E_0 = 10 mV) to an equivalent circuit. Up to 22 h (left of the dashed line) the scans are fitted to the circuit shown in Figure 3, and from 24 h on, to that shown in Figure 9.

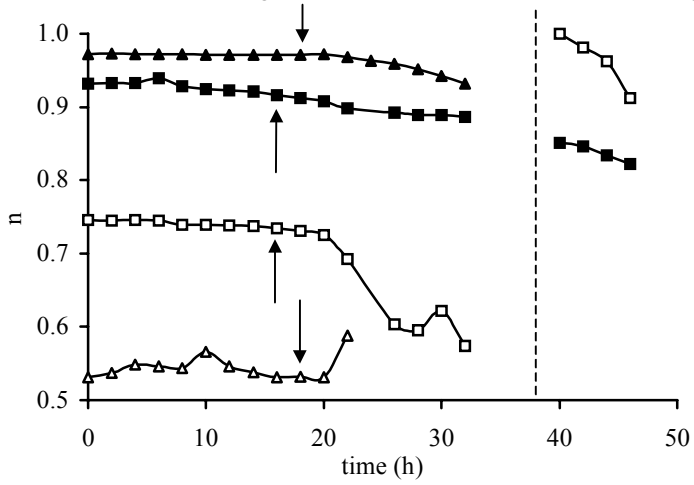

Figure 8. Change of the exponent (n) in Q_1 and Q_2 of TA (Q_1: ■, Q_2: □) and MUA (Q_1: ▲, Q_2:**Δ**) in time in buffered HCF(II/III) solution up to 16 and 18 h, respectively, in the dark, followed by exposure to light (indicated by arrows). The values of these elements have been derived from fitting the frequency scans (flow rate = 10 μL min^{-1}, f = 1 kHz – 50 mHz, E_{dc} = +0.2 V, E_0 = 10 mV) to the equivalent circuit shown in Figure 2. In case of MUA, from 24 h on (right of the dashed line) the scans are fitted to the equivalent circuit shown in Figure 9.

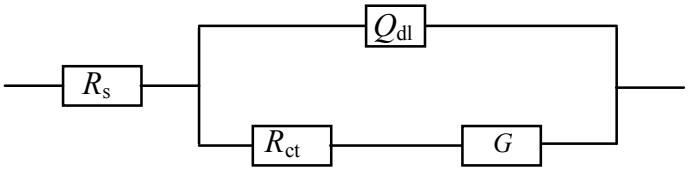

Figure 9. Equivalent circuit used to fit the frequency scans of MUA from 24 h on. The elements are explained in the text.

After exposure of the solution to light, a fast decrease of R_{diff} and R_{ct} and increase in Q_x and, to a lesser extent, of Q_{dl} occurs. After 6 h, the circuit shown in Figure 3 can no longer describe the MUA SAM. A better description is obtained with a circuit in which the parallel placed elements of R_{diff} and Q_x are replaced by a Gerischer element (G), as shown in Figure 9. A Gerischer element is not a very commonly found element. It describes the effect of chemical reactions coupled with faradaic diffusion, where Ox or Red is converted in an inactive complex, and thus depends on the rate constants of these reactions, diffusion and frequency.[58-60] The dc-value (R_{dc}) of this element, which can be approximated by $(Y_0 \cdot K^{½})^{-1}$, is comparable to R_{diff}, and Y_0 are shown in Figures 7a and b at the right site of the dashed line.

Probably, the change in circuit is related to the relatively rapid change in the MUA SAM compared to the TA SAM. In combination with the relatively low solubility of MUA in buffered HCF(II/III) solution, it means that desorbed MUA molecules remain in the cell and alter the behaviour of the WE. To be able to give an explanation of the occurrence of the Gerischer element in the MUA-system more information is required.

In case of the TA SAM, after exposure to light, R_{ct}, R_{diff} decreases and Q_x increases faster. The rate of increase in Q_{dl} is relatively low and doesn't increase after light activation. This can again be explained by removal of TA molecules from the SAM. An increase in the total area of exposed gold leads to an increased diffusion and charge transfer. Because the SAM is much more stable in the buffered HCF(II/III) solution before exposure to light, it is assumed that CN^- ions are responsible for the removal of TA molecules. A possible mechanism is the attack of the gold layer via pin-holes.

Mechanism of decreasing SAM quality

The assumption of etching of gold substrates by cyanide ions formed from HCF after illumination has further been investigated using thin (50 nm) gold layers on glass. The stability of these layers in a buffered HCF(II/III) solution has been tested by measuring the thickness of the gold layer spectrophotometrically (λ = 550 nm) at regular time intervals (see also Chapter 3). As shown in Figure 10, during 24 h in the dark only a slight decrease in thickness occurs compared to the

decrease observed after illumination of the solution. This supports the assumption that attack of SAMs proceeds by etching of the underlying gold.

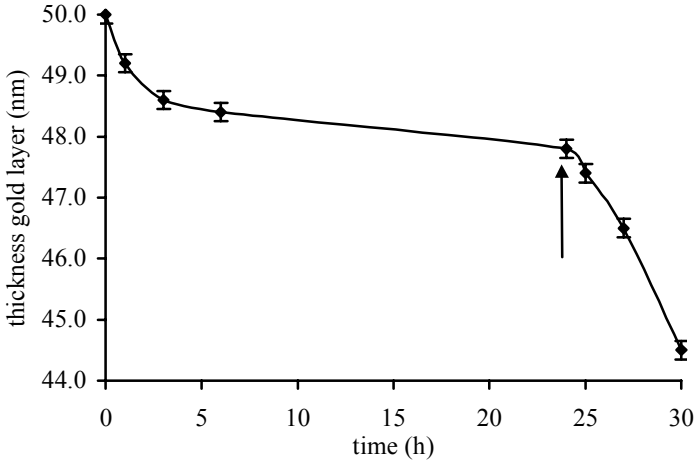

Figure 10. Thickness of a gold layer on glass as a function of time in buffered HCF(II//III) solution, calculated from VIS ($\lambda = 550$ nm) measurements. After 24 h, the solution is exposed to light (indicated by the arrow).

A further indication of the complexity of the mechanism can be obtained from comparison of the values of the circuit elements before SAM formation and at the end of the experiment, as shown in Table 2. From the large differences found between values for the SAMs and bare gold, it can be concluded that the effect of illuminated buffered HCF(II/III) solution on the SAM is not a simple removal of the SAM from the gold electrode. As is generally known, gold is never perfectly clean, and contaminations influence the characteristics. However, because we found that after cleaning (with our potential pulse treatment)[47, 48] the gold still behaves differently than before SAM formation, we assume that a change in the structure takes place. This is probably caused by etching of the gold by CN^-.

Table 2. Values of R_s, R_{ct}, R_{diff}, and Q_{dl} (Y_0 and n), and Q_x (Y_0 and n) found after incubation of the TA and MUA SAMs in exposed buffered HCF(II/III) solution, compared to those found for a bare gold electrode. The frequency scans are fitted using the CNLS method.[50]

	Bare gold	TA (56 h)	MUA (42 h) *
R_s (Ω cm^2)	2.9 ± 0.03	9.6 ± 0.5	10.5 ± 0.1
R_{ct} (Ω cm^2)	10 ± 0.3	690 ± 5	211.9 ± 0.6
R_{diff} (Ω cm^2)	1.7 ± 0.2	133 ± 6	
Q_{dl}: Y_0 (Ω^{-1} cm^{-2} s^n)	(1.4·± 0.2)·10^{-4}	(3.09± 0.06)·10^{-5}	(9.8 ± 0.1)·10^{-6}
n	0.88 ± 0.01	0.822 ± 0.003	0.932 ± 0.002
Q_x: Y_0 (Ω^{-1} cm^{-2} s^n)	(9.7·± 0.07)·10^{-5}	(1.51 ± 0.08)·10^{-3}	G: Y_0 = (2.70 ± 0.02)·10^{-3}
n	0.52 ± 0.004	0.91 ± 0.03	K = 5.0

* Using the equivalent circuit shown in Figure 9, for further information, see text.

Effect of changes at different frequencies

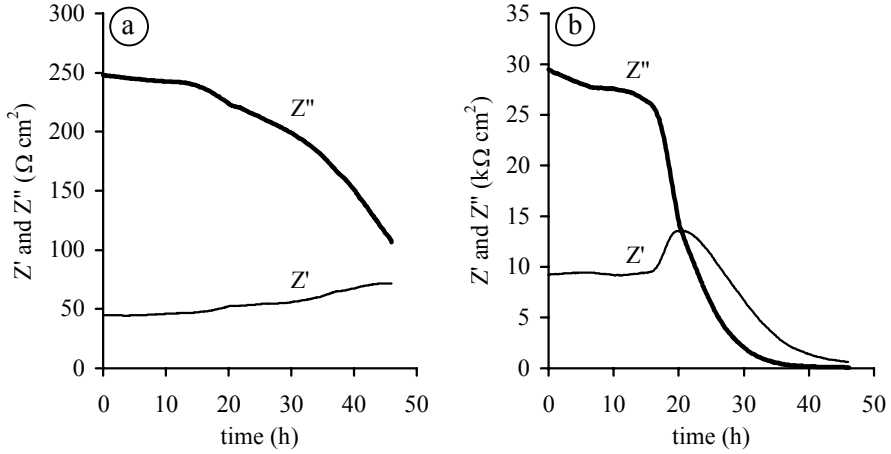

Figure 11. Monitoring of Z' and Z'' in time (flow rate = 10 μL min^{-1}, E_{dc} = 0.2 V, E_0 = 10 mV) for a SAM of TA in buffered HCF(II/III) solution at (a) 113 Hz and (b) 0.5 Hz. Note the different vertical scales.

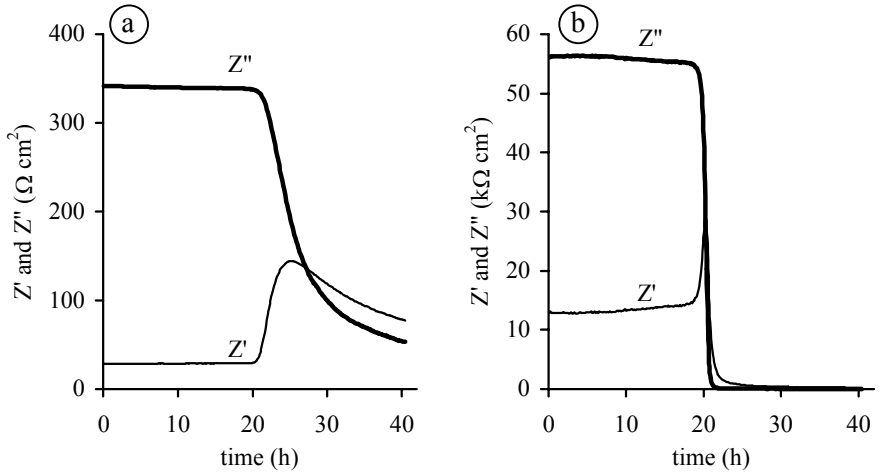

Figure 12. Monitoring of Z' and Z'' in time (E_{dc} = 0.2 V, E_0 = 10 mV) for a SAM of MUA in buffered HCF(II/III) solution at (a) 113 Hz and (b) 0.5 Hz. Note the different vertical scales.

Besides by recording frequency scans at regular time intervals, the impedance can also be monitored at a single frequency. However, this frequency has to be chosen carefully. In presence of a redox probe, mass transfer is more probable as the frequency is lower. This means that in some cases, more or different information is obtained, as the frequency is lower. From Figures 11a and 11b, where the effect measured at 113 Hz and 0.5 Hz is shown, it can be observed that light exposure causes a much larger change at 0.5 Hz. From comparison of Figures

11 and 12, it can also be seen that the effect of light exposure of the buffered HCF(II/III) solution is larger with MUA than with TA, as has also been concluded above from the fits of the frequency scans.

From a mechanistically point of view, however, much less information can be obtained from a simple scan at preselected frequencies, because the circuit elements both influence Z' and Z''.

CONCLUSIONS

The stability of SAMs of TA and MUA in buffered HCF(II/III) solutions pH 7.4 has been investigated, both in the dark and exposed to light, with impedance measurements at E_{dc} = +0.2 V versus SCE, E_0 = 10 mV and 10 kHz ≥ f ≥ 50 mHz. From CNLS-modelling of the frequency scans, it was found that unmodified gold and a SAM of TA or MUA can be described by the same equivalent circuit at 1 kHz ≥ f ≥ 50 mHz, and using a weighting factor of $\omega^{-½}$ (with different values of the elements).

As expected, before exposure to light, a MUA SAM is more stable and provides a better shielding of the gold electrode, which is expressed in a combination of lower values of Q_{dl} and Q_x and higher values of R_{ct} and R_{diff}. After exposure to light, a relatively rapid decrease of the quality of the SAMs is observed, and the MUA SAM is attacked faster than the TA SAM. Large changes occur in the elements of the model, and in case of the MUA SAM, the model even has to be modified.

The way in which the elements of the equivalent circuit change, suggests that TA molecules are removed from the SAM gradually. A possible mechanism is etching of the gold substrate by CN^- ions through pin-holes in the SAM. Support of this mechanism is obtained from the large difference in characteristics of the gold electrode before SAM formation and after long-term incubation in illuminated HCF(II/III), pointing to a change in the structure of the gold, and by the observation that thin gold layers are etched in this solution.

REFERENCES

1 Wink, T.; van Zuilen, S. J.; Bult, A.; van Bennekom, W. P. Self-assembled monolayers for biosensors (A tutorial review), *Analyst* **1997**, *122*, 43R-50R.

2 Delamarche, E.; Michel, B.; Biebuyck, H. A.; Gerber, C. Golden interfaces: the surface of self-assembled monolayers, *Advan. Mater.* **1996**, *8*, 719-729.

3 Finklea, H. O. In *Electroanalytical Chemistry*; Bard, A. J.Rubinstein, I., Eds.; Marcel Dekker, Inc.: New York, **1996**; Vol. 19, p. 110-318.

4 Mandler, D.; Turyan, I. Applications of self-assembled monolayers in electroanalytical chemistry, *Electroanalysis* **1995**, *8*, 207-213.

5 Disley, D. M.; Cullen, D. C.; You, H.-X.; Lowe, C. R. Covalent coupling of Immunoglobulin G to self-assembled monolayers as a method for immobilizing the interfactial recognition layer of a surface plasmon resonance immunosensor, *Biosens. Bioelectron.* **1998**, *13*, 1213-1225.

6 Mirsky, V. M.; Riepl, M.; Wolfbeis, O. S. Capacitive monitoring of protein immobilization and antigen-antibody reactions on monomolecular alkythiol films on gold electrodes, *Biosens. Bioelectron.* **1997**, *12*, 977-990.

7 Storri, S.; Santoni, T.; Minunni, M.; Mascini, M. Surface modifications for the development of piezoimmunosensors, *Biosens. Bioelectron.* **1998**, *13*, 347-357.

8 Wagner, P.; Hegner, M.; Kernen, P.; Zaugg, F.; Semenza, G. Covalent immobilization of native biomolecules onto Au(111) via N-hydroxysuccinimide ester functionalized self-assembled monolayers for scanning probe microscopy, *Biophys. J.* **1996**, *70*, 2052-2066.

9 Berggren, C.; Johansson, G. Capacitance measurements of antibody-antigen interactions in a flow system, *Anal. Chem.* **1997**, *69*, 3651-3657.

10 Creager, S. E.; Hocket, L. A.; Rowe, G. K. Consequences of microscopic surface roughness for molecular self-assembly, *Langmuir* **1992**, *8*, 854-861.

11 Guo, L.-H.; Facci, J. S.; McLendon, G.; Mosher, R. Effect of Gold Topography and Surface Pretreatment on the Self-Assembly of Alkanethiol Monolayers, *Langmuir* **1994**, *10*, 4588-4593.

12 Schlenoff, J. B.; Li, M.; Ly, H. Stability and self-exchange in alkanethiol monolayers, *J. Am. Chem. Soc.* **1995**, *117*, 12528-12536.

13 Chung, C.; Lee, M. Exchange of self-assembled thiol monolayers on gold: characterization by FT-IR external reflection spectroscopy, *J. Electroanal. Chem.* **1999**, *468*, 91-97.

14 Poirier, G. E. Characterization of organosulfur molecular monolayers on Au (111) using scanning tunneling microscopy, *Chem. Rev.* **1997**, *97*, 1117-1127.

15 Edinger, K.; Gölzhäuser, A.; Demota, K.; Wöll, C.; Grunze, M. Formation of self-assembled monolayers of n-alkanethiols on gold: a scanning tunneling microscopy study on the modification of substrate morphology, *Langmuir* **1993**, *9*, 4-8.

16 Hu, K.; Bard, A. J. In situ monitoring of kinetics of charged thiol adsorption on gold using an atomic force microscope, *Langmuir* **1998**, *14*, 4790-4794.

17 Xu, S.; Cruchon-Dupeyrat, S. J. N.; Garno, J. C.; Liu, G. Y.; Jennings, G. K.; Yong, T. H.; Laibinis, P. E. In situ studies of thiol self assembly on gold from solution using atomic force microscopy, *J. Chem. Phys.* **1998**, *108*, 5002-5012.

18 Debono, R. F.; Loucks, G. D.; Dellamanna, D.; Krull, U. J. Self assembly of short and long chain n-alkyl thiols onto gold surfaces. A real time study using surface plasmon resonance techniques, *Can. J. Chem.* **1996**, *74*, 677-688.

19 Peterlinz, K. A.; Georgiadis, R. In situ kinetics of self-assembly by surface plasmon resonance spectroscopy, *Langmuir* **1996**, *12*, 4731-4740.

20 Kim, Y. T.; Mccarley, R. L.; Bard, A. J. Observation of n-octadecanethiol multilayer formation from solution onto gold, *Langmuir* **1993**, *9*, 1941-1944.

21 Fruböse, C.; Doblhofer, K. In situ quartz microbalance study of the self assembly and stability of aliphatic thiols on polarized gold electrodes, *J. Chem. Soc. Faraday Trans.* **1995**, *91*, 1949-1953.

22 Perry, S. S.; Somorjai, G. A. Characterization of organic surfaces, *Anal. Chem.* **1994**, *66*, 403A-415A.

23 Cheng, Q.; Brajter-Toth, A. Permselectivity and high sensitivity at ultrathin monolayers. Effect of film hydrophobicity, *Anal. Chem.* **1995**, *67*, 2767-2775.

24 Chidsey, C. E. D.; Loiacono, D. N. Chemical functionality in self-assembled monolayers: structural and electrochemical properties, *Langmuir* **1990**, *6*, 682-691.

25 Yang, Z.; Gonzalez-Cortes, A.; Jourquin, G.; Viré, J.-C.; Kauffmann, J.-M.; Delplancke, J.-L. Analytical application of self assembled monolayers on gold electrodes: critical importance of surface pretreatment, *Biosens. Bioelectron.* **1995**, *10*, 789-795.

26 Porter, M. D.; Bright, T. B.; Allara, D. L.; Chidsey, C. E. D. Spontaneously organized molecular assemblies. 4. Structural characterization of n-alkyl thiol monolayers on gold by optical ellipsometry, infrared spectroscopy, and electrochemistry, *J. Am. Chem. Soc.* **1987**, *109*.

27 Miller, C.; Cuendet, P.; Grätzel, M. Adsorbed w-hydroxy thiol monolayers on gold electrodes: evidence for electron tunneling to redox species in solution, *J. Phys. Chem.* **1991**, *95*, 877-886.

28 Krysinski, P.; Brzostowska-Smolska, M. Three-probe voltammetric characterisation of octadecanethiol self-assembled monolayer integrity on gold electrodes, *J. Electroanal. Chem.* **1997**, *424*, 61-67.

29 Krysinski, P.; Brzostowska-Smolska, M. Capacitance characteristics of self-assembled monolayers on gold electrode, *Bioelectrochem. Bioenerg.* **1998**, *44*, 166-168.

30 Cheng, Q.; Brajter-Toth, A. Selectivity and sensitivity of self-assembled thioctic acid electrodes, *Anal. Chem.* **1992**, *64*, 1998-2000.

31 Cheng, Q.; Brajter-Toth, A. Permselectivity, sensitivity, and amperometric pH sensing at thioctic acid monolayer microelectrodes, *Anal. Chem.* **1996**, *68*, 4180-4185.

32 Flink, S.; Boukamp, B. A.; Vandenberg, A.; van Veggel, F. C. J. M.; Reinhoudt, D. N. Electrochemical detection of electrochemically inactive cations by self assembled monolayers, of crown ethers, *J. Am. Chem. Soc.* **1998**, *120*, 4652-4657.

33 Finklea, H. O.; Avery, S.; Lynch, M. Blocking oriented monolayers of alkyl mercaptans on gold electrodes, *Langmuir* **1987**, *3*, 409-413.

34 Taira, H.; Nakano, K.; Maeda, M.; Takagi, M. Electrode modification by long-chain, dialkyl disulfide reagent having terminal dinitrophenyl group and its application to impedimetric immunosensors, *Anal. Sci.* **1993**, *9*, 199-206.

35 Diao, P.; Guo, M.; Jiang, D.; Jia, Z.; Cui, X.; Gu, D.; Tong, R.; Zhong, B. Fractional coverage of defects in self-assembled thiol monolayers on gold, *J. Electroanal. Chem.* **2000**, *480*, 59 - 63.

36 Diao, P.; Jiang, D. L.; Cui, X. L.; Gu, D. P.; Tong, R. T.; Zhong, B. Studies of structural disorder of self-assembled thiol monolayers on gold by cyclic voltammetry and ac impedance, *J. Electroanal. Chem.* **1999**, *464*, 61-67.

37 Flink, S.; van Veggel, F.; Reinhoudt, D. N. Recognition of cations by self-assembled monolayers of crown ethers, *J. Phys. Chem.* **1999**, *B103*, 6515-6520.

38 Protsailo, L. V.; Fawcett, W. R. Studies of electron transfer through self-assembled monolayers using impedance spectroscopy, *Electrochim. Acta* **2000**, *45*, 3497-3505.

39 Rickert, J.; Göpel, W.; Beck, W.; Jung, G.; Heiduschka, P. A mixed self-assembled monolayer for an impedimetric immunosensor, *Biosens. Bioelectron.* **1996**, *11*, 757-768.

40 Kuramitz, H.; Sugawara, K.; Nakamura, H.; Tanaka, S. Electrochemical evaluation of interaction between avidin and biotin self-assembled using marker ions, *Chem. Lett.* **1999**, *8*, 725-726.

41 Knichel, M.; Heiduschka, P.; Beck, W.; Jung, G.; Göpel, W. Utilization of a self-assembled peptide monolayer for an impedimetric immunosensor, *Sens. Actuators* **1995**, *B28*, 85-94.

42 Patolsky, F.; Filanovsky, B.; Katz, E.; Willner, I. Photoswitchable antigen-antibody interactions studied by impedance spectroscopy, *J. Phys. Chem* **1998**, *B102*, 10359-10367.

43 Xia, Y.; Zhao, X.-M.; Kim, E.; Whitesides, G. M. A selective etching solution for use with patterned self-assembled monolayers of alkanethiolates on gold, *Chem. Mater.* **1995**, *7*, 2332-2337.

44 Chadwick, B. M.; Sharpe, A. G. In: *Advances in inorganic chemistry and radiochemistry,* Emeléus, H. J.; Sharpe, A. G., Eds. Academic Press, London **1966,** vol 8, p. 112-159.

45 Milazzo, G.; Caroli, S. *Tables of standard electrode potentials,* John Wiley & Sons, Chichester: **1978**.

46 Li, Y.-Q.; Chailapakul, O.; Crooks, R. M. Electrochemical scanning tunneling microscopy study of the electrochemical behavior of naked and n-alkanethiol-modified Au(111) surfaces in F^-- and CN^--containing electrolyte solutions, *J. Vac. Sci. Technol.* **1995**, *13*, 1300-1306.

47 Hoogvliet, J. C.; Dijksma, M.; Kamp, B.; van Bennekom, W. P. Electrochemical pretreatment of gold electrode surfaces for molecular self-assembly: a study of bulk polycrystalline gold electrodes in phosphate buffer pH 7.4, *Anal. Chem.* **2000**, *72*, 2016-2021. (Chapter 2 of this Ph.D. thesis)

48 Dijksma, M.; Kamp, B.; Hoogvliet, J. C.; van Bennekom, W. P. Formation and Electrochemical Characterization of Self-Assembled Monolayers of Thioctic Acid on Polycrystalline Gold Electrodes in Phosphate buffer pH 7.4, *Langmuir* **2000**, *16*, 3852-3857. (Chapter 3 of this Ph.D. thesis)

49 Dalhuijsen, A. J.; van der Meer, T. H.; Hoogendoorn, C. J.; Hoogvliet, J. C.; van Bennekom, W. P. Hydrodynamic properties and mass transfer characteristics of electrochemical flow-through cells of the confined wall-jet type, *J. Electroanal. Chem.* **1985**, *182*, 295-313.

50 Boukamp, B. A. A nonlinear least squares fit procedure for analysis of immitance data of electrochemical systems, *Solid State Ionics* **1986**, *20*, 31-44.

51 Boukamp, B. A. A linear Kronig-Kramers transform test for immittance data validation, *J. Electrochem. Soc.* **1995**, *142*, 1885 - 1894.

52 Sadkowski, A. On the ideal polarisability of electrodes displaying cpe-type capacitance dispersion, *J. Electroanal. Chem.* **2000**, *481*, 222-226.

53 Lang, G.; Heusler, K. E. Remarks on the energetics of interfaces exhibiting constant phase element behaviour, *J. Electroanal. Chem.* **1998**, *457*, 257.

54 Zoltowski, P. On the electrical capacitance of interfaces exhibiting constant phase element behaviour, *J. Electroanal. Chem.* **1998**, *443*, 149-154.

55 Bisquert, J.; Garcia-Belmonte, G.; Fabregat-Santiago, F.; Compte, A. Anomalous transport effects in the impedance of porous film electrodes, *Electrochem. Commun.* **1999**, *1*, 429-435.

56 Dijksma, M.; Kamp, B.; Hoogvliet, J. C.; van Bennekom, W. P. Development of an electrochemical immunosensor for direct detection of interferon-γ at attomolar level, *Anal. Chem. accepted* (Chapter 6 of this Ph.D. thesis)

57 Brett, C. M.; Oliveira Brett, A. M. *Electrochemistry, principles, methods and applications,* Oxford University Press Inc.: New York, USA, **1993**.

58 Makkus, R. C.; Hemmer, K.; de Wit, H. J. *Ber. Bunsenges. Phys. Chem.* **1990**, *94*, 847.

59 Sluyters-Rehbach, M.; Sluyters, J. H. In *Comprehensive Treatise of Electrochemistry*; Yeager, E., Bockris, J. O. M., Conway, B. E.Saragapani, S., Eds.; Plenum Press: New York, **1984**; Vol. 9, p. 274

60 Wu, Y.M.; Rapp, R.A. Electrochemical impedance studies of hot corrosion of preoxidized Ni by a thin-fused Na_2SO_4 film. *J. Electrochem. Soc.* **1991**, *138*, 2683-2688

5

Development of an Electrochemical Immunosensor for Direct Detection of Interferon-γ using a Self-Assembled Monolayer of Thioctic Acid

ABSTRACT

An electrochemical immunosensor for direct detection of the 15.5-kDa protein interferon-γ (IFN-γ) has been developed. A self-assembled monolayer (SAM) of thioctic acid is formed on an electropolished polycrystalline Au electrode. In an on-line procedure in the flow (50 mM phosphate buffer pH 7.4, thermostatted at 23.0°C) a specific antibody (MD-2) against IFN-γ is covalently attached following carbodiimide/succinimide activation of the carboxylic endgroups of the SAM. The formation of the immunosensor is monitored impedimetrically at a frequency of 113 Hz, a potential of 0.2 V and a superimposed sinusoidal potential with an amplitude of 10 mV. Despite the fact that 2 fg mL^{-1} could be detected, this sensor is not yet applicable to determining IFN-γ in samples containing other proteins (i.e., interleukin-2), because specific and nonspecific adsorption can not be distinguished.

INTRODUCTION

An immunosensor is a device that is able to detect the interaction between an antibody (Ab) and an antigen (Ag). Immunosensors are mainly applied in areas where both a high sensitivity and a high selectivity are required.[1] Direct detection of the interaction is preferred over the use of labels. Although with direct detection discrimination between specific and nonspecific proteins is often a problem, the use of labeling means a larger analysis time, while the extra steps increase the complexity of the procedure.

Direct detection can be performed with optical, e.g., surface plasmon resonance (SPR),[2] piezoelectrical, e.g., quartz crystal microbalance (QCM),[3] surface scanning, e.g., atomic force microscopy (AFM)[4-6] and electrochemical[7] transducers.

Electrochemical devices are very suitable for direct detection of low amounts. The impedance technique is the most frequently used method (see Chapter 1)[8] and has been applied to detection of proteins with antibodies immobilized in polypyrrole,[9, 10] on Si/SiO_2[11-14], on silanized metal[9, 15-18] and on gold via self-assembled monolayers (SAMs),[19-23] that is, monolayers that are spontaneously formed from sulfur-containing molecules on gold or silver.[24]

In immunosensors based on SAMs, antibodies are often immobilized after activation of carboxylic groups with carbodiimide, usually in combination with *N*-hydroxysuccinimide. Mirsky et al.[21] used this procedure, after testing different methods, for building an immunosensor for human serum albumin on SAMs of ω-mercaptohexadecanoic acid, which has a high stability and a detection limit of 1 $\mu g\ mL^{-1}$.[21] However, using SAMs of shorter-chain molecules, much lower detection limits have been obtained.[25]

Berggren and Johansson[25] reported a method for sensitive measurement of proteins in the $pg\ mL^{-1}$ range using chronoamperometry, by sampling the current with 50 kHz after application of a potential step (0 – 50 mV). Antibodies were immobilized on mechanically polished and plasma-cleaned polycrystalline gold rod electrodes via a carbodiimide-activated SAM of thioctic acid (TA), followed by postcoating with 1-dodecanethiol. From the difference in current response before and after injection of the analyte, the proteins interleukin-2 (IL-2), human chorionic gonadotropin hormone (HCG) and human serum albumin (HSA) could be detected, with detection limits in the $pg\ mL^{-1}$ range. With antibodies immobilized on cystamine after epoxy-activation, interleukin-6 (IL-6) could be detected at a level of 10 $fg\ mL^{-1}$.[19]

Reduction of nonspecific adsorption, or distinguishing between specific and nonspecific adsorption, is an important topic in the development of immunosensors.[8] In SAM-based immunosensors, a large, not distinguishable, amount of nonspecific adsorption has been found by Mirsky et al.[21] and Taira et al.[26] However, Berggren and Johansson[19, 25] and Snejdarkova et al.[27] report no influence of nonspecific proteins on the signal.

Another problem in SAM-based immunosensors is the reproducibility of sensor formation. Berggren and Johansson[25] reported that at least half of the electrodes did not produce any changes in capacitance when antigens were injected. Taira et al.[26] found differences in the impedance of the SAMs, arising from poor reproducibility of the roughness of the polished gold electrode. A method for reproducible formation of stable SAMs of TA on polished gold electrodes has been described. Reproducibility is accomplished on electropolished electrodes when during formation a potential of +0.2 V versus SCE is applied to the electrode.[28, 29]

In this chapter the development of a sensitive impedimetric immunosensor for detection of interferon-γ (IFN-γ) is described. A SAM of TA is formed on an electropolished gold electrode and antibodies against IFN-γ (MD-2) are coupled to the carboxylic endgroups of the SAM after carbodiimide/succinimide activation.[30-32] Spontaneous decay of the remaining succinimide groups is compared with deactivation using ethanolamine.[30-32] The sensitivity and selectivity of the sensor are investigated.

EXPERIMENTAL SECTION

Chemicals

All chemicals were of analytical grade and used as received, unless mentioned otherwise. DL-6,8-thioctic acid (> 99%), 1-ethyl-3-[3-(dimethylamino)propyl]-carbodiimide·hydrochloride (EDC), *N*-hydroxysulfosuccinimide (NHS), and ethanolamine·hydrochloride (EA) were purchased from Sigma (St. Louis, MO, USA). All water used was demineralized. Solutions of EDC (0.4 M in water) and NHS (0.1 M in water) were stored at -20°C. After thawing, equal volumes were mixed prior to activation of a SAM. A solution of EA (1 M in water, adjusted to pH 8.5 with NaOH) was prepared.

Phosphate buffer pH 7.4 (50 or 100 mM) was prepared by mixing solutions of Na_2HPO_4 and NaH_2PO_4 (both from Merck, Darmstadt, Germany). 100 mM KCl (Merck) solution was prepared in water. Recombinant interferon-γ (IFN-γ) and the antibody MD-2 have been a kind gift from Dr. P. H. van der Meide (U-Cytech, Utrecht, The Netherlands).[33] Interleukin-2 (IL-2, Proleukin®) was kindly donated by Dr. R.F.M. Rombouts (Chiron, Amsterdam, The Netherlands). After addition of water to the freeze-dried samples of MD-2, IFN-γ or IL-2, solutions of 0.1 mg mL^{-1} in 125 mM phosphate buffered saline pH 7.4 were prepared and stored at -80°C. Prior to use they were thawed and further diluted with 50 mM phosphate buffer pH 7.4. Trehalose, present in the MD-2 and IFN-γ samples when received, does not interfere in our measurements.

Mechanical pretreatment of the electrodes

The working electrodes consist of a gold wire (99.99%, Engelhard-Clal, Amsterdam, The Netherlands) with a diameter of 1.00 mm (geometric surface area of 0.785 mm^2) and are press-fitted in Kel-F. They are polished during 30 min with Gamma micropolish B deagglomerated alumina suspension (0.05 µm, Buehler, Lake Bluff, USA), using a Metaserve automatic polisher (Buehler, Coventry, U.K.), with polishing cloth Alphacloth (Metprep, Coventry, U.K.). Finally the electrodes are cleaned ultrasonically in water for 15 min.

Electrochemical equipment

For electrochemical measurements, a confined wall-jet flow-through cell is used, with a saturated calomel reference electrode (SCE) and a glassy-carbon disc auxiliary electrode.[34] All potentials are versus SCE. The flow system further consisted of a HPLC pump (LKB 2150, Bromma, Sweden) and PEEK capillaries. The PEEK injector was provided with a 50-µL loop. For potential pulses an Autolab PGSTAT10 digital potentiostat/galvanostat with GPES 4.5 software (Eco Chemie, Utrecht, The Netherlands), and for impedance measurements a FRA module with FRA 2.3 software (Eco Chemie) was used.

Electrochemical methods

After polishing, the electrodes were pretreated by application of triple-pulse sequences (+1.6, 0.0, –0.8 V, each 0.1 s) for 30 - 120 min in flow (0.1 mL min^{-1}).[28] Measurements of impedance in time have been performed in 100 mM phosphate buffer pH 7.4 at an applied potential E_{dc} of +0.2 V, with a superimposed alternating potential with an amplitude E_0 of 10 mV, at a frequency f of 113 Hz, in flow (10 µL min^{-1}). The real (Z') and imaginary (Z'') component of the impedance Z are plotted against time.

Formation and removal of self-assembled monolayers

SAMs were formed on potential-pulse pretreated electrodes from 50 mM solutions of TA in 100 mM phosphate buffer pH 7.4 at room temperature by adsorption at E = +0.2 V, in batch, while stirring. SAMs were removed from the electrodes in 100 mM phosphate buffer pH 7.4 by application of potential pulses (+1.6, 0.0, -0.8 V versus SCE, each 0.1 s) for 15 min in the flow (0.5 mL min^{-1}).

RESULTS AND DISCUSSION

Immobilization of MD-2 antibodies

Mechanically polished gold electrodes are electropolished, and TA SAMs are formed as described in the experimental section. MD-2 antibodies are covalently coupled to the carboxylic groups of the SAM after activation with EDC/NHS (Figure 1a), followed by deactivation of the remaining succinimide groups with

ethanolamine (Figure 1b)[30-32] or spontaneous decay. The formation of the immunosensor has been performed in a flow of 10 µL min^{-1} of 50 mM phosphate buffer pH 7.4 and monitored at E_{dc} = +0.2 V, E_0 = 10 mV and f = 113 Hz. At 113 Hz, an optimal signal-to-noise ratio is obtained and injections of IFN-γ only influences Z''.

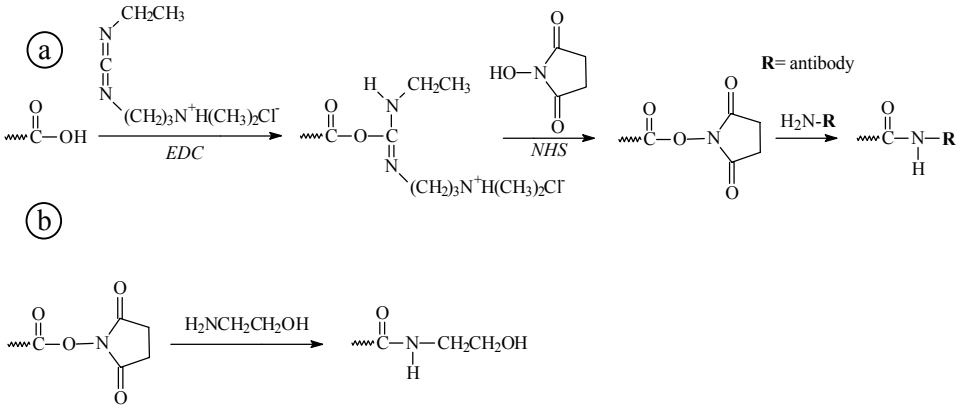

Figure 1. (a) Activation of carboxylic groups with EDC, followed by NHS and coupling of MD-2 antibodies. (b) Deactivation of remaining succinimide groups with ethanolamine.[32]

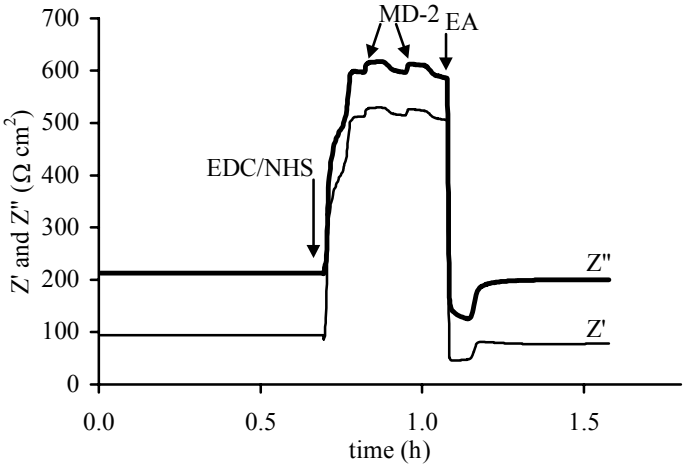

Figure 2. Monitoring of the immunosensor build up on a TA SAM. The real (Z') and the imaginary (Z'') component of the impedance Z as a function of time are shown, measured at f = 113 Hz, E_{dc} = +0.2 V, E_0 = 10 mV, in 50 mM phosphate buffer pH 7.4, with a flow-rate of 10 µL min^{-1}. The arrows indicate the start of an injection. First the SAM is activated with EDC/NHS, next MD-2 (50 µg mL^{-1}) is injected twice and finally, the remaining succinimide groups are deactivated by a single injection of ethanolamine (EA).

As shown in Figure 2, activation of a TA SAM leads to a large increase in both Z' and Z''. Due to the difference in impedance between a solution with and without

proteins, the impedance is larger during the time a protein-containing solution is in contact with the electrode (5 min). The covalent attachment of MD-2 results in a shift in both Z' and Z''. Because, in general, no effect has been observed from a third injection of MD-2 it is assumed that two injections are sufficient to saturate the surface with antibody. Due to steric hindrance, it is not possible to use all succinimide groups. To prevent antigens from binding to remaining succinimide groups, these groups have to be deactivated before antigen is injected. This can be achieved by either spontaneous decay or injection of ethanolamine.

From an UV-assay a half-life of 14 min has been observed for a succinimide group.[35] From Figure 3, where the decay of succinimide groups monitored with impedance measurements is shown, it can be observed that after 2 h most succinimide groups have decayed. However, still a small amount remains, which can be derived from the (still) slowly decreasing impedance. To be certain that all succinimide groups are deactivated, and to be able to build up the immunosensor in less time, ethanolamine is used.

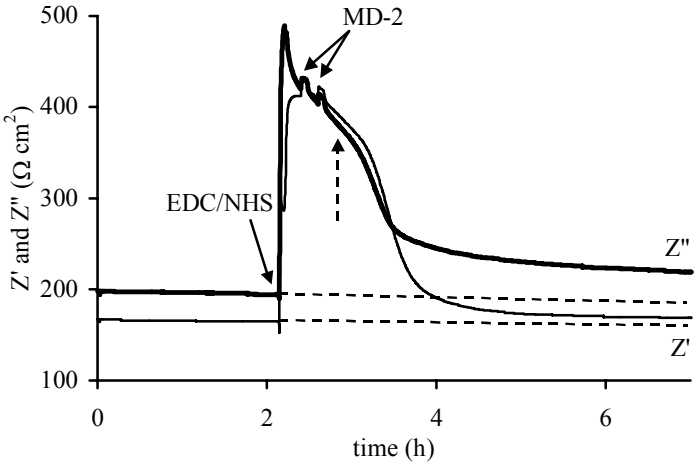

Figure 3. Monitoring of Z' and Z'' during activation with EDC/NHS, coupling of MD-2 and decomposition of remaining succinimide groups, measured in 50 mM phosphate buffer pH 7.4, with flow-rate 10 μL min^{-1}, at E_{dc} = +0.2 V, E_0 = 10 mV and f = 113 Hz. At the time indicated by the upward arrow usually EA is injected.

Usually, characteristics of SAMs are described in terms of the double layer capacitance (C_{dl}) and the charge-transfer resistance (R_{ct}). The relation between these and the SAM type has been investigated. It was found that R_{ct} is larger and C_{dl} smaller as the alkyl chain is longer. Further, C_{dl} decreases and R_{ct} increases with increasing hydrophobicity.[36, 37]

Detection of IFN-γ

In contrast to activation, coupling of antibodies, and deactivation, binding of IFN-γ to the immobilized antibodies only leads to a shift in Z'' (Figure 4a), while in Z' only a temporal effect of a difference in composition of the injected solution compared to the flowing buffer is observed (Figure 4b).

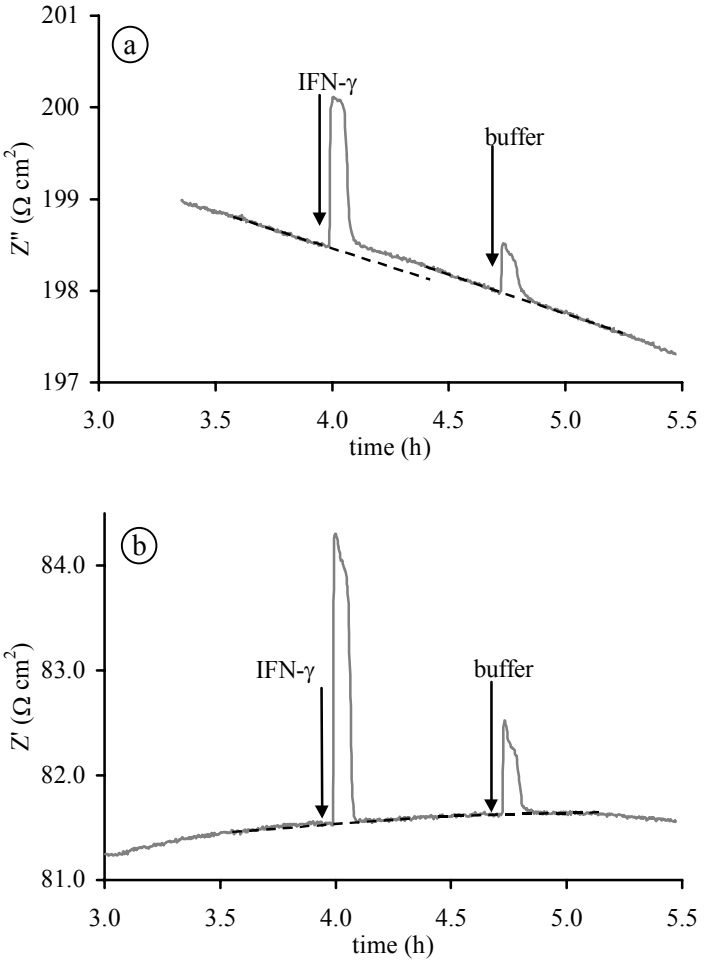

Figure 4. Monitoring of the effect of an injection of IFN-γ (2 fg mL^{-1}) followed by a blank one on MD-2 immobilized on a TA SAM. The (a) real (Z') and (b) imaginary (Z'') component of the impedance Z as a function of time are shown.

A clear effect can be observed from injections of IFN-γ-concentrations as low as 2 fg mL^{-1}. When the cumulative change in Z'' from 5 subsequent injections is plotted against the total injected amount, a linear relation ($r^2 = 0.9968$) is obtained, as shown in Figure 5.

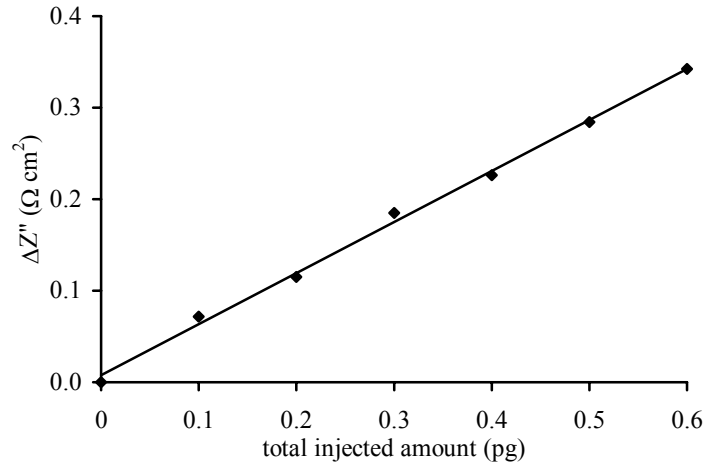

Figure 5. Calibration curve of IFN-γ. The cumulative change in Z'' ($\Sigma\Delta Z''$) is plotted as a function of the total amount of IFN-γ injected.

However, this result is not obtained each time the same procedure is performed. This irreproducibility is also apparent from the difference in shift caused by injection of EDC/NHS in Figures 2 and 3. This is a clear example of the lack of reproducibility resulting from differences in the surface due to the use of different electrodes, or the mechanical polishing treatment. Formation of an immunosensor on a single gold electrode and detection of IFN-γ is reproducible within about 10%.[28, 29] Also, injections of IL-2 lead to shifts in Z'', thus we cannot be sure whether the signal of IFN-γ arises from specific adsorption, nonspecific or a combination. This means that determination of the specific dynamic range is impossible.

Nonspecific adsorption

A possibility for distinguishing specific and nonspecific adsorption was expected in the removal of nonspecifically adsorbed proteins with injections of a solution with a different ionic strength or pH. However, injections of phosphate buffer pH 7.4 in concentrations higher than 50 mM have no effect, phosphate buffer solutions with a higher or lower pH than 7.4 resulted in a negative or positive shift in Z'', respectively, and injections of NaCl or KCl lead to a positive shift.

In Figure 6 the effect of KCl on the sensor is shown. The fact that injections of KCl lead to an increase in Z'' does not mean that no removal of nonspecifically adsorbed proteins occurs. Possibly, the observed change is dominated by the effect of KCl itself.

Further efforts will be put in the search for a solution of a substance able to reduce nonspecific adsorption. The final goal of this study is to be able to measure

a protein specifically in real samples. Because of the observed relation between detection limit and thickness of the SAM, the possibility to detect concentrations lower than 2 fg mL^{-1} by using (acetyl)cysteine will be investigated.

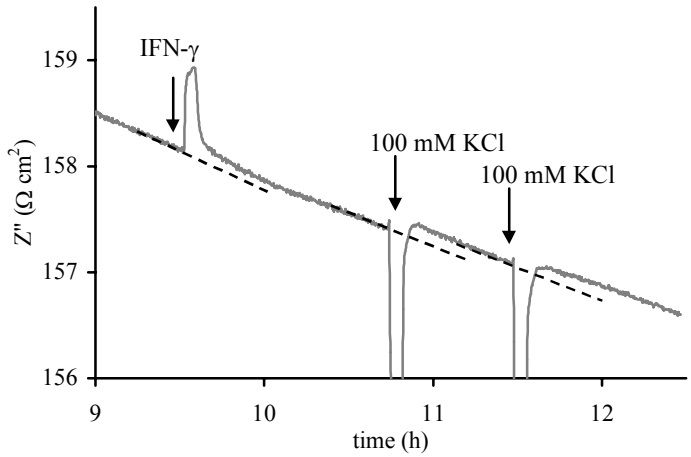

Figure 6. Monitoring Z' and Z'' during injections of IFN-γ and 100 mM KCl on MD-2 immobilized on a TA SAM.

CONCLUSIONS

On MD-2 antibodies immobilized on SAMs of TA, unlabeled IFN-γ can be detected, using impedance measurements at $E_{dc} = 0.2$ V, $E_0 = 10$ mV and $f = 113$ Hz. Detection of 2 fg mL^{-1} has been achieved, however, the selectivity of the sensor is very low. We have not been able to distinguish specific and nonspecific adsorption by injection of solutions with a different pH or ionic strength.

ACKNOWLEDGMENT

This work has been supported by grant UFA44.3392 from the Dutch Technology Foundation (STW). The authors gratefully acknowledge Dr. P. H. van der Meide (U-Cytech) for the donation of MD-2 and IFN-γ and Dr. R.F.M. Rombouts (Chiron) for the gift of IL-2.

REFERENCES

1 Byfield, M. P.; Abuknesha, A. Biochemical aspects of biosensors, *Biosens. Bioelectron.* **1994**, *9*, 373-400.

2 Homola, J.; Yee, S. S.; Gauglitz, G. Surface plasmon resonance sensors: review, *Sens. Actuators* **1999**, *B54*, 3-15.

3 O'Sullivan, C. K.; Vaughan, R.; Guilbault, G. G. Piezoelectric immunosensors - Theory and applications, *Anal. Lett.* **1999**, *32*, 2353-2377.

4 Allen, S.; Chen, X.; Davies, J.; Davies, M. C.; Dawkes, A. C.; Edwards, J. C.; Roberts, C. J.; Sefton, J.; Tendler, S. J. B.; Williams, P. M. Detection of antigen-antibody binding events with the atomic force microscope, *Biochem.* **1997**, *36*, 7457-7463.

5 Perrin, A.; Lanet, V.; Theretz, A. Quantification of specific immunological reactions by atomic force microscopy, *Langmuir* **1997**, *13*, 2557-2563.

6 Dong, Y.; Shannon, C. Heterogeneous immunosensing using antigen and antibody on gold surfaces with electrochemical and scanning probe detection, *Anal. Chem.* **2000**, *72*, 2371-2376.

7 Skládal, P. Advances in electrochemical immunosensors, *Electroanalysis* **1997**, *9*, 737-745.

8 Dijksma, M.; van Bennekom, W. P. Direct electrochemical immunosensors - review, *manuscript in preparation.* (Chapter 1 of this Ph.D. thesis)

9 Ameur, S.; Maupas, H.; Martelet, C.; Jaffrezic-Renault, N.; Ben Ouada, H.; Cosnier, S.; Labbe, P. Impedimetric measurements on polarized functionalized platinum electrodes: application to direct immunosensing, *Mater. Sci. and Eng.* **1997**, *c5*, 111-119.

10 Sargent, A.; Sadik, O. A. Monitoring antibody-antigen reactions at conducting polymer-based immunosensors using impedance spectroscopy, *Electrochim. Acta* **1999**, *44*, 4667-4675.

11 Maupas, H.; Saby, C.; Martelet, C.; Jaffrezic-Renault, N.; Soldatkin, A. P.; Charles, M.-H.; Delair, T.; Mandrand, B. Impedance analysis of Si/SiO_2 heterostructures grafted with antibodies: an approach for immunosensor development, *J. Electroanal. Chem.* **1996**, *406*, 53-58.

12 Jaffrezic-Renault, N.; Martelet, C. Semiconductor-based micro-biosensors, *Synthetic metals* **1997**, *90*, 205-210.

13 Berney, H.; Alderman, J.; Lane, W.; Collins, J. K. A differential capacitive biosensor using polyethylene glycol to overlay the biolayer, *Sens. Actuators,* **1997**, *B44*, 578-584.

14 Berney, H.; Alderman, J.; Lane, W.; Collins, J. K. Development of a generic IC compatible silicon transducer for immunoreactions, *Sens. Actuators* **1999**, *B57*, 238-248.

15 Maupas, H.; Soldatikin, A. P.; Martelet, C.; Jaffrezic-Renault, N.; Mandrand, B. Direct immunosensing using differential electrochemical measurements of impedimetric variations, *J. Electroanal. Chem.* **1997**, *421*, 165-171.

16 DeSilva, M. S.; Zhang, Y.; Hesketh, P. J.; Maclay, G. J.; Gendel, S. M.; Stetter, J. R. Impedance based sensing of the specific binding reaction between staphylococcus enterotoxin B and its antibody on an ultra-thin platinum film, *Biosens. Bioelectron.* **1995**, *10*, 675-682.

17 Varlan, A. R.; Suls, J.; Sansen, W.; Veelaert, D.; De Loof, A. Capacitive sensor for the allatostatin direct immunoassay, *Sens. Actuators* **1997**, *B44*, 334-340.

18 Feng, C.; Xu, Y.; Song, L. Study on highly sensitive potentiometric IgG immunosensor, *Sens. Actuators* **2000**, *B66*, 190-192.

19 Berggren, C.; Bjarnason, B.; Johansson, G. An immunological interleukin-6 capacitive biosensor using perturbation with a potentiostatic step, *Biosens. Bioelectron.* **1998**, *13*, 1061-1068.

20 Rickert, J.; Göpel, W.; Beck, W.; Jung, G.; Heiduschka, P. A mixed self-assembled monolayer for an impedimetric immunosensor, *Biosens. Bioelectron.* **1996**, *11*, 757-768.

21 Mirsky, V. M.; Riepl, M.; Wolfbeis, O. S. Capacitive monitoring of protein immobilization and antigen-antibody reactions on monomolecular alkythiol films on gold electrodes, *Biosens. Bioelectron.* **1997**, *12*, 977-990.

22 Ameur, S.; Martelet, C.; Jaffrezic-Renault, N.; Chovelon, J. M.; Plossu, C.; Barbier, D.; Ouada, H. B. Immunosensing using electrochemical impedance spectroscopy on functionalized gold electrodes, *Proc. - Electrochem. Soc.* **1997**, *97-19*, 1019-1023.

23 Jie, M.; Ming, C. Y.; Jing, D.; Cheng, L. S.; Na, L. H.; Jun, F.; Xiang, C. Y. An electrochemical impedance immunoanalytical method for detecting immunological interaction of human mammary tumor associated glycoprotein and its monoclonal antibody, *Electrochem. Commun.* **1999**, *1*, 425-428.

24 Wink, T.; van Zuilen, S. J.; Bult, A.; van Bennekom, W. P. Self-assembled monolayers for biosensors (A tutorial review), *Analyst* **1997**, *122*, 43R-50R.

25 Berggren, C.; Johansson, G. Capacitance measurements of antibody-antigen interactions in a flow system, *Anal. Chem.* **1997**, *69*, 3651-3657.

26 Taira, H.; Nakano, K.; Maeda, M.; Takagi, M. Electrode modification by long-chain, dialkyl disulfide reagent having terminal dinitrophenyl group and its application to impedimetric immunosensors, *Anal. Sci.* **1993**, *9*, 199-206.

27 Snejdarkova, M.; Csaderova, L.; Rehak, M.; Hianik, T. Amperometric immunosensor for direct detection of human IgG., *Electroanalysis* **2000**, *12*, 940-945.

28 Hoogvliet, J. C.; Dijksma, M.; Kamp, B.; van Bennekom, W. P. Electrochemical pretreatment of gold electrode surfaces for molecular self-assembly: a study of bulk polycrystalline gold electrodes in phosphate buffer pH 7.4, *Anal. Chem.* **2000**, *72*, 2016-2021.

29 Dijksma, M.; Kamp, B.; Hoogvliet, J. C.; van Bennekom, W. P. Formation and electrochemical characterization of self-assembled monolayers of thioctic acid on polycrystalline gold electrodes in phosphate buffer pH 7.4, *Langmuir* **2000**, *16*, 3852-3857. (Chapter 3 of this Ph.D. thesis)

30 Disley, D. M.; Cullen, D. C.; You, H.-X.; Lowe, C. R. Covalent coupling of Immunoglobulin G to self-assembled monolayers as a method for immobilizing the interfactial recognition layer of a surface plasmon resonance immunosensor, *Biosens. Bioelectron.* **1998**, *13*, 1213-1225.

31 Vaughan, R. D.; O'Sullivan, C. K.; Guilbault, G. G. Sulfur based self-assembled monolayers (SAM's) on piezoelectric crystals for immunosensor development, *Fresenius J. Anal. Chem.* **1999**, *364*, 54-57.

32 O'Shannessy, D. J.; Brigham-Burke, M.; Peck, K. Immobilization chemistries suitable for use in the BIAcore surface plasmon resonance detector, *Anal. Biochem.* **1992**, *205*, 132-136.

33 Van der Meide, P. H.; Dubbeld, M.; Schellekens, H. Monoclonal antibodies to human immune interferon and their use in a sensitive solid-phase ELISA, *J. Immunol. Methods* **1985**, *79*, 293-305.

34 Dalhuijsen, A. J.; van der Meer, T. H.; Hoogendoorn, C. J.; Hoogvliet, J. C.; van Bennekom, W. P. Hydrodynamic properties and mass transfer characteristics of electrochemical flow-through cells of the confined wall-jet type, *J. Electroanal. Chem.* **1985**, *182*, 295-313.

35 Parker, M.-C.; Davies, M. C.; Tendler, S. J. B. Effect of controlled hydration on scanning tunneling microscopy images of covalently immobilized proteins, *J. Phys. Chem.* **1995**, *99*, 16155-16161.

36 Swietlow, A.; Skoog, M.; Johansson, G. Double layer capacitance measurements of self-assembled layers on gold electrodes, *Electroanalysis* **1992**, *4*, 921-928.

37 Cheng, Q.; Brajter-Toth, A. Permselectivity and high sensitivity at ultrathin monolayers. Effect of film hydrophobicity, *Anal. Chem.* **1995**, *67*, 2767-2775.

6

Development of an Electrochemical Immunosensor for Direct Detection of Interferon-γ at the Attomolar Level

ABSTRACT

An electrochemical immunosensor for direct detection of the 15.5-kDa protein interferon-γ (IFN-γ) at attomolar level has been developed. Self-assembled monolayers (SAMs) of cysteine or acetylcysteine are formed on electropolished polycrystalline Au electrodes. IFN-γ adsorbs physically to each of these SAMs. With injections of 100 mM KCl, IFN-γ can be removed in the flow without damaging the acetylcysteine SAM. However, the cysteine SAM is affected by these KCl injections.

In an on-line procedure in the flow, a specific antibody (MD-2) against IFN-γ is covalently attached following carbodiimide/succinimide activation of the SAM. The activation of the carboxylic groups, attachment of MD-2, and deactivation of the remaining succinimide groups with ethanolamine are monitored impedimetrically at a frequency of 113 Hz, a potential of +0.2 V versus SCE, and a superimposed sinusoidal potential with an amplitude of 10 mV. Plots of the real (Z') and imaginary (Z'') component of the impedance versus time provide the information to control these processes.

In the thermostatted setup (23.0°C), samples of unlabeled IFN-γ (in phosphate buffer pH 7.4) are injected and the binding with immobilized MD-2 is monitored with impedance or potential-step methods. While the chronoamperometric results are rather poor, the impedance approach provides unsurpassed detection limits, as low as 0.02 fg mL^{-1} (~1 aM) IFN-γ.

From a calibration curve (i.e., Z'' versus the amount injected), recorded by multiple 50-μL injections of 2 pg mL^{-1} of IFN-γ, a dynamic range of 0-12 pg mL^{-1} could be derived. However, when nonspecific adsorption is taken into account, which has been found to be largely reduced through injections of 100 mM KCl, a much smaller dynamic range of 0-0.14 fg mL^{-1} remains.

The immunosensor can be regenerated by using a sequence of potential pulses in the flow by which the SAM with attached MD-2 and bound IFN-γ is completely removed. When the developed procedures described above are repeated, the response of the immunosensor is reproducible within 10%.

M. Dijksma, B. Kamp. J.C. Hoogvliet and W.P. van Bennekom, *Anal. Chem,* accepted.

INTRODUCTION

Immunosensors are mainly applied in areas where both a high selectivity and a high sensitivity are required.[1] An immunosensor is a device that is able to detect the interaction between an antibody (Ab) and an antigen (Ag). One of the binding partners is immobilized, frequently, via a self-assembled monolayer (SAM), i.e., a monolayer formed on a gold surface by spontaneous adsorption of sulfur-containing molecules.[2, 3] The recognition protein is covalently attached to these sulfur compounds either before[4-6] or after[7-14] the SAM formation.

The conversion of the binding event into a measurable signal, in particular at a low concentration of the analyte, the method of immobilization, the prevention or elimination of nonspecific interactions, the regenerability, and reusability are, among other topics, major challenges in immunosensor development research.

Direct detection of immunochemical interactions, i.e., when none of the reaction partners is labeled, can be performed with optical, e.g., surface plasmon resonance (SPR),[15] piezoelectrical, e.g., quartz crystal microbalance (QCM),[16] surface scanning, e.g., atomic force microscopy (AFM)[17-19] and electrochemical[20] transducers. Since the detection limit of SPR, QCM and AFM is usually in the nM range, many strategies have been developed for improvement including, for SPR, the use of liposomes,[21] latex beads,[22, 23] colloidal gold,[24] or hydrogels[25] and plasma-polymerized films[26] with stacked binding locations.[27]

Direct electrochemical detection of proteins can be performed, e.g., with potential-step or impedance methods, by measuring (small) differences in capacitance and/or resistance of an electrode. Mirsky et al.[7] achieved with impedance methods a detection limit of ~1 $\mu g\ mL^{-1}$ (~15 nM) for human serum albumin (HSA) with antibodies immobilized on a SAM of ω-mercapto-hexadecanoic acid. Göpel and co-workers[4, 5] impedimetrically measured a concentration of 1.74 $\mu g\ mL^{-1}$ (~12 nM) of an antibody using an immobilized synthetic antigen.

A major break-through has been published by Berggren et al.[8, 9] showing the capability of a potential-step approach to determine (small changes of) the interfacial capacitance. With antibodies immobilized on a SAM of thioctic acid or cysteamine, detection limits as low as 1 $pg\ mL^{-1}$ (~10 fM) were reported for interleukin-2, interleukin-6, human chorionic gonadotropin hormone, and HSA. While Mirsky et al.[7] only used long-chain alkanethiols, Berggren et al.[8, 9] showed that much lower concentrations can be detected with antibodies immobilized via sulfur-containing compounds with a shorter chain. Since the initial capacitance is larger, the changes are relatively large when a protein is bound by the immobilized antibody.[9]

As mentioned above, elimination or prevention of nonspecific adsorption is another topic of paramount importance in immunosensor research. It has been demonstrated (for SPR), that the amount of nonspecific binding at immuno-globulin G (IgG) immobilized via a short-chain SAM is less than at physically

adsorbed IgG.[10] Cysteine, in particular, has very beneficial characteristics: it exhibits a low amount of nonspecific adsorption, making detection of lower concentrations with SPR possible,[10] and it facilitates the immobilization of proteins to surfaces because of the presence of a thiol group for binding to the gold surface, and a carboxylic acid moiety for attachment of the recognition protein. Cysteine has also been used to introduce a thiol moiety in proteins before self-assembly.[28-30] Other small molecules reported for attaching proteins via SAMs to Au surfaces are cystamine[31, 32] and cysteamine.[9, 33, 34] Silin et al.[35] reported a large amount of nonspecific adsorption of IgG and bovine serum albumine on SAMs of cysteine, probably due to charge interactions of these proteins with the protonated NH_2 groups of cysteine. Therefore, acetylcysteine would be, because of its *N*-acetyl functionality, an alternative for immobilizing proteins.

Regeneration of immunosensors is not straightforward. The use of chaotropic reagents to accomplish dissociation of the Ab:Ag interaction leads to damage of the SAMs or decreased sensitivity of the sensor.[4, 5, 8, 36] Reproducible sensing is only accomplished by reproducible formation of a SAM on a smooth surface. Using a small sulfur-containing molecule like thioctic acid, SAMs with similar characteristics can be formed repeatedly on electropolished gold electrodes.[37, 38] This procedure will be used for the cysteine- and acetylcysteine-based immuno-sensors.

In this paper we describe the development of a sensitive impedimetric immunosensor for detection of interferon-γ (IFN-γ), a relatively small protein of 15.5 kDa. On an electropolished polycrystalline Au electrode a SAM of cysteine or acetylcysteine is formed to which, through activation with carbodiimide/ succinimide, an antibody (MD-2) against IFN-γ is covalently attached. The remaining succinimide groups are deactivated with ethanolamine.[10, 13, 39] For detection of IFN-γ both impedance and potential-step methods are applied.

EXPERIMENTAL SECTION

Chemicals

All chemicals were of analytical grade and used as received, unless mentioned otherwise. *N*-acetyl-L-cysteine, L-cysteine·hydrochloride, 1-ethyl-3-[3-(dimethyl-amino)propyl]carbodiimide·hydrochloride (EDC), *N*-hydroxy-sulfosuccinimide (NHS), and ethanolamine·hydrochloride (EA) were purchased from Sigma (St. Louis, MO, USA). All water used was demineralized.

Solutions of EDC (0.4 M in water) and NHS (0.1 M in water) were stored at -20°C. After thawing, equal volumes were mixed prior to activation of a SAM. A solution of EA (1 M in water) was prepared.

Phosphate buffer pH 7.4 (10 or 100 mM) was prepared by mixing solutions of Na_2HPO_4 and NaH_2PO_4 (both from Merck, Darmstadt, Germany). 100 mM KCl (Merck) solution was prepared in water. Recombinant IFN-γ and the antibody

MD-2 have been a kind gift from Dr. P. H. van der Meide (U-Cytech, Utrecht, The Netherlands).[40] IL-2 (Proleukin®) was kindly donated by Dr. R.F.M. Rombouts (Chiron, Amsterdam, The Netherlands).

After addition of water to the freeze-dried samples of MD-2, IFN-γ or IL-2, solutions of 0.1 mg mL^{-1} in 125 mM phosphate buffered saline pH 7.4, were prepared and stored at -80°C. Prior to use they were thawed and further diluted with 10 mM phosphate buffer pH 7.4. Trehalose, present in the MD-2 and IFN-γ samples when received, does not interfere with our measurements.

Mechanical polishing of the electrode

The working electrodes consist of a gold wire (99.9%, Engelhard-Clal, Amsterdam, The Netherlands) with a diameter of 1.00 mm (geometric surface area of 0.785 mm^2) and are press-fitted in Kel-F. They are polished during 30 min with gamma-micropolish B deagglomerated alumina suspension (0.05 μm, Buehler, Lake Bluff, IL) using a Metaserve automatic polisher (Buehler, Coventry, U.K.). Finally, the electrodes are cleaned ultrasonically in water for 15 min.

Experimental setup

For electrochemical pretreatment of the Au working electrodes a confined wall-jet flow-through cell is used, with a saturated calomel reference electrode (SCE) and a glassy-carbon disk auxiliary electrode. The distance between the working and auxiliary electrode is 100 μm. Details of this homemade flow-through cell were described previously.[41] All potentials mentioned are versus SCE. The flow system further consisted of an HPLC pump (LC-10AD, Shimadzu, Kyoto, Japan), a packed HPLC column for additional reduction of flow variations, PEEK capillaries, a fixed-loop injector (50 μL), and a thermostat/cryostat (Julabo F12, Julabo Labortechnik, Seelbach, Germany).

For application of the potential pulses or steps an Autolab PGSTAT10 digital potentiostat/galvanostat was used with GPES 4.5 software (Eco Chemie, Utrecht, The Netherlands). The potential-step measurements were performed with an additional module (Eco Chemie) that allows the current to be sampled at a frequency of 750 kHz. For impedance measurements a FRA-2 module with software version 4.7 (Eco Chemie) was used.

Formation of the immunosensor

After mechanical polishing, the Au electrodes are electropolished by application of potential pulses (+1.6, 0.0, -0.8 V, each 0.1 s) for 30-120 min in 100 mM phosphate buffer, flow 0.1 mL min^{-1}, until a minimum surface roughness has been obtained.[37] Such a pretreated smooth electrode is immersed in a phosphate solution of 1 M cysteine or acetylcysteine (pH 1.25 and 2.30, respectively) during at least 17 h at room temperature. After thoroughly rinsing with water, the electrode with the cysteine or acetylcysteine SAM is transferred to

a thermostatted (23.0°C) flow-through cell. The immunosensor is built up in flow (10 μL min^{-1} of 10 mM phosphate buffer pH 7.4), by successive injections of EDC/NHS, MD-2 (50 μg mL^{-1}) and EA. Then, the antigen IFN-γ is injected in various concentrations. Formation of the immunosensor and detection of IFN-γ have been monitored with both impedance methods and chronoamperometry. IL-2 is used to investigate the nonspecific adsorption.

Chronoamperometry

In chronoamperometry, after each injection, potential steps were applied from 0 to 50 mV versus SCE until successive current-time responses became identical. The current after potential-step application is sampled at a frequency of 750 kHz, usually for 2 ms, i.e., generating about 1500 data points.

According to Berggren et al.[8, 9] the current-time response of an electrode modified with antibody before and after antigen binding, can be described by an equivalent circuit consisting of the solution resistance (R_s) and a double-layer capacitance (C_{dl}) in series. This non-faradaic process can be described by Equation 1:

$$I(t) = \frac{\Delta E}{R_s} \cdot \exp\left(\frac{-t}{R_s \cdot C_{dl}}\right) \qquad \text{(Equation 1)}$$

where *I(t)* is the current as a function of time *t* and ΔE is the potential step. From the slope and intercept of the (linear part of the) log *I(t)*-*t* plot, R_s and C_{dl} could be calculated.[8, 9]

Impedance method

In the impedance measurements[42] an alternating potential (E_{ac}), with an amplitude of 10 mV at various frequencies (*f*) in the range from 10 kHz to 3 Hz, superimposed on a fixed potential (E_{dc} = +0.2 V versus SCE) is applied to the electrode. The impedance *Z* is expressed in terms of a real (*Z′*) and an imaginary (*Z″*) component. Monitoring has been performed at *f* = 113 Hz.

Repeatability of SAM formation

For reproducible formation of the acetylcysteine or cysteine SAM, the method described for thioctic acid SAMs was used.[38] After removal of the SAM from the electrode with a sequence of potential pulses, a new SAM can be formed reproducibly on the same electrode. Then SAMs have more or less identical characteristics. However, we used a large set of Au electrodes, each with slightly different characteristics. This explains (at least partly) the differences in the impedance between experiments.

RESULTS AND DISCUSSION

Selection of the measurement method

SAMs of cysteine or acetylcysteine were formed on electropolished polycrystalline gold electrodes. To detect the binding between MD-2 immobilized via the SAM and IFN-γ in solution, both impedance and chronoamperometry[8, 9] can be used. In immunosensing with impedance measurements, usually, measurements at a single optimized frequency as a function of time provide the required analytical information.[4, 5, 7] The best signal-to-noise ratio is obtained in the frequency range from 80 to 240 Hz. We have adopted a frequency of 113 Hz, following Göpel and co-workers.[4, 5]

Because the goal of our work was to find a method for direct detection of very low concentrations of IFN-γ, impedance and chronoamperometry were compared. The SAM is formed in batch on an electropolished Au electrode. Before and after (see "Au" and "cysteine" in Figure 1b) the SAM formation, potential steps are applied for characterization. Then, in the flow, the SAM is activated with EDC/NHS, MD-2 is immobilized, and the remaining succinimide groups are deactivated with EA.[10, 13, 39] These processes are impedimetrically monitored at f = 113 Hz (Figure 1a). Before IFN-γ is injected, the ac monitoring is interrupted for recording the potential-step response (see (1) in Figures 1a and 1b). The ac monitoring is reestablished and IFN-γ is injected (Figure 1a). Finally, the ac monitoring is terminated for applying a potential step again (see (2) in Figures 1a and 1b).

In Figure 1a, at f = 113 Hz, Z'' shows the immunosensor buildup and detection of IFN-γ. The shift ($\Delta Z''$), the consequence of binding of IFN-γ to immobilized MD-2, is clearly detected (see (2) in Figure 1a). However, the chronoamperometric response of the immunosensor before and after binding of IFN-γ is almost identical (see (1) and (2) in Figure 1b). The difference becomes more clear in a log $I(t)$-t plot (Figure 1c) but remains very small. Apparently, at larger delay times (> 1 ms), the difference increases. This is, at least partly, masked by an increase of noise (see Figure 1c). Moreover, a linear part of the log $I(t)$-t plot as reported by Berggren et al.[8, 9] is absent in our experiments which becomes even more clear in Figure 1d.

We cannot fully explain the discrepancy, but there are differences. Berggren et al.[8, 9] used a homemade four-electrode system, used other SAM-forming compounds, and sampled the current at 50 kHz usually for 0.2 ms after potential-step application, i.e., generating 10 data points for fitting the RC circuit (see Chronoamperometry).[43] Moreover, it turns out that the equivalent circuit of our systems is much more complicated than their simple RC circuit (data not shown).

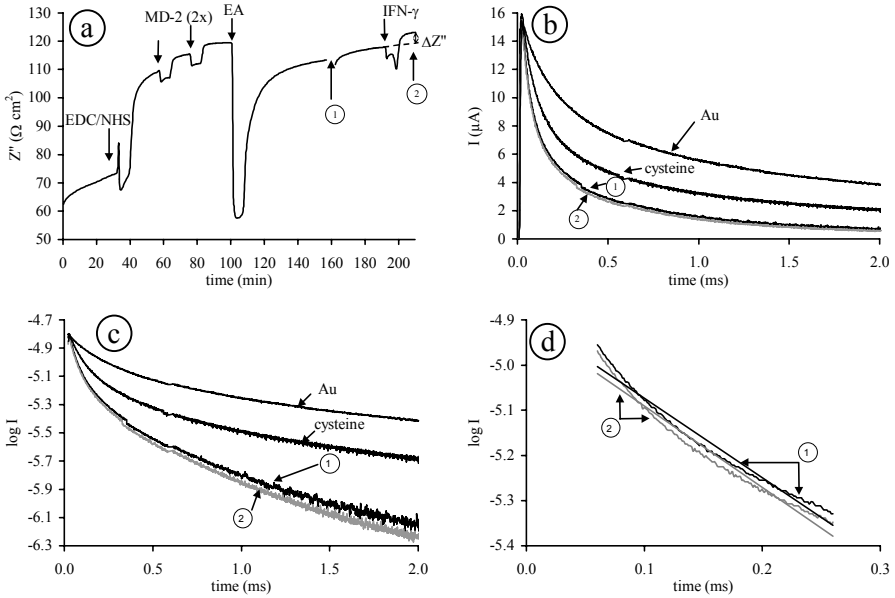

Figure 1. Monitoring of the various stages during immunosensor buildup on a cysteine SAM with impedance measurements and chronoamperometry, and the detection of IFN-γ. Experimental conditions: (a) impedance measurements, the imaginary component of the impedance (Z'') is recorded with $E_{dc} = 0.0$ V, $E_0 = 10$ mV, $f = 113$ Hz; (b) chronoamperometry, the potential is stepped from 0 to +50 mV; (c) logarithmic $I(t)$-t plot of the data presented in (b); (d) log $I(t)$-t plot of the data shown in (b) using the time window as applied by Berggren et al.[8, 9] The current is plotted from 60 to 260 μs; linear regression fits of (1) give a slope of-1.76 and an intercept of -4.90 ($r^2 = 0.973$) and of (2) a slope of -1.80 and an intercept = -4.91 ($r^2 = 0.973$). The experiments are performed in a FIA setup (flow 10 μL min^{-1} of 10 mM phosphate buffer pH 7.4). Injections (50-μL) of EDC/NHS, MD-2 (50 μg mL^{-1}), EA, and IFN-γ (1 μg mL^{-1}). The start of an injection is indicated by an arrow.

It can be concluded that the difference in capacitance caused by binding of IFN-γ to immobilized MD-2 is too small to be measured chronoamperometrically with our instrumentation. Therefore, since for an acetylcysteine-based immunosensor comparable results have been obtained (data not shown), it is clear that for our equipment the impedance method is superior and thus preferred over the potential-step method.

Note: The binding of antibody MD-2 (~160 kDa) to IFN-γ (15.5 kDa) immobilized via a cysteine SAM, gives rise to clear differences in the current-time response (data not shown).

Selection of acetylcysteine

Although from impedance measurements SAMs of cysteine and acetyl-cysteine appear to have comparable characteristics and nonspecific adsorption takes place on both, acetylcysteine has a beneficial characteristic in the possibility to remove nonspecifically adsorbed proteins such as IFN-γ with an injection of 100 mM KCl. Figure 2 shows that IFN-γ (injections 1 and 3) physically adsorbs to the acetylcysteine SAM. However, after injection of 100 mM KCl (injections 2 and 4) the signal returns to the baseline, which indicates that IFN-γ is completely removed without damaging the SAM. On the other hand, injections of KCl on cysteine SAMs leads to an increase in Z''. Therefore, acetylcysteine SAMs will be used for the further development of the electrochemical immunosensor.

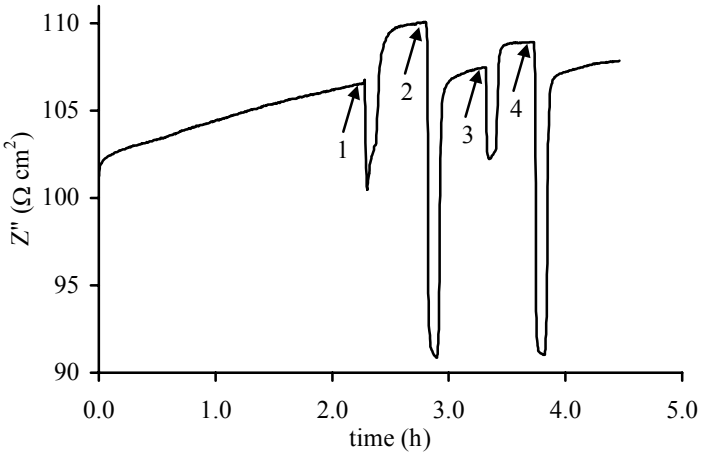

Figure 2. Influence of KCl injections on the desorption of physically adsorbed IFN-γ from an acetylcysteine SAM. The imaginary component of the impedance (Z'') is shown. Injections of (1) 20 fg mL^{-1} IFN-γ, (2) 100 mM KCl, (3) 0.2 fg mL^{-1} IFN-γ, and (4) 100 mM KCl as indicated by the arrows. Experimental conditions: E_{dc} = +0.2 V, E_0 = 10 mV, f = 113 Hz, flow 10 µL min^{-1} of 10 mM phosphate buffer pH 7.4, injection volume; 50 µL.

Immobilization of MD-2 antibodies

The buildup of an immunosensor on an acetylcysteine SAM was monitored impedimetrically. In Figures 3a and 3b the real Z' and the imaginary Z'' part of the impedance Z, measured at 113 Hz during this immobilization process, are shown, respectively. The acetylcysteine SAM is activated using EDC/NHS. Then, the MD-2 antibodies are immobilized. For deactivation of the remaining succinimide groups EA was used.

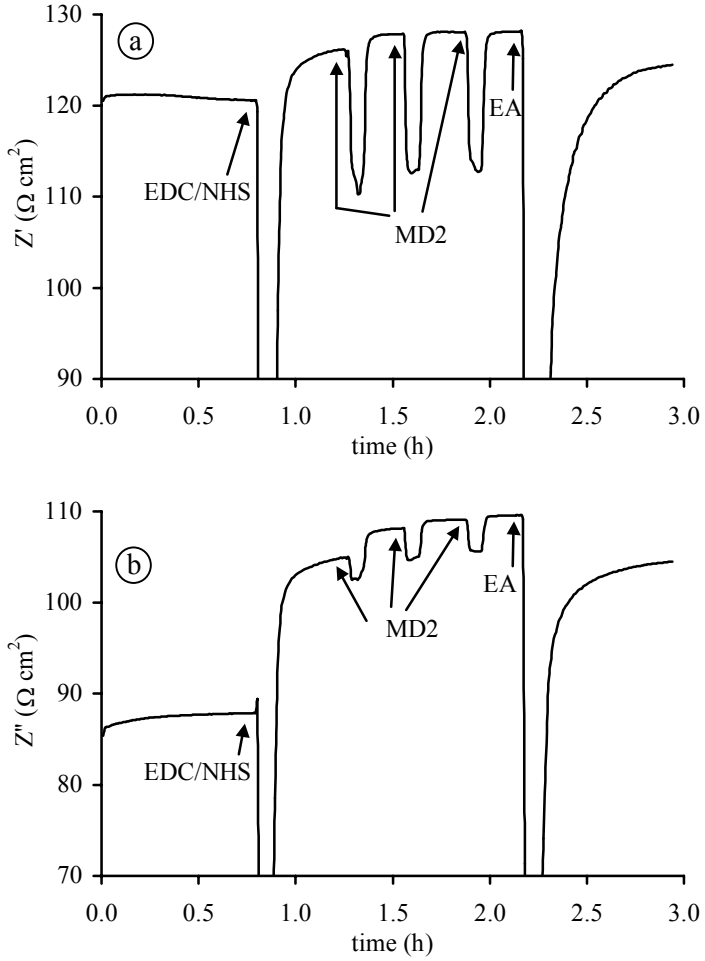

Figure 3. Monitoring of the immunosensor buildup on an acetylcysteine SAM. The (a) real (Z') and (b) imaginary (Z'') component of the impedance Z as a function of time are shown. The arrows indicate the start of an injection. First the SAM is activated with a single injection of EDC/NHS. Next, MD-2 (50 μg mL^{-1}) is injected 3 times. Finally the remaining succinimide groups are deactivated by a single injection of EA. Experimental conditions, see Figure 2.

After three injections of MD-2 both Z' and Z'' are more or less stable indicating maximal coverage of the surface area. From Z'' (Figure 3b) it can be concluded that each MD-2 injection leads to a further increase in Z'', indicating attachment of more MD-2 molecules. By the injection of EA, physically adsorbed MD-2 is desorbed and the remaining succinimide groups are inactivated. EA has a large effect on the configuration/conformation of the sensing layer and the electrical double-layer of the electrode, as reflected by the very long time required for returning to a stable baseline.

Detection of IFN-γ

Using this immunosensor, IFN-γ can be detected with a very high sensitivity. The result of repeated injections of IFN-γ (2 pg mL^{-1}) is shown, both in Z' (Figure 4a) and Z'' (Figure 4b).

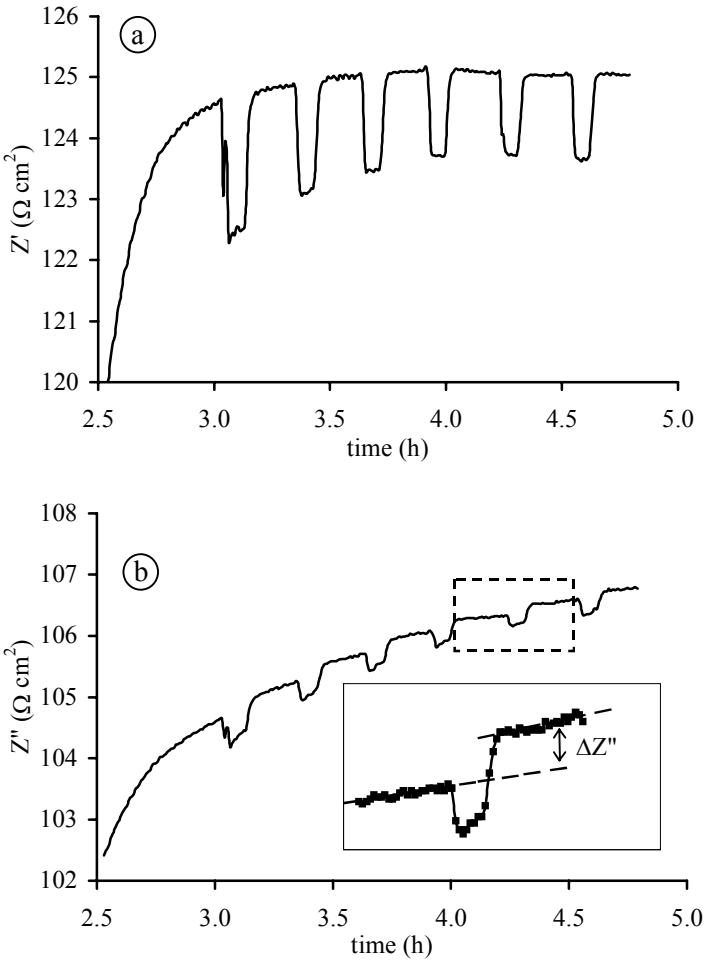

Figure 4. Monitoring of the binding of IFN-γ to MD-2 immobilized via an acetylcysteine SAM. The (a) real (Z') and (b) imaginary (Z'') components of the impedance Z as a function of time are shown. IFN-γ (2 pg mL^{-1}) is injected 6 times. In the inset (Figure 4b) the determination of $\Delta Z''$ due to a 50-µL injection is illustrated. Experimental conditions, see Figure 2.

While activation, attachment of MD-2 and deactivation of the remaining succinimide groups leads to changes both in Z' and Z'' (see Figure 3), binding of IFN-γ primarily leads to changes in Z'' (see Figures 4a and 4b). The effect of each injection was determined by extrapolating the baseline (see inset in Figure 4b).

The corresponding calibration curve is shown in Figure 5 where the change in Z'' ($\Delta Z''$) is plotted versus the cumulative amount of IFN-γ injected. The IFN-γ immunosensor appears to have a reasonable dynamic range at least from 0 to 0.6 pg corresponding to 0 to 12 pg mL^{-1}.

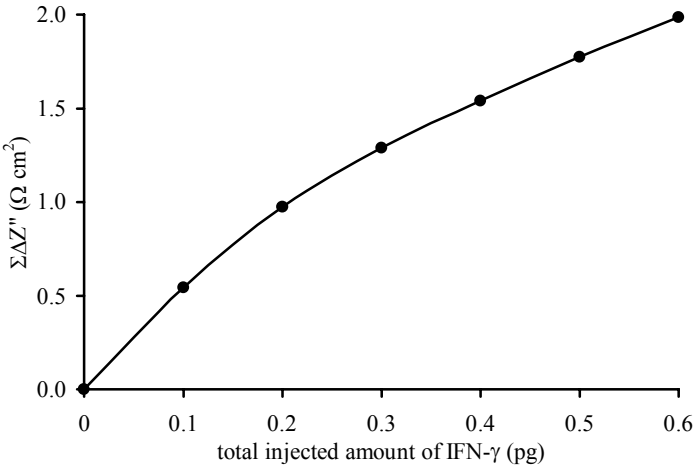

Figure 5. Calibration curve of IFN-γ. The cumulative change in Z'' ($\Sigma\Delta Z''$) is plotted as a function of the total amount of IFN-γ injected. Experimental conditions, see Figures 2 and 4.

Nonspecific interactions

However, it turns out by injections of other proteins, including IL-2, that the response is a combination of specific and nonspecific interactions. This nonspecific adsorption is a major problem in immunosensing, since nonspecific adsorption cannot be distinguished from specific adsorption in (capacitive) electrochemical sensing of unlabeled antigens. Therefore, an additional procedure is required to correct for (or to eliminate) the nonspecific contribution. Many agents in various concentrations have been tested (e.g., KCl, glycine, buffers with various pH) for achieving the desired result: return of the impedance to the baseline after injection. We found that nonspecifically adsorbed proteins can be removed for the greater part by tuning the ionic strength, i.e., by injection of a low concentration of KCl (100 mM in water) without damaging the SAM, the immobilized antibody (and thus maintaining the sensitivity), or desorbing specifically bound antigen. Higher concentrations of KCl result in an instable baseline (Z''), probably caused by a damage of the SAM.[8, 36]

In Figure 6, the effect of several injections of 100 mM KCl on adsorbed proteins is shown. Buffer (1, 2), 0.2 fg mL^{-1} IFN-γ (3, 4), and 100 mM KCl (5) were injected, successively. As expected due to injections (3, 4) Z'' increases, but after the KCl injection (5) a decrease in Z'' occurs, which is assumed to correspond to the removal of nonspecifically adsorbed IFN-γ. An injection (6) of 20 pg mL^{-1}

IL-2 leads to a shift in Z'', but Z'' returns to the baseline after injections of KCl (7, 8). An injection (9) of 20 pg mL^{-1} IFN-γ leads again to a shift, of which a residual shift remains after injections of KCl (10, 11). From these experiments it can be concluded that by the 100-mM KCl injections the nonspecific adsorption (i.e., IL-2) is removed. Moreover, it is assumed that nonspecifically adsorbed IFN-γ is also removed by the KCl injections.

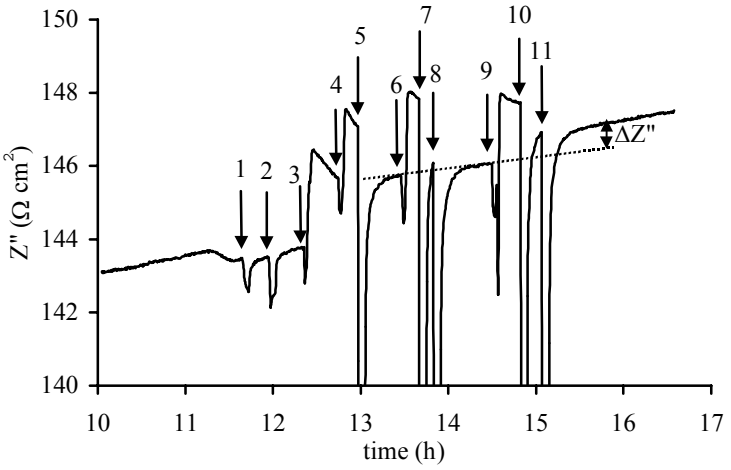

Figure 6. Influence of KCl injections on the desorption of nonspecifically adsorbed proteins from MD-2 immobilized via an acetylcysteine SAM. Z'' as a function of time is shown. As indicated by the arrows, injections of 10 mM phosphate buffer (1, 2), 0.2 fg mL^{-1} IFN-γ (3, 4), 100 mM KCl (5), 20 pg mL^{-1} IL-2 (6), 100 mM KCl (7, 8), 20 pg mL^{-1} IFN-γ (9), and 100 mM KCl (10, 11). Experimental conditions, see Figure 2.

By performing multiple injections of a low concentration of IFN-γ the cumulative change in Z'' is determined. The calibration curve is shown in Figure 7. The result of 12 injections of 0.02 fg mL^{-1} IFN-γ, each followed by an injection of 100 mM KCl, is shown. In this experiment, initially no desorption of protein (IFN-γ) after injection of KCl was observed. However, after multiple injections either no shift occurs upon injection of protein, or the shift is undone by injection of 100 mM KCl. This means that all available specific binding locations are occupied; i.e., the surface is saturated.

After 7 injections, no IFN-γ is bound anymore, because the sensor becomes saturated. Assuming that 7 ag of IFN-γ / 50 μL injection can be bound by the sensor, the upper limit of the dynamic range for application can be approximated by about 0.14 fg mL^{-1}. From Figure 7 it is clear that 1 ag IFN-γ/50-μL injection can be detected, so the detection limit of the sensor is better than 0.02 fg mL^{-1}. As revealed in Figure 7, the statistical variation due to the 50-μL injections is very low. However, the repeatability (the same electrode) is within 10%, since the exact position of the electrode as well as the distance between working and auxiliary

electrode has to be adjusted manually. These uncertainties introduce systematic errors because the effective cell volume will vary to some extent, in addition to the variations in the immunochemical layer (see Repeatability of SAM formation).

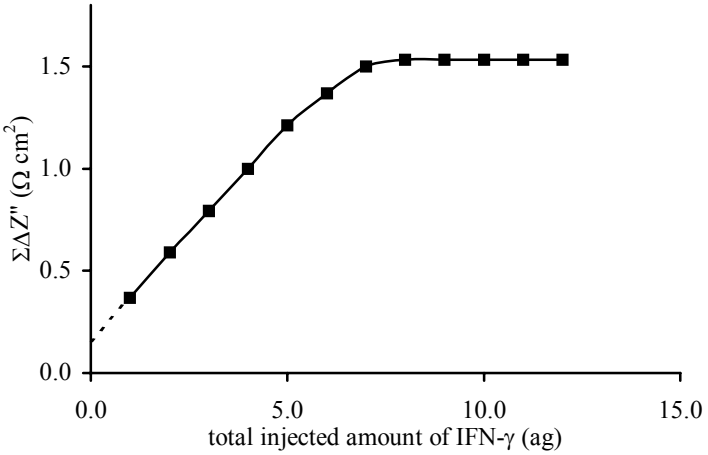

Figure 7. Calibration curve of IFN-γ. The cumulative change of Z'' ($\Sigma\Delta Z''$) of multiple injections of IFN-γ (0.02 fg mL^{-1}), each injection followed by a 100 mM KCl injection, is shown. Experimental conditions, see Figure 2.

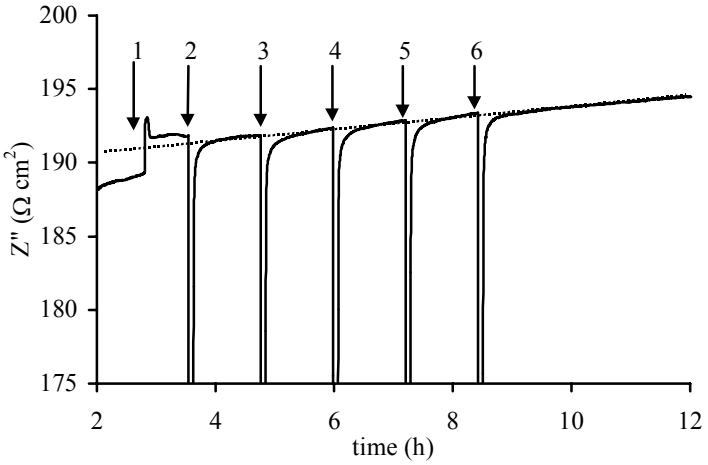

Figure 8. Effect of multiple 100 mM KCl injections on specifically bound IFN-γ. Z'' is shown as a function of time. Injection of 2 pg mL^{-1} IFN-γ (1), followed by 5 injections of 100 mM KCl (2-6). Experimental conditions, see Figure 2.

It turns out that the shift caused by the first injection of IFN-γ is always larger than the shift caused by a subsequent indentical injection. This means that the

change in impedance of a clean surface with only MD-2 is different from that of a MD-2 surface with IFN-γ bound.

In Figure 8 is shown that an injection of 2 pg mL^{-1} IFN-γ causes a shift of 2.5 Ω cm^2. After several injections of 100 mM KCl, a shift of 1.9 Ω cm^2 remains, which is explained by specifically bound IFN-γ. We assume that nonspecifically adsorbed IFN-γ is removed by the first KCl injection(s).

Research is in progress to investigate the applicability of this method in the determination of IFN-γ and other proteins in real samples (e.g., plasma and serum). We are also extending the research for measuring simultaneously the impedance and the response of SPR. In this study, the quantitative and mechanistic aspects of the immunosensor are being investigated further and in more detail.

CONCLUSIONS

An electrochemical immunosensor for direct detection of IFN-γ at attomolar level has been developed. SAMs of cysteine or acetylcysteine, formed on electropolished polycrystalline Au electrodes, have in phosphate buffer pH 7.4 comparable electrochemical characteristics as turns outs from impedance measurements. IFN-γ, that physically adsorbs to these SAMs, can be removed in the flow from the acetylcysteine SAM without damage by use of 100 mM KCl injections. The cysteine SAM is affected by this treatment. Therefore acetylcysteine is preferred over cysteine.

In an on-line procedure in the flow, the carboxylic groups of the SAM are activated by EDC/NHS, a specific antibody (MD-2) against IFN-γ is covalently attached, and the remaining succinimide groups are inactivated with EA. These processes are controlled by monitoring both Z' and Z'' at f = 113 Hz, E_{dc} = +0.2 V, and E_0 = 10 mV.

In the thermostatted setup (23.0°C), samples of unlabeled IFN-γ (in phosphate buffer pH 7.4) are injected and the binding with immobilized MD-2 is monitored with impedance or potential-step methods. While the impedance approach provides unsurpassed detection limits, as low as 0.02 fg mL^{-1} (~1 aM) IFN-γ, the chronoamperometric results are rather poor.

The results as published by Berggren et al.[8, 9] could not be reproduced for detecting IFN-γ with immobilized MD-2. However, MD-2 can clearly be detected chronoamperometrically with immobilized IFN-γ. Therefore, for our goals, impedance methods are preferred.

From a Z''-concentration calibration curve, a dynamic range of 0-12 pg mL^{-1} IFN-γ was established. However, when nonspecific adsorption is taken into account, which can largely be reduced through injections of 100 mM KCl, a much smaller range of IFN-γ remains (0-0.14 fg mL^{-1}).

The immunosensor can be regenerated by using a sequence of potential pulses in the flow by which the SAM with attached MD-2 and bound IFN-γ is completely

removed. When the developed procedures are repeated, the response of the immunosensor is reproducible within 10%.

It is assumed that these extremely low levels of IFN-γ could be detected because of our optimized experimental setup: the thermostatted flow-system, a low flow rate, the electrochemical confined wall-jet flow-through cell for favorable mass-transfer, the electrode pretreatment for optimal smoothness, the immobilization of MD-2 via the acetylcysteine SAM as well as the impedance method employed.

ACKNOWLEDGMENT

This work has been supported by grant UFA44.3392 from the Dutch Technology Foundation (STW). The authors gratefully acknowledge Dr. P. H. van der Meide (U-Cytech) for the donation of MD-2 and IFN-γ and Dr. R.F.M. Rombouts (Chiron) for the gift of IL-2.

REFERENCES

1 Byfield, M. P.; Abuknesha, A. Biochemical aspects of biosensors, *Biosens. Bioelectron.* **1994**, *9*, 373-400.

2 Wink, T.; van Zuilen, S. J.; Bult, A.; van Bennekom, W. P. Self-assembled monolayers for biosensors (A tutorial review), *Analyst* **1997**, *122*, 43R-50R.

3 Tam Chang, S.-W.; Iverson, I. In *Studies in Surface Science and Catalysis*; Dabrowski, A., Eds.; Elsevier: Amsterdam, **1999**; Vol. 120A, p. 917-950.

4 Knichel, M.; Heiduschka, P.; Beck, W.; Jung, G.; Göpel, W. Utilization of a self-assembled peptide monolayer for an impedimetric immunosensor, *Sens. Actuators* **1995**, *B28*, 85-94.

5 Rickert, J.; Göpel, W.; Beck, W.; Jung, G.; Heiduschka, P. A mixed self-assembled monolayer for an impedimetric immunosensor, *Biosens. Bioelectron.* **1996**, *11*, 757-768.

6 Taira, H.; Nakano, K.; Maeda, M.; Takagi, M. Electrode modification by long-chain, dialkyl disulfide reagent having terminal dinitrophenyl group and its application to impedimetric immunosensors, *Anal. Sci.* **1993**, *9*, 199-206.

7 Mirsky, V. M.; Riepl, M.; Wolfbeis, O. S. Capacitive monitoring of protein immobilization and antigen-antibody reactions on monomolecular alkythiol films on gold electrodes, *Biosens. Bioelectron.* **1997**, *12*, 977-990.

8 Berggren, C.; Johansson, G. Capacitance measurements of antibody-antigen interactions in a flow system, *Anal. Chem.* **1997**, *69*, 3651-3657.

9 Berggren, C.; Bjarnason, B.; Johansson, G. An immunological interleukin-6 capacitive biosensor using perturbation with a potentiostatic step, *Biosens. Bioelectron.* **1998**, *13*, 1061-1068.

10 Disley, D. M.; Cullen, D. C.; You, H.-X.; Lowe, C. R. Covalent coupling of Immunoglobulin G to self-assembled monolayers as a method for immobilizing the interfactial recognition layer of a surface plasmon resonance immunosensor, *Biosens. Bioelectron.* **1998**, *13*, 1213-1225.

11 Duschl, C.; Sévin-Landais, A.-F.; Vogel, H. Surface engineering: optimization of antigen presentation in self-assembled monolayers, *Biophys. J.* **1996**, *70*, 1985-1995.

12 Storri, S.; Santoni, T.; Minunni, M.; Mascini, M. Surface modifications for the development of piezoimmunosensors, *Biosens. Bioelectron.* **1998**, *13*, 347-357.

13 Vaughan, R. D.; O'Sullivan, C. K.; Guilbault, G. G. Sulfur based self-assembled monolayers (SAM's) on piezoelectric crystals for immunosensor development, *Fresenius J. Anal. Chem.* **1999**, *364*, 54-57.

14 Wagner, P.; Kernen, P.; Hegner, M.; Ungewickell, E.; Semenza, G. Covalent anchoring of proteins onto gold-directed NHS-terminated self-assembled monolayers in aqueous buffers: SFM images of clathrin cages and triskelia, *FEBS Lett.* **1994**, *356*, 267-271.

15 Homola, J.; Yee, S. S.; Gauglitz, G. Surface plasmon resonance sensors: review, *Sens. Actuators* **1999**, *B54*, 3-15.

16 O'Sullivan, C. K.; Vaughan, R.; Guilbault, G. G. Piezoelectric immunosensors- Theory and applications, *Anal. Lett.* **1999**, *32*, 2353-2377.

17 Allen, S.; Chen, X.; Davies, J.; Davies, M. C.; Dawkes, A. C.; Edwards, J. C.; Roberts, C. J.; Sefton, J.; Tendler, S. J. B.; Williams, P. M. Detection of antigen-antibody binding events with the atomic force microscope, *Biochem.* **1997**, *36*, 7457-7463.

18 Perrin, A.; Lanet, V.; Theretz, A. Quantification of specific immunological reactions by atomic force microscopy, *Langmuir* **1997**, *13*, 2557-2563.

19 Dong, Y.; Shannon, C. Heterogeneous immunosensing using antigen and antibody on gold surfaces with electrochemical and scanning probe detection, *Anal. Chem.* **2000**, *72*, 2371-2376.

20 Skládal, P. Advances in electrochemical immunosensors, *Electroanalysis* **1997**, *9*, 737-745.

21 Wink, T.; van Zuilen, S.; Bult, A.; van Bennekom, W. P. Liposome-mediated enhancement of the sensitivity in immunoassays of proteins and peptides in surface plasmon resonance spectrometry, *Anal. Chem.* **1998**, *70*, 827-832.

22 Severs, A. H.; Schasfoort, R. B. M. Enhanced surface plasmon resonance inhibition test (ESPRIT) using latex particles, *Biosens. Bioelectron.* **1993**, *8*, 365-370.

23 De Vries, E. F. A.; Schasfoort, R. B. M.; van der Plas, J.; Greve, J. Nucleic acid detection with surface plasmon resonance using cationic latex, *Biosens. Bioelectron.* **1994**, *9*, 509-514.

24 Lyon, L. A.; Musick, M. D.; Natan, M. J. Colloidal Au-Enhanced Surface Plasmon Resonance Immunosensing, *Anal. Chem.* **1998**, *70*, 5177-5183.

25 Löfås, S.; Johnsson, B. A novel hydrogel matrix on gold surfaces in surface plasmon resonance sensors for fast and efficient covalent immobilization of ligands, *J. Chem. Soc. Chem. Commun.* **1990**, *21*, 1526-1528.

26 Nakamura, R.; Muguruma, H.; Ikebukuro, K.; Sasaki, S.; Nagata, R.; Karube, I.; Pedersen, H. A plasma-polymerized film for surface plasmon resonance immunosensing, *Anal. Chem.* **1997**, *67*, 4649-4652.

27 Zubritsky, E. New choices for SPR. Emerging products are filling niches in the SPR market., *Anal. Chem.* **2000**, *72*, 289A-292A.

28 Bladon, C. M.; Kindermann, J.; Sommerdijk, N.; Wright, J. D. A surface plasmon resonance study of the binding of antibody LDS47 to self-assembled monolayers of cysteine containing peptides, *J. Chem. Res.* **1999**, *1*, 42-43.

29 Duschl, C.; Liley, M.; Corradin, G.; Vogel, H. Biologically Addressable Monolayer Structures Formed by Templates of Sulfur Bearing Molecules, *Biophys. J.* **1994**, *67*, 1229-1237.

30 You, H. X.; Lin, S. M.; Lowe, C. R. A Scanning tunneling microscopic study of site specifically immobilized Immunoglobulin G on gold, *Micron* **1995**, *26*, 311-315.

31 Moore, A. N. J.; Katz, E.; Willner, I. Immobilization of pyrroloquinoline quinone on gold by carbodiimide coupling to adsorbed polyamines: stability comparison to attachment via a chemisorbed thiol monolayer, *Electroanalysis* **1996**, *8*, 1092-1094.

32 Ben-Dov, I.; Willner, I. Piezoelectric Immunosensors for urine specimens of *Chlamidia trachomatis* employing quartz crystal microbalance microgravimetric analysis, *Anal. Chem.* **1997**, *69*, 3506-3512.

33 Hianik, T.; Snejdarkova, M.; Sokolikova, L.; Meszar, E.; Krivanek, R.; Tvarozek, V.; Novotny, I.; Wang, J. Immunosensors based on supported lipid membranes, protein films and liposomes modified by antibodies, *Sens. Actuators* **1999**, *B57*, 201-212.

34 Ameur, S.; Martelet, C.; Chovelon, J. M.; Ben Ouada, H.; Jaffrezic-Renault, N.; Barbier, D. Sensitive electrochemical detection of antigens using gold electrodes functionalized with antibody moieties, *Eurosensors XII, Proc. 12th Eur. Conf. Solid-State Transducers 9th UK Conf. Sens. Their Appl.* **1998**, *2*, 797-800.

35 Silin, V.; Weetall, H.; Vanderah, D. J. SPR studies of the nonspecific adsorption kinetics of human IgG and BSA on gold surfaces modified by self assembled monolayers (SAMs), *J. Colloid Interface Sci.* **1997**, *185*, 94-103.

36 Liu, M.; Rechnitz, G. A.; Li, K.; Li, Q. X. Capacitive immunosensing of polycylic aromatic hydrocarbon and protein conjugates, *Anal. Lett.* **1998**, *31*, 2025-2038.

37 Hoogvliet, J. C.; Dijksma, M.; Kamp, B.; van Bennekom, W. P. Electrochemical pretreatment of gold electrode surfaces for molecular self-assembly: a study of bulk polycrystalline gold electrodes in phosphate buffer pH 7.4, *Anal. Chem.* **2000**, *72*, 2016-2021. (Chapter 2 of this Ph.D. thesis)

38 Dijksma, M.; Kamp, B.; Hoogvliet, J. C.; van Bennekom, W. P. Formation and electrochemical characterization of self-assembled monolayers of thioctic acid on polycrystalline gold electrodes in phosphate buffer pH 7.4, *Langmuir* **2000**, *16*, 3852-3857. (Chapter 3 of this Ph.D. thesis)

39 O'Shannessy, D. J.; Brigham-Burke, M.; Peck, K. Immobilization chemistries suitable for use in the BIAcore surface plasmon resonance detector, *Anal. Biochem.* **1992**, *205*, 132-136.

40 Van der Meide, P. H.; Dubbeld, M.; Schellekens, H. Monoclonal antibodies to human immune interferon and their use in a sensitive solid-phase ELISA, *J. Immunol. Methods* **1985**, *79*, 293-305.

41 Dalhuijsen, A. J.; van der Meer, T. H.; Hoogendoorn, C. J.; Hoogvliet, J. C.; van Bennekom, W. P. Hydrodynamic properties and mass transfer characteristics of electrochemical flow-through cells of the confined wall-jet type, *J. Electroanal. Chem.* **1985**, *182*, 295-313.

42 Bard, A. J.; Faulkner, L. R. *Electrochemical methods. Fundamentals and Applications,* John Wiley & Sons Ltd: New York, **1980**.

43 Berggren, C.; Bjarnason, B.; Johansson, G. Instrumentation for direct capacitive biosensors, *Instrum. Sci. Techn.* **1999**, *27*, 131-140.

7

General Conclusions and Perspectives

The achieved improvement in the sensitivity of electrochemical immunosensors (as described in Chapter 6) has been accomplished by optimizing all experimental conditions. It is assumed that extremely low amounts could be detected because of the thermostatted flow-system, the low flow rate, the favorable mass-transfer of the electrochemical confined wall-jet flow-through cell, the developed electrode pretreatment for optimal smoothness, immobilization of the antibody MD-2 via the acetylcysteine SAM as well as the impedance method employed.

Discrimination between specifically and nonspecifically bound proteins can be accomplished by injections of KCl. It remains to be investigated if this approach can be applied in general, for achieving the final goal: direct measurement of proteins in real samples like plasma or serum.

Another strategy to be investigated would be the use of antibody fragments, i.e., Fab' or $F(ab)_2$. It is expected that, because of the smaller size of these fragments, a better sensitivity of electrochemical immunosensing can be achieved.

The possibility to detect very small amounts of proteins and peptides offers various opportunities. Diseases can be diagnosed in a much earlier stage. An example of a protein indicating a disease is IFN-γ, which is used as model compound in this Ph.D. thesis. This protein is elicited in reaction to inflammation. Another example would be the early detection of, e.g., toxins in low concentration, a major problem in biotechnology.

Furthermore, the sensor may be applied in the investigation of the kinetics of interaction, since the sensor responds in real time.

Application of this type of sensor in a multichannel setup, with a different antibody immobilized in each channel, affords detection of different proteins in a single sample at the same time. Using high-throughput screening a range of compounds can be tested for interaction with a certain protein or peptide, immobilized on an electrode. This method may be explored in combinatorial chemistry and proteomics.

A reproducibility of about 10% in the results is found, because of variation in the position of the working and auxiliary electrode. The reproducibility can be improved by performing all actions in the flow, which was one of our goals. However, for a SAM to be reproducible and stable it has to be allowed to form during at least 17 h. We have not applied this prolonged pumping of TA through the cell.

Good reproducibility is achieved on a single electrode. Non-reproducibility arises for the larger part because of the inherent sensitivity of the impedance method applied. A small difference in the SAM structure causes large differences in the impedance results. To solve the problem of the differences in SAM formation on different electrodes, their cause has to be found. By using hexacyanoferrate(II/III) more information about the SAM formation can be obtained. However, in the presence of this redox probe, the characterization method influences the SAM characteristics. The differences in structure of the surface and the SAM can be further investigated using surface characterization methods like scanning tunnelling microscopy or atomic force microscopy.

Currently, electrochemistry is being applied in combination with surface plasmon resonance (SPR). These methods are complementary in some cases. For example, while binding of a large compound to a layer, that has a very low capacitance, is not observed in impedimetry, in SPR the binding results in a large shift. A combination of electrochemistry and quartz crystal microbalance (QCM) yields information on changes in resistance, capacitance and mass. Combinations can be made with various methods to obtain the required information.

Another problem we encountered which remains to be solved, is the large difference in behaviour for SAM formation on thin-layer versus polycrystalline gold electrodes. Since the SPR and QCM methods use evaporated gold layers on glass with a titanium or chromium adhesion layer, the "polycrystalline" results cannot be extrapolated directly to "thin-layer" results.

Summary

In this Ph.D. thesis, the development of an immunosensor for direct electrochemical detection of unlabeled proteins is described. This immunosensor is based upon antibodies immobilized on a self-assembled monolayer (SAM) of sulfur-containing molecules on a gold electrode. Because a reliable sensor has to be both stable and reproducible, preparation of stable SAMs was of paramount importance. Further, to be able to measure extremely low protein concentrations, a sensing layer with a high capacitance (i.e., a thin layer) is required. Also, the sensor has to be specific and reusability is preferred.

In **Chapter 1**, an overview of literature on electrochemical immunosensors capable of measuring unlabeled proteins has been given. Sensors have been described based on antibodies (or antigens) immobilized in or on silanized Si/SiO_2, silanized metal, polypyrrole, SAMs on gold electrodes and bilayer lipid membranes. Various electrochemical detection methods have been used, including amperometry and impedimetry. While the research on most methods is not continued because of the many disadvantages, sensors based on SAMs offer opportunities for sensitive and direct detection of unlabeled proteins and peptides.

For the formation of reproducible and stable SAMs, the actual state of the gold surface plays an important role. In **Chapter 2**, a method for decreasing the surface roughness of mechanically polished gold electrodes is described. This electro-polishing effect is obtained by alternately oxidizing and reducing the gold in a flow system (100 mM phosphate buffer pH 7.4). The most effective method is a triple pulse potential of +1.6, 0.0, and –0.8 V versus SCE and pulse widths of 100 ms for each potential, for prolonged time (2000 - 5000 s).

The investigation of the influence of the conditions and time of SAM formation on the characteristics is described in **Chapter 3**. SAMs are characterized with impedimetry at 0.2 V versus SCE and a superimposed sinusoidal potential with an amplitude of 10 mV, in the frequency range from 10 kHz to 50 mHz. Stable SAMs of thioctic acid (TA) are reproducibly formed on electropolished gold electrodes from a stirred 50 mM solution in 100 mM phosphate buffer pH 7.4 at an applied potential of 0.0 or +0.2 V versus SCE. The TA SAMs are stable in 100 mM phosphate buffer pH 7.4, and when protected from light, also in buffered 2 mM hexacyanoferrate(II/III) solution. Using the triple pulse treatment for 15 min, the TA SAM can be removed completely, recovering the initial state of the gold electrode, as deduced from potential-step experiments (chronoamperometry). This way TA SAMs can be formed and removed repeatedly and reproducibly on a single electrode.

In **Chapter 4,** the influence of hexacyanoferrate(II/III), a redox probe often applied in the characterization of SAMs and impedimetric immunosensing, on SAMs of TA and 11-mercaptoundecanoic acid (MUA) is described. The change in characteristics of these SAMs is studied in the dark and during subsequent

exposure of the solution to light, with impedimetry by recording frequency scans (ranging from 10 kHz to 50 mHz) at regular time intervals at 0.2 V versus SCE and a superimposed sinusoidal potential with an amplitude of 10 mV. These frequency scans have been modelled with an electrochemical equivalent circuit. From this model it was found that, as expected from the chain lengths of TA and MUA, charge transfer and diffusion of the redox probe are hindered more by a MUA SAM than by a TA SAM, and that the capacitive component is lower in case of a MUA SAM.

After exposure of the solution to light, a relatively rapid decrease in the resistances and increase in the double-layer capacitance is observed. The manner in which resistances and capacitances change in case of the TA SAM, suggests that TA molecules are gradually removed from the SAM. A possible mechanism is etching of the gold substrate by CN^- ions through pin-holes in the SAM. Support of this mechanism is obtained from the large difference in characteristics of the gold electrode before SAM formation and after long-term incubation in illuminated buffered hexacyanoferrate(II/III) solution, pointing to a change in the structure of the gold, and the etching of thin gold-layers in this solution.

It can be concluded that, because stability is an important property of an immunosensor, measurements can better be performed in absence of this redox probe.

In **Chapter 5** the development of an impedimetric immunosensor based upon SAMs of TA on an electropolished gold electrode is described. In an on-line procedure in the flow (50 mM phosphate buffer pH 7.4, thermostatted at 23.0°C) a specific antibody (MD-2) against interferon-γ (IFN-γ, a small protein with molecular weight 15.5 kDa) is covalently attached following carbodiimide/ succinimide activation of the carboxylic groups of the SAM. This procedure is monitored impedimetrically at a frequency of 113 Hz, a potential of 0.2 V versus SCE and a superimposed sinusoidal potential with an amplitude of 10 mV. Despite the fact that 2 fg mL^{-1} could be detected, this sensor is not yet applicable to determine IFN-γ in samples containing other proteins (i.e., interleukin-2), because specific and non-specific adsorption could not be distinguished.

The application of SAMs of cysteine and acetylcysteine has been studied in an immunosensor for IFN-γ using both chronoamperometry and impedimetry, as described in **Chapter 6.** SAMs of acetylcysteine are found to have beneficial characteristics in the possibility to remove non-specifically adsorbed proteins with injections of 100 mM KCl, which leads in case of cysteine SAMs to damage. In the thermostatted setup (23.0°C), samples of unlabeled IFN-γ (in phosphate buffer pH 7.4) are injected and the binding with immobilized MD-2 is monitored with impedimetry or chronoamperometry. While the chronoamperometric results are rather poor, the impedance approach provides unsurpassed detection limits.

From a calibration curve (i.e., Z'' versus the amount injected), recorded by multiple 50-μL injections of 2 pg mL^{-1} of IFN-γ, a dynamic range of 0-12 pg mL^{-1}

could be derived. However, when non-specific adsorption is taken into account, which has been found to be largely reduced through injections of 100 mM KCl, a much smaller dynamic range of 0-0.14 fg mL^{-1} remains. The detection limit is as low as 0.02 fg mL^{-1} (~1 aM) IFN-γ.

These immunosensors can be regenerated by using a sequence of potential pulses in the flow by which the SAM with attached MD-2 and bound IFN-γ is completely removed. When repeating the developed procedures described above, the response of the immunosensor is reproducible within 10%.

In conclusion, a tremendous improvement in the sensitivity of immunosensing has been accomplished by optimizing the experimental conditions, including pretreatment of the gold, the formation of thin SAMs, and the measurement method. This method can, for example, be applied in the early detection of diseases. In a multichannel set-up, with a different protein immobilized in each channel, detection of various proteins in a sample at the same time is possible.

Samenvatting

In dit proefschrift wordt de ontwikkeling van een immunosensor voor directe electrochemische detectie van ongelabelde eiwitten beschreven. De immunosensor bestaat uit antilichamen geïmmobiliseerd op een zelf-assemblerende monolaag (SAM) van zwavelbevattende moleculen op een goudelectrode. Omdat een sensor alleen betrouwbaar is als deze stabiel en reproduceerbaar is, is de vorming van een stabiele SAM (de basis van de sensor) van groot belang. Om een zeer lage concentratie eiwit te kunnen meten, is het bovendien vereist dat de sensorlaag een grote electrische capaciteit heeft (d.w.z. dun is). Daarnaast moet de sensor specifiek zijn en bij voorkeur regenereerbaar.

In **Hoofdstuk 1** wordt een overzicht gegeven van de literatuur over electrochemische immunosensoren waarmee ongelabelde eiwitten kunnen worden gemeten. De beschreven sensoren zijn gebaseerd op antilichamen (of antigenen), geïmmobiliseerd in of op gesilaniseerd Si/SiO_2, gesilaniseerd metaal, polypyrrool, SAMs op goudelectroden en lipide dubbellaag membranen. Verscheidene electrochemische detectietechnieken zijn toegepast, waaronder amperometrie en impedimetrie. Hoewel het onderzoek aan de meeste methoden inmiddels gestopt is, vanwege de vele nadelen, blijken sensoren op basis van SAMs uitstekende mogelijkheden te bieden voor gevoelige en directe detectie van ongelabelde eiwitten en peptiden.

Voor de vorming van reproduceerbare en stabiele SAMs is de staat van het goudoppervlak van groot belang. In **Hoofdstuk 2** wordt een methode beschreven om de oppervlakteruwheid van mechanisch gepolijste goudelectroden te verminderen. Dit electropolijsten van het goudoppervlak wordt bereikt door afwisselend te oxideren en te reduceren in een doorstroomsysteem (100 mM fosfaat buffer pH 7,4). De meest effectieve methode is het aanleggen van een pulspotentiaal van +1,6, 0,0 en -0,8 V versus de verzadigde calomel electrode (SCE) met pulsbreedten van 100 ms voor elke potentiaal, gedurende langere tijd (2000 – 5000 s).

In **Hoofdstuk 3** wordt het onderzoek naar de invloed van condities en tijdsduur van SAM-vorming op de eigenschappen van die SAM beschreven. De SAMs worden gekarakteriseerd met impedimetrie bij een potentiaal van 0,2 V versus SCE en een gesuperpositioneerde wisselspanning met een amplitude van 10 mV en frequencies van 10 kHz tot 50 mHz. Stabiele SAMs van thioctic acid (TA) worden reproduceerbaar gevormd op geëlectropolijste goudelectroden in een 50 mM oplossing van dit disulfide in 100 mM fosfaatbuffer pH 7,4 bij een aangelegde potentiaal van 0,0 of +0,2 V versus SCE, onder roeren. De TA SAMs zijn stabiel in 100 mM fosfaatbuffer pH 7,4, en indien afgeschermd van licht ook in een gebufferde (pH 7,4) 2 mM hexacycanoferraat(II/III) oplossing. Door de eerder genoemde pulsmethode toe te passen gedurende 15 minuten, wordt de TA SAM volledig verwijderd. Uit potentiaalstap experimenten (chronoamperometrie)

kan worden afgeleid dat de goudelectrode hierdoor inderdaad terugkomt in zijn begintoestand. Op deze manier kunnen TA SAMs reproduceerbaar worden gevormd op en verwijderd van één enkele electrode.

In **Hoofdstuk 4** wordt de invloed van hexacyanoferraat(II/III), een redoxkoppel dat regelmatig is toegepast in de karakterisering van SAMs en bij impedimetrische immunosensoren, op SAMs van TA en 11-mercapto-undecaanzuur (MUA) beschreven. De verandering in de karakteristieken van deze SAMs is bestudeerd in het donker en de daaropvolgende blootstelling aan licht, met impedimetrie door het regelmatig opnemen van frequentiescans (met een bereik van 10 kHz tot 50 mHz) bij 0,2 V versus SCE en een gesuperpositioneerde wisselspanning met een amplitude van 10 mV. Vervolgens is er een equivalent circuit afgeleid waarmee deze frequentiescans kunnen worden beschreven. Uit dit model bleek, zoals verwacht op basis van de ketenlengte van TA en MUA, dat ladings-overdracht en diffusie van het redoxkoppel meer gehinderd wordt door een MUA SAM dan door een TA SAM en dat de capacitieve component van de MUA SAM lager is.

Na blootstelling aan licht nemen de weerstanden relatief snel af terwijl de dubbellaagcapaciteit toeneemt. De manier waarop weerstand en capaciteit veranderen in het geval van de TA SAM wijst erop dat TA moleculen geleidelijk uit de SAM worden verwijderd. Een mogelijk mechanisme is etsing van het goudsubstraat door CN^- ionen via kleine openingen (zogenaamde pin-holes) in de SAM. Verdere aanwijzingen hiervoor zijn: het grote verschil in de eigenschappen van de goudelectrode vóór de SAM-vorming en ná een lange incubatie van de SAM in een belichte gebufferde hexacyanoferraat(II/III) oplossing (wat wijst op verandering in de goudstruktuur), en het feit dat dunne goudlagen worden geëtst in die oplossing.

Aangezien een immunosensor stabiel moet zijn, is het gebruik van dit redox-koppel af te raden.

In **Hoofdstuk 5** wordt de ontwikkeling van een impedimetrische immuno-sensor op basis van TA SAMs op een geëlectropolijste goudelectrode beschreven. In een doorstroom systeem (50 mM fosfaatbuffer pH 7,4, gethermostreerd bij 23,0ºC) wordt een specifiek antilichaam (MD-2) tegen interferon γ (IFN-γ, een klein eitwit met een molecuulgewicht van 15,5 kDa) covalent gebonden aan de SAM na activering van de carboxylgroepen met carbodiimide/succinimide. Deze procedure is impedimetrisch gevolgd bij een frequentie van 113 Hz, een potentiaal van 0,2 V versus SCE en een gesuperpositioneerde wisselspanning met een amplitude van 10 mV. Ondanks het feit dat 2 fg mL^{-1} gedetecteerd kon worden, is deze sensor vooralsnog niet toepasbaar om IFN-γ te detecteren in monsters die ook andere eitwitten bevatten (b.v. interleukine-2), omdat geen onderscheid gemaakt kan worden tussen specifieke en niet-specifieke adsorptie.

Het gebruik van SAMs van cysteine en acetylcysteine in een immunosensor voor IFN-γ is bestudeerd met chronoamperometrie en impedimetrie, zoals

beschreven in **Hoofdstuk 6**. Met SAMs van acetylcysteine blijkt het mogelijk te zijn om niet-specifiek geadsorbeerde eiwitten te verwijderen met injecties van 100 mM KCl, terwijl SAMs van cysteine hierdoor worden aangetast. In de gethermostreerde opstelling (23,0ºC) worden monsters van IFN-γ (in fosfaatbuffer pH 7,4) geïnjecteerd. De binding aan geïmmobiliseerd MD-2 wordt gevolgd met impedimetrie of chronoamperometrie. De chronoamperometrische techniek leverde slechte resultaten op, met de impedimetrische techniek werden daarentegen onovertroffen detectielimieten bereikt.

Uit een ijkcurve (Z'' versus de geïnjecteerde hoeveelheid) opgenomen door meerdere malen 50 µL van 2 pg mL^{-1} IFN-γ te injecteren, kon een dynamisch bereik van 0-12 pg mL^{-1} worden afgeleid. Echter, als rekening wordt gehouden met de niet-specifieke adsorptie, die sterk gereduceerd blijkt te kunnen worden door injecties van 100 mM KCl, blijft er een dynamisch bereik van 0-0.14 fg mL^{-1} over. De detectielimiet is 0.02 fg mL^{-1} (~1 aM) IFN-γ, wat betekent dat extreem kleine hoeveelheden gedetecteerd kunnen worden.

Deze immunosensoren kunnen worden geregenereerd met de pulsmethode. Hierbij wordt de SAM met gebonden MD-2 en IFN-γ volledig verwijderd. Na herhaling van bovenstaande procedure is de respons van de immunosensor reproduceerbaar binnen 10%.

Concluderend, er is een enorme verbetering in gevoeligheid van dit type immunosensoren bereikt door de experimentele omstandigheden te optimaliseren met inbegrip van de voorbehandeling van het goud, de vorming van de SAM en de keuze van de meetmethode. Deze methode kan bijvoorbeeld worden toegepast voor diagnose van bepaalde ziektes in een vroeg stadium. In een meerkanaalsopstelling, waarbij in ieder kanaal een ander eiwit is geïmmobiliseerd, is detectie van verschillende eiwitten in een monster tegelijkertijd mogelijk.

Dankwoord

Het onderzoek waar ik me de afgelopen 4 jaren mee heb beziggehouden, heeft uiteindelijk toch tot mooie resultaten geleid, ondanks het nogal demotiverende eerste jaar van dit onderzoek waarin we tevergeefs geprobeerd hebben een veelbelovend lijkende methode te reproduceren. Aan dit resultaat hebben velen een bijdrage geleverd.

Gelukkig is Wout van Bennekom in staat geweest om dit onderzoek te blijven begeleiden. Door zijn plotselinge ziekte in het eerste jaar is dat nog een tijdlang erg onzeker geweest. In het schrijven van wetenschappelijke publicaties heb ik een goede leerschool gehad en ik zal de opgedane kennis zeker goed kunnen gebruiken nu ik in de wetenschap verder ben gegaan.

De gesprekken met Auke Bult waren altijd erg gezellig en leerzaam. Het was alleen jammer dat we niet over electrochemie konden praten. Het is nu toch gebleken deze techniek ontzettend interessante mogelijkheden biedt in de analyse van eiwitten. Ook mijn tweede promotor, Fred Hagen bedank ik voor zijn inbreng, als lid van de gebruikerscommissie van STW en als promotor. Ook voor hun kritische blik op de tekst van mijn artikelen en/of dit proefschrift bedank ik Wout, Auke, Fred en Joop Hoogvliet.

Bertwin Kamp is iemand van wie ik altijd op aan kon (al besefte ik dat niet meteen). Bertwin, jij gaf mij de mogelijkheid te praten over literatuur en onze eigen ervaringen, zodat ik mijn gedachten kon ordenen. Je stak, gelukkig, je eigen mening ook nooit onder stoelen of banken. Zeker in de tijd toen Wout, ziek was, heb ik erg veel profijt gehad van jouw aanwezigheid. Je handigheid is ook vaak goed van pas gekomen. De indeling van het lab werd steeds praktischer. Jouw aandeel in het werk is enorm belangrijk voor de resultaten die uiteindelijk bereikt zijn. Ik ben blij dat je het hebt volgehouden in Utrecht te werken ondanks je enorm lange reistijd. Of moet ik zeggen dat ik geluk gehad heb dat er zo weinig banen zijn in het oosten des lands?

Ook vele andere collega's hebben direct dan wel indirect een rol gespeeld bij het tot stand komen van dit proefschrift. Thijs Wink heeft destijds in onze groep de eerste stappen gezet voor het gebruik van SAMs, wat uiteindelijk een belangrijk onderdeel van mijn onderzoek is geworden. Martin Bart heeft me, door zijn enthousiasme, door een paar moeilijkere momenten heen gesleept. Martin, ik vond het erg prettig met jou uitgebreid te kunnen filosoferen over literatuur en (schijnbaar) vreemde resultaten. Helaas komt mijn vertrek je gezondheid niet ten goede: de belemmering tegen roken op de zitkamer is verdwenen. Peter van Os was lange tijd de spil waar de groep om draaide. Wie kan er nu werken zonder een kop koffie of thee op z'n tijd? Ook met computerproblemen kon ik altijd bij jou terecht. Bedankt ook voor het opofferen van een aantal van je SPR-plaatjes aan het hexacyanoferraat-geweld. Helma van der Horst heeft een enorme indruk op mij achtergelaten. Ik bewonder je om je vermogen om anderen op te beuren,

ondanks je eigen problemen. Onze zinnige en minder zinnige gesprekken hebben mij enorm geholpen. Je hebt een enorm goede kijk op het onderzoek en hebt er zeker aan bijgedragen dat ik inmiddels een stuk mondiger ben. Ik vond het erg leuk dat je de afgelopen jaren regelmatig even langskwam om bij te praten.

Aan het onderzoek hebben ook een aantal studenten een bijdrage geleverd. Menno Jelluma heeft vol inzet gewerkt in een periode waarin nog niets leek te lukken. In een keuzevak heeft Esther van den Born later het werk van Menno voortgezet, wat uiteindelijk in een publicatie is verwerkt. Dat het mogelijk is om in korte tijd toch prachtige resultaten te krijgen, wordt bewezen door de poster van Floris van Haselen en Martin Bart, die op "Eirelec '98 in Dublin is gepresenteerd.

Ron van't Hof bedank ik voor zijn hulp bij de problemen met de eiwitten en Matthias Wahls voor zijn inleidende werk aan de infrarood metingen. Jammer dat zij ons snel al weer verlieten. Natuurlijk zal ik de gezellige gesprekken in de "wandelgangen" en koffie/thee en lunch-pauzes niet snel vergeten. Marnix Hoitink, Gerard Wiese, Jan Teeuwsen, Thom Stroink, Johan Rozenbrand, Mirjam Damen, Jan de Groot, Rianne van Maanen, Rolf Sparidans, Willy Underberg, alle al eerder genoemde collega's, en alle studenten die in de tijd voorbij trokken:Gerald, Hans, Inge, Matthijs, Charles, Sicco, Steven, Annemarie, Karen, Jeroen, Diana, Martin-Jan, Pim, Petra en Tom, bedankt hiervoor.

Aangezien het project gefinancierd werd door NWO, vond er ieder half jaar een vergadering plaats waarin geïnteresseerden, in de gebruikers-commissie van STW, op de hoogte werden gebracht van de stand van zaken. Vaak kwamen daar interessante discussies uit voort. Ik wil de leden van de commissie, de heren Boontje, Bos, Holthuis, Van Dijk, Van Es, Bijleveld bedanken voor hun interesse en hun inbreng.

In de gebruikerscommissie was ook steeds Eco Chemie zeer actief vertegenwoordigd: in eerste instantie Gertjan Brug en later Timoer Frelink. Ik heb erg veel gehad aan de steun en belangstelling voor het onderzoek die we kregen vanuit dit bedrijf. Timoer, bedankt voor je hulp bij de impedantiemetingen. Ondanks je drukke werk kon ik toch altijd bij je terecht met vragen. En was er een probleem met de software: een telefoontje naar Sef Coenen gaf altijd resultaat.

Bernard Boukamp bedank ik voor zijn hulp bij het fitten van de impedantiemetingen, waardoor ik een mechanisme voor de afbraak van de SAMs heb kunnen omschrijven.

Zoals vaak bij een chemisch onderzoek, was ook voor mij de hulp van de instrumentele dienst van groot belang. Ik wil speciaal Hans Vonk bedanken voor het maken van de elektrodes. De mensen van de glasblazerij wil ik bedanken voor de vele meetcellen die zij in de afgelopen jaren hebben gemaakt. Het is gebleken dat als er één breekt, er nog snel een aantal volgen. Toch zaten we nooit zonder. Ik hoefde me ook nooit zorgen te maken over de toevoer van eiwitten. Een telefoontje aan Peter van der Meide (U-Cytech) was genoeg. Voor de prachtige

posters om het onderzoek te presenteren en ook de omslag van dit boekje bedank ik de grafische dienst.

Voor alle administratieve zaken en af en toe dat gezellige praatje bedank ik Anneke Warnaar en Nel Annen. Ook Linda Hutzezon was altijd bereikbaar voor vragen en heeft me menigmaal op weg geholpen. Bert Janssen bedank ik voor zijn vertrouwen en hulp. Als ik dat niet gehad had, zou ik waarschijnlijk het onderzoek niet hebben afgerond.

Om een promotieonderzoek te kunnen voltooien is ook de steun van familie en vrienden van belang. Hierover had ik niet te klagen, al bleef het moeilijk uit te leggen dat ik niet bezig was met “afstuderen” of mijn “scriptie”. Mijn ouders hebben me altijd gestimuleerd om zoveel mogelijk te doen met mijn capaciteiten en hebben herhaaldelijk getracht me mijn onzekerheid over mijn eigen kunnen uit het hoofd te praten. Het is eindelijk doorgedrongen dat een beetje meer zelfvertrouwen wel op zijn plaats is. Ook Wouter heeft gelijk gekregen met zijn “Niet zeuren zus, je haalt het toch wel, dat is al vaker gebleken.” Ik vind het wel jammer dat je dit nu in Mexico-stad moet lezen en niet bij de promotie aanwezig zult zijn. Ik en vele anderen hadden je graag eens gezien in een chique pak (als paranimf).

En dan Martijn. Je wordt als laatste genoemd, maar dat wil zeker niet zeggen dat je het minst belangrijk was. Integendeel, met je rustige en begrijpende aard ben je de afgelopen jaren een enorme steun voor me geweest. Naast het geven van morele steun heb je ook concreet bijgedragen aan dit proefschrift. Het uniform maken van de grafieken was opeens een stuk eenvoudiger toen je er een makro voor geschreven had (waar overigens ook door anderen al dankbaar gebruik van wordt gemaakt). Ook was je hulp bij de tekstopmaak zeer welkom. Sommigen zetten er vraagtekens bij of het wel verstandig was om in het laatste jaar van mijn promotieonderzoek te trouwen. Ik heb er zelf geen moment spijt van gehad.

Curriculum Vitae

Martine Dijksma werd op 8 februari 1973 in Delft geboren. Het VWO diploma werd behaald in 1991 aan het Christelijk Lyceum Delft en hetzelfde jaar werd gestart met de studie Scheikunde aan de Universiteit Utrecht. Het afstudeeronderzoek, met als onderwerp de substraatspecificiteit van vetzuur-hydroperoxide lyases, werd gedaan bij de vakgroep Bio-Organische chemie van de Faculteit Scheikunde. Daarnaast zijn er nog een drietal stages uitgevoerd. Bij de vakgroep Voedingsmiddelen van Dierlijke Oorsprong van de Faculteit Diergeneeskunde van de Universiteit Utrecht werd een HPLC methode ontwikkeld voor het scheiden en detecteren van het diergeneesmiddel oxytetracycline en afbraakprodukten in vlees. Bij de vakgroep Biomedische analyse van de Faculteit Farmacie, Universiteit Utrecht is gewerkt aan de ontwikkeling van een Liposome Immunoassay (LISA) voor humaan IFN-γ. Tenslotte heeft zij bij Organon in Oss gewerkt aan de conformatieanalyse van een anti-thrombotisch pentasaccharide met behulp van verschillende NMR-technieken.

Op 1 oktober 1996 is zij gestart met het promotieonderzoek bij de disciplinegroep Biomedische Analyse van de Universiteit Utrecht, met dit proefschrift als resultaat.

Sinds 1 februari 2001 is zij werkzaam aan de Technische Universiteit Eindhoven als postdoc op het gebied van electrochemische energieopslag.

List of Publications

Hoogvliet, J. C.; Dijksma, M.; Kamp, B.; van Bennekom, W. P. Electrochemical pretreatment of gold electrode surfaces for molecular self-assembly: a study of bulk polycrystalline gold electrodes in phosphate buffer pH 7.4, *Anal. Chem.* **2000**, *72(9)*, 2016-2021.

Dijksma, M.; Kamp, B.; Hoogvliet, J. C.; van Bennekom, W. P. Formation and electrochemical characterization of self-assembled monolayers of thioctic acid on polycrystalline gold electrodes in phosphate buffer pH 7.4, *Langmuir* **2000**, *16(8)*, 3852-3857.

Dijksma, M.; Kamp, B.; Hoogvliet, J. C.; van Bennekom, W. P. Development of an electrochemical immunosensor for direct detection of interferon-γ at attomolar level, *Anal. Chem, accepted. Web Release Date: January 27*, **2001**.

Dijksma, M.; Boukamp, B. A.; Kamp, B.; van Bennekom, W. P. Effect of hexacyanoferrate(II/III) on self-assembled monolayers of thioctic acid and 11-mercaptoundecanethiol on gold, *in preparation*.

Dijksma, M.; van Bennekom, W. P. Direct electrochemical immunosensing – review, *in preparation.*